DOE/RL-2016-37
Revision 0

PROTOTYPE HANFORD BARRIER 1994 TO 2015

Prepared for the U.S. Department of Energy

U.S. DEPARTMENT OF ENERGY | Richland Operations Office

P.O. Box 550
Richland, Washington 99352

This page intentionally left blank.

DOE/RL-2016-37
Revision 0

Prototype Hanford Barrier 1994 to 2015

Date Published
March 2016

Prepared for the U.S. Department of Energy

P.O. Box 550
Richland, Washington 99352

APPROVED
By Janis D. Aardal at 12:54 pm, Mar 31, 2016

Release Approval Date

Approved for Public Release;
Further Dissemination Unlimited

TRADEMARK DISCLAIMER

Executive Summary

A surface barrier (also known as a surface cover) is a technology commonly used to isolate and contain subsurface contaminants. The key functions of a surface barrier are to isolate underlying waste from intrusion and to reduce or eliminate the movement of meteoric precipitation into the waste zone. Drainage resulting from this precipitation could trigger contaminant transport towards the underlying groundwater.

After a decade of development activities, the Prototype Hanford Barrier (PHB) was constructed between late 1993 and 1994 over the 216-B-57 Crib at the Hanford Site in southeastern Washington State as part of a *Comprehensive Environmental Response, Compensation, and Liability Act of 1980* (CERCLA) treatability test of barrier performance for the 200-BP-1 Operable Unit. The barrier was monitored extensively between November 1994 and September 1998 to evaluate surface-barrier constructability, construction costs, and hydrologic and structural performance at the field scale. The results of the 4-year (fiscal years 1995 to 1998) treatability test are documented in *200-BP-1 Prototype Barrier Treatability Test Report.*[1] The CERCLA treatability test included an enhanced precipitation stress test during the water years 1995 to 1997 to determine barrier response to extreme precipitation events.

After fiscal year 1998, monitoring focused on a more limited set of water balance, stability, and biotic parameters to evaluate the barrier's hydrologic, structural, and ecological performance. The only stress test during this period was a controlled fire in 2008. The purpose of this report is to compile the monitoring data, evaluate the monitoring systems, summarize the findings and lessons learned, and provide recommendations.

The PHB consists of four main components: (1) An evapotranspiration-capillary (ETC) barrier that consists of a silt loam evapotranspiration layer and an underlying capillary break consisting of gravels grading into large basalt, which is intended to prevent intrusion; (2) an asphalt concrete (AC) barrier with a polymer-modified fluid applied asphalt coating and a compacted soil layer beneath it; (3) a gentle pit-run gravel side slope in the west (10:1); and (4) a steep basalt riprap side slope in the east (2:1). The ETC barrier is the portion of the PHB that sits directly above the waste zone. The role of the ETC barrier is to store precipitation and release the stored water into the atmosphere and to deter intrusion from the barrier surface by plants, animals, or humans. The AC barrier diverts drainage, hinders intrusion, and thus acts as a backup to the ETC barrier should the functionality of the latter be compromised. The two side slopes maintain barrier stability so that the ETC barrier remains intact and retains its functionality.

Based on a comprehensive review and analysis of the data collected from 1994 to 2013, the main findings with respect to the performance of the barrier components are as follows:

- The ETC barrier of the PHB performed much better than the drainage design goal of 0.5 mm yr^{-1}.
    - During each winter season, the silt loam layer was recharged by precipitation. The capillary break considerably enhanced the barrier's storage capacity.
    - During each summer season, all of the summer precipitation and nearly all of the stored water from the winter season was returned to the atmosphere by evapotranspiration. These seasonal

[1] DOE-RL. 1999. *200-BP-1 Prototype Barrier Treatability Test Report*, DOE/RL-99-11, Rev. 0, U.S. Department of Energy Richland Operations Office, Richland, Washington.

observations were consistent year to year and thus explained why average drainage (0.005 mm yr^{-1}) was so much lower than the design goal.

  - After the controlled fire in September 2008, far less vegetation reestablished in the burned section of the PHB than in the unburned section. The reestablished grasses still removed nearly all the stored water in the burned section, but at a slower rate than in the unburned section, which had fully grown shrubs. Initially after the fire, the soil showed decreased wettability, but gradually returned to normal in the years that followed.
  - No detectable settlement or compression of the ETC barrier occurred.
  - The number and sizes of animal holes on the barrier surface were small and did not discernibly affect barrier function.
- Both side slopes remained stable and well-drained.
- The AC barrier remained stable and allowed negligible water percolation.

From 1994 to 2013—during which time the barrier experienced 3 years of enhanced precipitation, three 1000-year return, 24-hour simulated rainstorms, and a controlled fire—the PHB limited drainage to well below the 0.5 mm yr^{-1} design criterion and had minimal erosion. Although the test period represents only 2% of the design life, the observations suggest the PHB is robust enough to control drainage and isolate subsurface contaminants. Future barrier performance will depend on barrier stability and hydrology. Given the 19-year record of successful performance and considering all processes and mechanisms that could degrade barrier stability and hydrology in the future, the results suggest that the PHB is very likely to perform for at least the remainder of its 1000-year design life. This conclusion is based on two assumptions: (1) the exposed subgrade receives protection against erosion and (2) institutional controls prevent inadvertent human activity on the barrier.

Acknowledgments

Numerous individuals contributed to the Hanford Barrier program during its existence. Their contributions range from design and engineering to field monitoring support and analysis. Key individuals include Dr. Glendon W. Gee of Pacific Northwest National Laboratory (PNNL), the principal scientist for design and installation of the barrier, and Dr. Kevin D. Leary of the Department of Energy, who directed monitoring activities and is the inspiration behind the controlled burn and subsequent natural recovery monitoring. Other key individuals include PNNL's Dr. Mike J. Fayer (test of barrier design at the lysimeter scale) and Dr. Andy L. Ward and Dr. Z. Fred Zhang (routine monitoring and reporting).

The following list of contributors was compiled from previous barrier documents or activities, but some contributors may have been missed. Organizational affiliations listed are from the time of the individuals' contributions. This summary report and/or some of the appendices have been reviewed by Dr. Michael J. Fayer, Dr. Mart Oostrom, Mr. Michael J. Truex, Dr. Janelle L. Downs, Dr. Christopher Strickland, and Dr. Yang Gao of PNNL. Dr. Craig H. Benson of the University of Virginia and Dr. William H. Albright of the Desert Research Institute reviewed the report and provided valuable comments and suggestions.

Pacific Northwest National Laboratory
Cadwell, L. L.
Campbell, M. D.
Clayton, R. E.
Davis, R.
Dennis, G. W.
Draper, K. E.
Freeman, H. D.
Fayer, M. J.
Freshley, M. D.
Gee, G. W.
Gilmore, B. G.
Hasan, N.
Keller, J. M.
Kirkham, R. R.
Ligotke, M. W.
Link, S. O.
O`Neil, T. K.
Perkins, W. A.
Ritter, J.C.
Rod, K.
Romine, R. A.
Seedahmed, G. H.
Smith, S. K.
Strickland, C. E.
Thomle, J. N.
Wellman, D. W.
Walters, W. H. Jr.
Ward, A. L.
Zhang, Z. F.

Westinghouse Hanford Company
Wing, N. R.

Bechtel Hanford, Inc.
Berlin, G. T.
Buckmaster, M. A.
Cammann, J. W.
Consort, S. D.
Corpuz, F. M.
Duranceau, D. A.
Fort, D. L.
Myers, D. R.
Petersen, K. L.
Sonnichsen, J. C.

CH2M Hill Hanford Group, Inc.
Linville, J. K.
Wittreich, C. D.

U.S. Department of Energy
Leary, K. D.
Morse, J. G.

Acronyms and Abbreviations

Acronym	Description
AC	asphalt concrete
CERCLA	*Comprehensive Environmental Response, Compensation, and Liability Act*
CG	creep gauge
DOE	U.S. Department of Energy
DVZ – AFRI	Deep Vadose Zone – Applied Field Research Initiative
ED	extreme dry
EDM	electronic distance measurement
ET	evapotranspiration
ETC	evapotranspiration-capillary
EW	extreme wet
FAA	fluid applied asphalt
FGB	fiberglass block
FLTF	Field Lysimeter Test Facility
FY	fiscal year
GTCC	Greater-Than-Class C
HDU	heat dissipation unit
MD	moderate dry
MW	moderate wet
NN	near normal
NP	neutron probe
NPL	National Priorities List
PET	potential evapotranspiration
PHB	Prototype Hanford Barrier
PNNL	Pacific Northwest National Laboratory
QA	Quality Assurance
RAO	remedial action objective
RCRA	*Resource Conservation and Recovery Act*
SPI	standardized precipitation index
TDR	time domain reflectometry
WY	water year
X	times

Definition of Symbols

Symbol	Description
a, a_0, a_1, a_2, b, c, d	constants
D	drainage (mm)
dx	change in the easting direction
dy	change in the northing direction
dz	change in the vertical direction
ET	evapotranspiration (mm)
ET_m	monthly evapotranspiration (mm)
ET_s	summer season evapotranspiration (mm)
ET_w	winter season evapotranspiration (mm)
ET_{w0}	average winter season evapotranspiration (mm)
G	cumulative probability
h	soil-water pressure head (m)
k	von Karman constant (≈0.41)
L	soil thickness
P	precipitation (mm)
P_a	annual precipitation (mm)
P_m	monthly precipitation (mm)
P_s	summer season precipitation (mm)
P_w	winter season precipitation (mm)
P^{avg}	long-term annual average precipitation (mm)
P_s^{avg}	long-term summer season average precipitation (mm)
P_w^{avg}	long-term winter season average precipitation (mm)
PET	potential evapotranspiration (mm)
$P50$	median precipitation
R	runoff (mm)
t	time
u_z	wind velocity (m s^{-1})
u_*	friction velocity (m s^{-1})
W	2-m water storage (mm)
x	easting distance (m)
y	northing distance (m)
z	height (m)
z_0	surface roughness (m)

Symbol	Description
α	a shape parameter
β	a scale parameter
σ	standard deviation
ΔV	voltage change (mV)
ΔW	water storage change (mm)
ΔW_s	summer season water storage change (mm)
ΔW_w	winter season water storage change (mm)
Γ	Gamma function
μ	mean
θ	volumetric water content ($m^3m^{-3)}$
θ_s	saturated volumetric water content ($m^3m^{-3)}$

Contents

Appendices

Figures

Tables

1.0 Introduction

1.1 Hanford Site Background and Mission

The Hanford Site is located in a semi-arid region of southeastern Washington State along the Columbia River, and is approximately 1517 square kilometers (586 square miles) in size. From the early 1940s to approximately 1989, the site's mission included defense-related nuclear research, development, and weapons production activities. During that period, nine nuclear reactors and associated processing facilities comprised the plutonium production mission.

The Hanford Site mission since 1989 has been environmental remediation, focused on cleaning up waste sites and remediating contaminated soils and groundwater. The emphasis of cleanup has been on remediating the river corridor to protect the Columbia River and reduce the overall footprint of the Hanford Site. Since about 2010, attention has turned to the Hanford Site Central Plateau (Figure 1.1), where facilities in the 200 Areas were used to separate special nuclear materials from spent nuclear fuel through chemical processing and for waste management. As a result of these activities, 200 Area waste sites are included on the U.S. Environmental Protection Agency's National Priorities List (NPL) (EPA 2013). The NPL listing encompasses the 200 Areas and portions of the 600 Area, and includes 44 operable units and more than 1000 waste sites, including *Comprehensive Environmental Response, Compensation, and Liability Act* (CERCLA) and *Resource Conservation and Recovery Act* (RCRA) past-practice waste sites; unplanned release sites; RCRA treatment, storage, and disposal units; and surplus facilities.

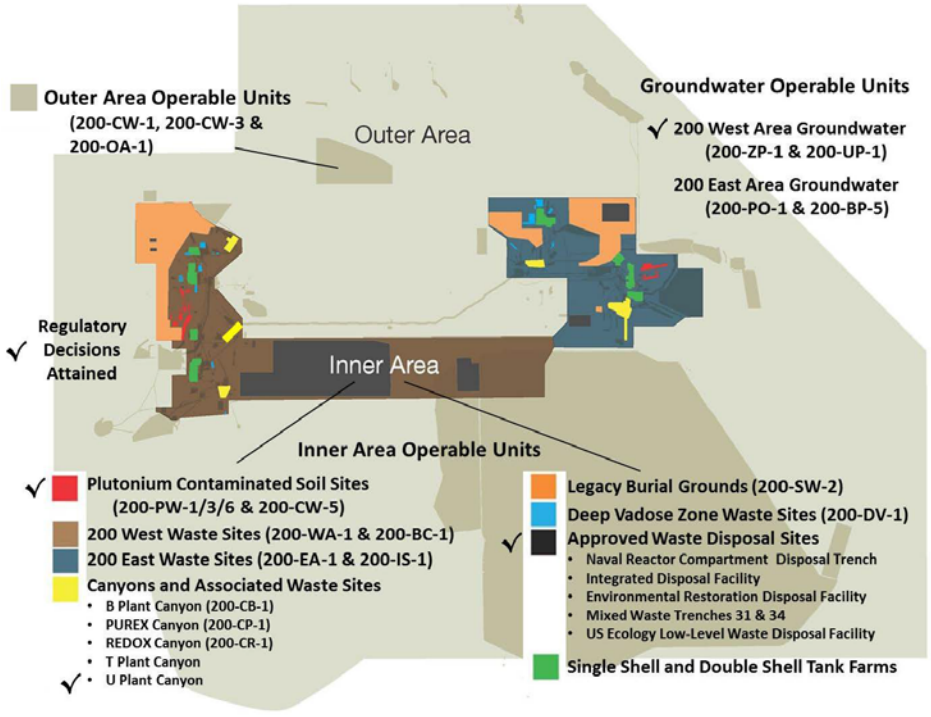

Figure 1.1. Central Plateau and primary decision groupings of waste sites, disposal facilities, tank farms, and canyon facilities for which final remedy and closure decisions will be needed (After Figure 4-1 of DOE-RL 2013).

1.2 Surface Barrier Technology for the Hanford Site Central Plateau

As part of the CERCLA remedial investigation and feasibility study process for the Hanford Central Plateau includes characterizing the nature and extent of contamination, assessing the risks to human health and the environment, evaluating and selecting remedial actions. In the early stages of the CERCLA process, the U.S. Department of Energy (DOE) identified the overall remedial action objectives (RAOs) for the Hanford Central Plateau:

> *Reduce the risk of harmful effects to the environment and human users of the area by isolating or permanently reducing the toxicity, mobility, or volume of contaminants from the source areas to meet applicable or relevant and appropriate requirements or risk-based levels that will allow industrial use of the area* (DOE-RL 1992a, b, c).

Potential remedial technologies were screened based on their effectiveness, implementability, and cost. Engineered surface covers (also termed surface barriers in this report) were identified and considered applicable to sites with radionuclides, heavy metals, inorganic compounds, and/or organic compounds. Surface barriers satisfied the RAOs of protecting human health and the environment from direct exposure to contaminated soil, biomobilization, and airborne contaminants. Specifically, surface barriers can minimize (1) infiltration of precipitation (*P*) into contaminated soil, thereby minimizing the driving force for downward migration of contaminants; (2) migration of windblown dust that originates from contaminated surface soils; (3) penetration of biota into the waste zone; (4) the potential for direct exposure to contamination; and (5) the migration of volatile organic compounds, radon, and tritium to the atmosphere.

DOE has identified surface barriers as one of several alternatives that could be applied broadly to contain various types of waste sites throughout the Hanford Central Plateau (DOE-RL 1992a, b, c). Because of the potential broad application of surface barriers to 200 Area sites, DOE recommended that a focused feasibility study be prepared to examine generic surface barrier designs for various waste categories rather than designs for specific waste sites.

A multi-year barrier development program was undertaken to develop, test, and evaluate the effectiveness of various barrier designs. The program was organized to develop and evaluate barrier design technology for long-term containment of subsurface radioactive waste in the field and at the Hanford Site's Field Lysimeter Test Facility (FLTF). The program also included evaluation of natural analogs. A team of engineers and scientists from ICF Kaiser Hanford Company, Westinghouse Hanford Company, Bechtel Hanford, Inc., and Pacific Northwest National Laboratory (PNNL) directed the barrier development effort and established the following key performance objectives (DOE-RL 1999) to address both CERCLA and RCRA criteria:

- Function in a semiarid to sub-humid climate.
- Have a design life of 1000 years.
- Limit drainage to less than 0.5 mm yr^{-1}.
- Limit runoff.
- Be maintenance free.
- Minimize erosion.
- Meet or exceed RCRA performance criteria.

After a decade of development activities from 1983 to 1993, the Prototype Hanford Barrier (PHB) was constructed between late 1993 and 1994 over the 216-B-57 Crib in the Central Plateau. The barrier was monitored from November 1994 to September 1998 as part of a CERCLA treatability test of barrier performance for the Hanford Site's 200-BP-1 Operable Unit. The results of the 4-year (fiscal years [FYs] 1995 to 1998) treatability test are documented in the *200-BP-1 Prototype Barrier Treatability Test Report* (DOE-RL 1999).

The PHB was also evaluated against RCRA criteria; however, not all of the RCRA criteria are defined quantitatively for all site conditions (Albright et al. 2010). The RCRA criteria require a design life of 30 years, a thickness of 0.9 m, and permeability of 10^{-7} cm s^{-1}. Strictly speaking, the permeability requirement is not a performance criterion; hence, it is interpreted here as drainage rate. Within treatability test, the PHB was designed for sites with Greater-Than-Class C (GTCC) low-level waste and/or GTCC mixed waste, and/or substantial inventories of transuranic constituents. The barrier was designed to function for a performance period of 1000 years and to provide the maximum practicable degree of containment and hydrologic protection of the evaluated designs. The barrier layers are designed to maximize moisture retention and evapotranspiration (ET) and to minimize moisture drainage and biointrusion, considering long-term variations in the Hanford Site climate. The primary structural differences between the PHB and other proposed barriers are increased thicknesses of individual layers, number of layers, the inclusion of a coarse-fractured basalt layer and the asphalt concrete (AC) layer, and side slopes to control biointrusion and to limit inadvertent human intrusion.

The purpose of the PHB demonstration was to evaluate surface barrier constructability, construction costs, and physical and hydrologic performance at field scale. Table 1.1 provides a timeline of main activities before and after construction of the PHB. Monitoring and data collection began in October 1994 and continued until the present (2015). Data collection focused on the following:

- Water-balance, consisting of precipitation, runoff (*R*, as well as sediment collection to evaluate the water erosion component), soil moisture storage (*W*), and drainage (*D*) measurements with ET calculated by difference;
- Structural stability, consisting of asphalt-layer-settlement, basalt-side-slope-stability, and surface elevation measurements due to such factors as wind and water erosion, compaction, settling, and changes in bulk density; and
- Vegetation community and animal activities.

Table 1.1. Timeline of main activities before and after construction of the Prototype Hanford Barrier.

Date	Activities
1985	Initiated the Hanford Site Permanent Isolation Surface Barrier Development Program
1987	Constructed the Field Lysimeter Test Facility to test barriers of different designs
1990	Initiated the PHB design
1992	Conducted peer review of the scope, need, results, and design; completed the PHB design
02/1993	Conducted a value engineering workshop to review plans for remaining barrier development activities and to reach stakeholder consensus. A minimum design life of 1000 years was selected (Myers and Duranceau 1994).
09/1993	Started PHB construction
08/1994	Completed PHB construction; started performance monitoring
11/1994	Revegetated the barrier surface; started the enhanced precipitation (treatability) test
02/1995	Initiated enhanced precipitation treatment to the north section of the barrier
09/2008	Conducted a controlled burn test on the north section of the barrier

1.3 Purpose and Scope

The purpose of this report is to summarize the performance of PHB during the monitoring period from the time it was constructed in 1994 through 2013. Monitoring data collected after 2013 are not included in this report. Three aspects of performance are evaluated: (1) hydrological performance based on data within, below, and around the barrier; (2) structural stability based the settlement of the barrier subgrade, elevation change of the barrier surface, and displacement of the riprap slope; and (3) ecological performance based on the vegetation characteristics and animal activities.

Because a large amount of monitoring data has been generated, this document consists of a summary report and a series of appendices. The appendices provide detailed information on barrier design and monitoring, and in-depth analysis of the monitoring results. The summary report describes the history, barrier design and study approach, and main findings based on the results in the appendices.

Section 2.0 briefly describes the approaches and methods used to test PHB performance. Section 3.0 discusses the results of barrier performance over the monitoring period. Section 4.0 is a summary of findings and Section 5.0 provides recommendations for the PHB and future barrier development. Quality assurance (QA) is described in Section 6.0 and a list of references is given in Section 7.0.

For more details, refer to Appendix A for the precipitation characteristics at Hanford, Appendix B for the design of and tests at the PHB, Appendix C for the monitoring system, Appendix D and Appendix E for the properties of the materials for constructing the PHB, Appendix F for the performance of the monitoring instruments, Appendix G and Appendix H for the hydrological characteristics at the silt loam barrier and the side slopes of the PHB, Appendix I for the structural stability of PHB, Appendix J and Appendix K for vegetation community and plant structure, Appendix L for animal activities, Appendix M and Appendix N for the controlled fire and fire impacts, and Appendix O for aerial photos of the PHB and surrounding area. A summary of elements worked, lessons learned, and recommendations is given in Appendix P. The list of the qualified monitoring data is given in Appendix Q and the data are provided in digital form on CD. Finally, the publications relevant to the PHB are compiled in Appendix R.

2.0 Study Approaches and Methods

This section briefly summarizes the approaches and methods used to test PHB performance.

2.1 Climate and Standardized Precipitation Index at Hanford

The Hanford Site has a steppe (semi-arid) climate with typical dry, hot summers and cool, wet winters (Hoitink et al. 2005). Under the Hanford climate, the most likely season for recharge is between November and March (termed the winter season), when ET is low (Gee et al. 1992; Gee et al. 2005). In addition to winter rains, snowmelt can be an important contributor to recharge. Vegetation consists of shrub-steppe plant communities composed of annual grasses and perennial grasses and shrubs (Rickard and Vaughan 1988). This shrub-steppe vegetation, a mixture of shallow- and deep-rooted plants, generally uses soil water very efficiently from April to October (termed the summer season). To be consistent with the precipitation pattern, a water year (WY) is defined as the 12-month period from November to October. As such, a WY consists of a 5-month winter season and a 7-month summer season. A specific WY is denoted by "WYyy," in which "yy" is the last two digits of a year. For example, WY1999 is denoted by WY99.

The average recharge rate to the subsurface beneath undisturbed natural vegetation at Hanford is usually no more than 5.0 mm yr^{-1} (Fayer and Keller 2007). However, in areas where there is no vegetation, the recharge rate can be as high as 50 to 100 mm yr^{-1} (Gee et al. 2005), depending on the texture of the surface soil. A coarser surface soil tends to produce higher recharge.

Precipitation tends to obey a gamma distribution (Thom 1966). The cumulative probability of an observed precipitation event is described as

$$G(P) = \int_0^P \frac{\xi^{\alpha-1}\exp(-\xi/\beta)}{\beta^{\alpha}\Gamma(\alpha)}d\xi \qquad [2.1]$$

$$\text{where } \Gamma(\alpha) = \int_0^{\infty} \xi^{\alpha-1}\exp(-\xi)d\xi \qquad for\ P > 0$$

where $\alpha > 0$ is a shape parameter, $\beta > 0$ is a scale parameter, $P > 0$ is the precipitation amount, ξ is the dummy variable of integration, and $\Gamma(\alpha)$ is the gamma function. Based on precipitation measured at Hanford from WY48 to WY14 (Appendix A), the precipitation data for the WYs, winter seasons, and summer seasons were used to fit α and β according to Eq. [2.1]. Table 2.1 shows the precipitation statistics and fitted α and β parameters. Figure 2.1 shows the cumulative probability of precipitation for a WY, winter season, and summer season. Although the model describes the observed precipitation data, the estimated precipitation at very low probability (e.g., 0.1%) is subject to extrapolation error.

In the following, subscripts *a*, *w*, and *s* denote a WY, winter season, and summer season, respectively, and a superscript *avg* denotes the average of a variable. The WY meteoric precipitation at the Hanford Site has an average, P^{avg}, of 171.3 mm and varies from 101.4 mm ($0.59P^{avg}$) to 293.6 mm ($1.71P^{avg}$, Table 2.1). On average, 58.7% (100.6 mm, P_w^{avg}) of the precipitation falls in the winter season and 41.3% (70.7 mm, P_s^{avg}) falls in the summer season. During the barrier monitoring period of WY95 to WY13, the average precipitation was 185.1 mm yr^{-1}, slightly (8.1%) higher than the long-term average.

Table 2.1. Precipitation statistics and the fitted parameters α and β for WY48 to WY14.

	Water Year	Winter Season	Summer Season
Min (mm)	101.4	29.7	14.2
Max (mm)	293.6	224.0	157.5
Average (mm)	171.3	100.6	70.7
Median (mm)	167.1	96.1	66.9
α	13.739	7.485	6.149
β	12.465	13.438	11.494

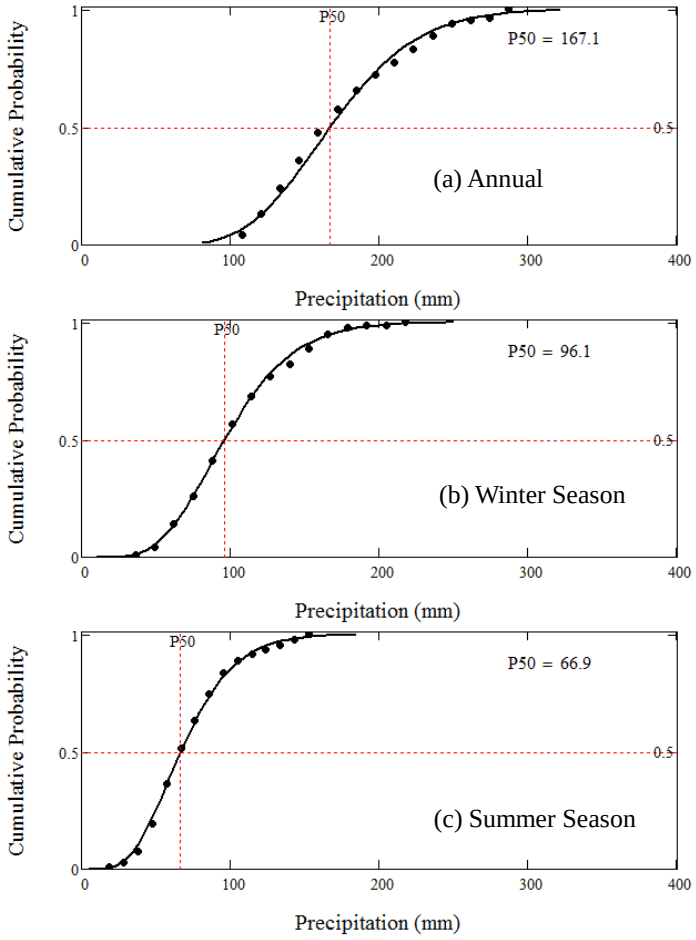

Figure 2.1. Cumulative probability of precipitation. The symbols denote data and the curves are the best fits. P50 is the median precipitation.

The maximum precipitation expected once every 1000 years was quantified by the 99.9th percentile. Based on Eq. [2.1], the estimated precipitation with 0.1% probability at Hanford is 350.5 mm for a WY, 253.0 mm for a winter season, and 191.9 mm for a summer season.

Precipitation was categorized with the standardized precipitation index (SPI) developed by McKee et al. (1993). The SPI is a probability index defined as the standard normal random variable (with mean $\mu = 0$ and standard deviation $\sigma = 1$) obtained from the cumulative probability (Eq. [2.1]). The nature of the SPI allows the quantification of an anomalously dry or wet event at a particular time (t) scale. According to

the SPI values, McKee et al. (1995) categorized the precipitation of a given period into seven classes: extreme wet, severe wet, moderate wet, near normal, moderate dry, severe dry, and extreme dry (Table 2.2). The precipitation, calculated SPIs, and precipitation classes during the barrier test period from WY95 to WY13 for the WYs, winter seasons, and summer seasons are given in Table 2.3 and shown in Figure 2.2. Of the 19 test years, 2 years (WY95 and WY97) were extremely wet, 4 moderately wet, 12 near normal, and 1 (WY05) severely dry. This means that the barrier had the highest precipitation stress in WY95 and WY97, even for the non-irrigated section.

Table 2.2. SPI classification following McKee et al. (1995).

SPI Values	Class Name	Class Symbol	Probability of Event (%)
SPI > 2.0	Extreme wet	EW	2.3
1.5 < SPI ≤ 2.0	Severe wet	SW	4.4
1.0 < SPI ≤ 1.5	Moderate wet	MW	9.2
-1.0 < SPI ≤ 1.0	Near normal	NN	68.3
-1.5 < SPI ≤ -1.0	Moderate dry	MD	9.2
-2.0 < SPI ≤ -1.5	Severe dry	SD	4.4
SPI ≤ -2.0	Extreme dry	ED	2.3

Table 2.3. Precipitation, SPI, and precipitation classes during the test period from WY95 to WY13.

WY	Annual			Winter Season			Summer Season		
	P_a (mm)	SPI	Class	P_w (mm)	SPI	Class	P_s (mm)	SPI	Class
WY95	279.1	2.058	EW	147.8	1.244	MW	131.3	1.84	SW
WY96	233.4	1.298	MW	173.5	1.757	SW	59.9	-0.261	NN
WY97	290.3	2.231	EW	224.0	2.64	EW	66.3	-0.022	NN
WY98	153.4	-0.309	NN	106.9	0.29	NN	46.5	-0.832	NN
WY99	130.8	-0.864	NN	85.9	-0.298	NN	45.0	-0.904	NN
WY00	169.2	0.044	NN	88.4	-0.222	NN	80.8	0.472	NN
WY01	150.9	-0.368	NN	79.5	-0.494	NN	71.4	0.159	NN
WY02	130.6	-0.87	NN	95.3	-0.025	NN	35.3	-1.402	MD
WY03	222.8	1.107	MW	144.5	1.174	MW	78.2	0.389	NN
WY04	239.0	1.396	MW	140.0	1.075	MW	99.1	1.018	MW
WY05	105.4	-1.571	SD	49.3	-1.617	SD	56.1	-0.413	NN
WY06	226.1	1.167	MW	120.1	0.621	NN	105.9	1.206	MW
WY07	159.5	-0.169	NN	104.1	0.217	NN	55.4	-0.444	NN
WY08	138.7	-0.664	NN	93.7	-0.068	NN	45.0	-0.904	NN
WY09	149.6	-0.398	NN	108.7	0.336	NN	40.9	-1.103	MD
WY10	215.9	0.981	NN	83.1	-0.383	NN	132.8	1.876	SW
WY11	182.6	0.33	NN	111.5	0.408	NN	71.1	0.15	NN
WY12	157.7	-0.21	NN	67.1	-0.913	NN	90.7	0.777	NN
WY13	181.9	0.314	NN	72.4	-0.728	NN	109.5	1.3	MW

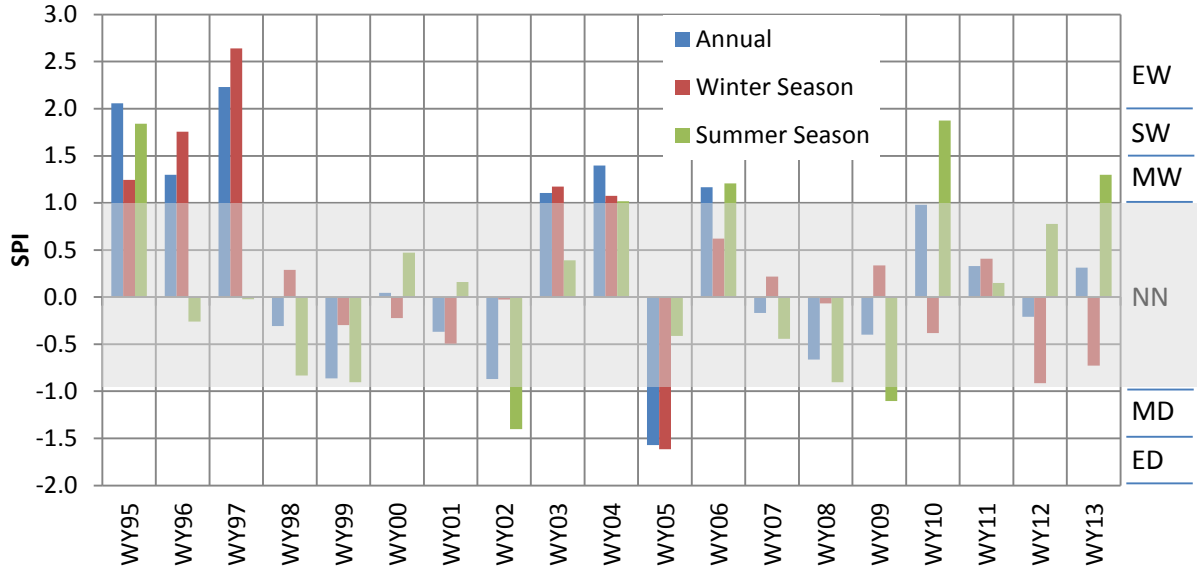

Figure 2.2. Standardized precipitation index and precipitation categories during the barrier demonstration period. The precipitation category symbols are defined in Table 2.2.The shaded area indicates the range of near-normal precipitation.

To mimic an extreme precipitation scenario, an irrigation system was used on the north section of the barrier from WY95 to WY97 such that the total precipitation was about three times (3X) the long-term average. More details about the enhanced precipitation test are given in Section 2.3.1. The total annual and winter precipitation and the corresponding SPI for the irrigated section are summarized in Table 2.4. The 3X precipitation was considerably more than the lowest precipitation amount with a 0.1% chance (350 mm annually or 253 mm for the winter season). The SPIs for the enhanced precipitation test period from WY95 to WY97 were larger than 4.2, except for the winter of WY95, which had an SPI of 3.079 because irrigation was delayed until February 1995. The estimated probability of P_a at the enhanced precipitation condition is extremely low, only 0.67, 0.68, and 0.47 times every 1 million years for WY95, WY96, and WY97, respectively. The estimated probability of P_w is 9 and 7 times every 1 million years for WY96 and WY97, respectively. In May 1998, 209.6 mm water was applied to the north section of the barrier for instrument calibration, bringing the total WY precipitation to 363.0 mm, which corresponds to an SPI of 3.265. The barrier was exposed to the natural precipitation conditions in WY99 and thereafter.

Table 2.4. Statistics of total (meteoric and irrigated) precipitation of the irrigated north section of the barrier from WY95 to WY98.

WY	Annual			Winter Season		
	P_a (mm)	SPI	Probability of P_a or higher	P_w (mm)	SPI	Probability of P_w or higher
WY95	493.3	4.834	6.68E-07	252.2	3.079	1.04E-03
WY96	493.1	4.832	6.75E-07	339.9	4.277	9.46E-06
WY97	499.7	4.905	4.68E-07	344.2	4.331	7.42E-06
WY98	363.0	3.265	5.46E-04	106.0	0.289	3.86E-01

2.2 Barrier Design

The description and design of the PHB are reported in other sources (e.g., DOE-RL 1994, 1999; Gee et al. 1997; KEH 1993; Myers and Duranceau 1994; Ward and Gee 1997; Wing and Gee 1994). They are also summarized in Appendix B and briefly in this section.

The PHB, with an area of 2.5 ha (6.2 acres), is located in the 200 East Area (46°34'01.23"N, 119°32'28.43"W) and was deployed over the 216-B-57 Crib in the 200-BP-1 Operable Unit (Figure 2.3). More information about the 216-B-57 Crib can be found in DOE-RL (1993).

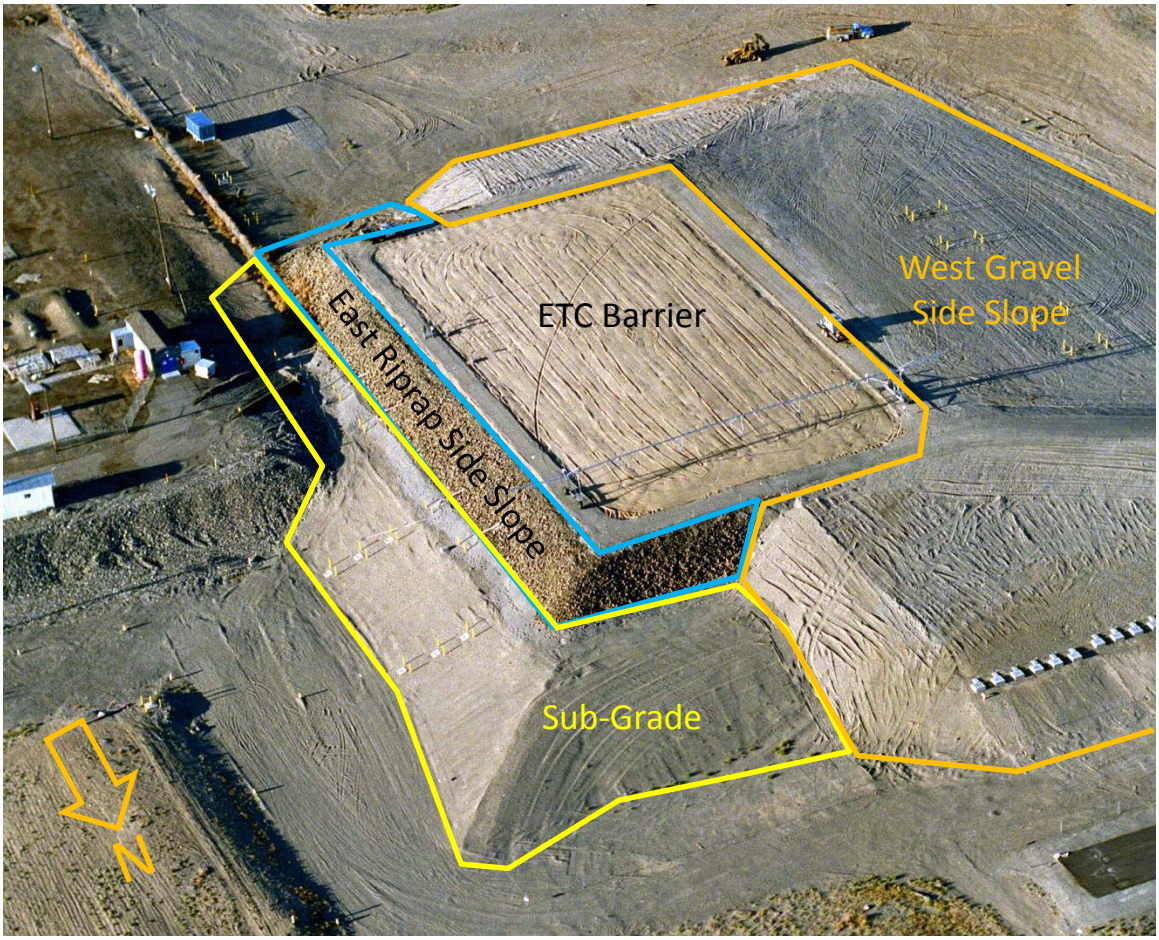

Figure 2.3. Plan view of the Prototype Hanford Barrier after completion of construction. (Photo taken on August 9, 1994. The lines show the approximate boundaries of the main barrier components.)

The PHB consists of four main components (Figure 2.4): (1) a silt loam ET layer with an underlying capillary break and an intrusion prevention layer, termed the evapotranspiration-capillary (ETC) barrier, in the middle: (2) an AC barrier with a polymer-modified fluid applied asphalt (FAA) coating and a compacted soil layer at the bottom; (3) a 10:1 gentle pit-run gravel side slope on the west side and partially on the north and south sides; and (4) a 2:1 steep basalt riprap side slope on the east side and partially on the north and south sides. The ETC barrier is the centerpiece of the PHB and sits directly above the waste zone (Figure 2.4). It is designed to store precipitation and release the stored water into the atmosphere and to deter intrusion by plants, animals, or humans from the barrier surface. The AC is

redundant with the overlying ETC barrier to divert drainage and to hinder intrusion. The two side slopes protect the ETC barrier from damage or intrusion from the sides.

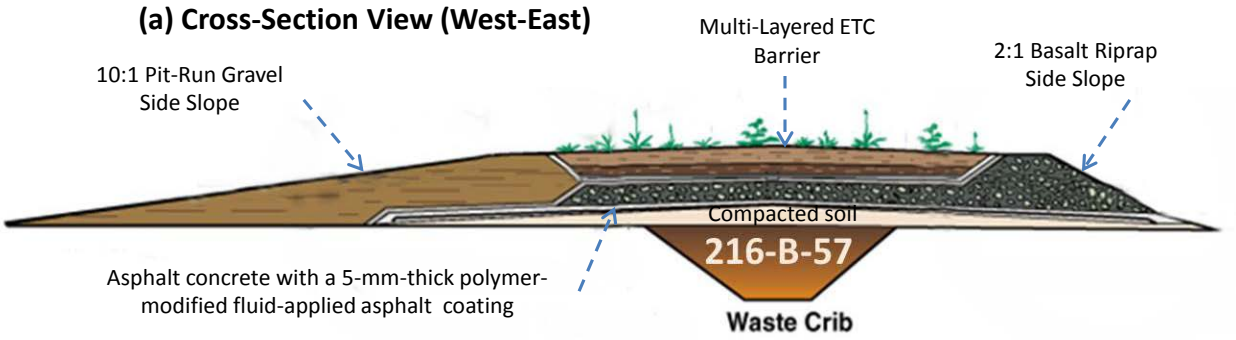

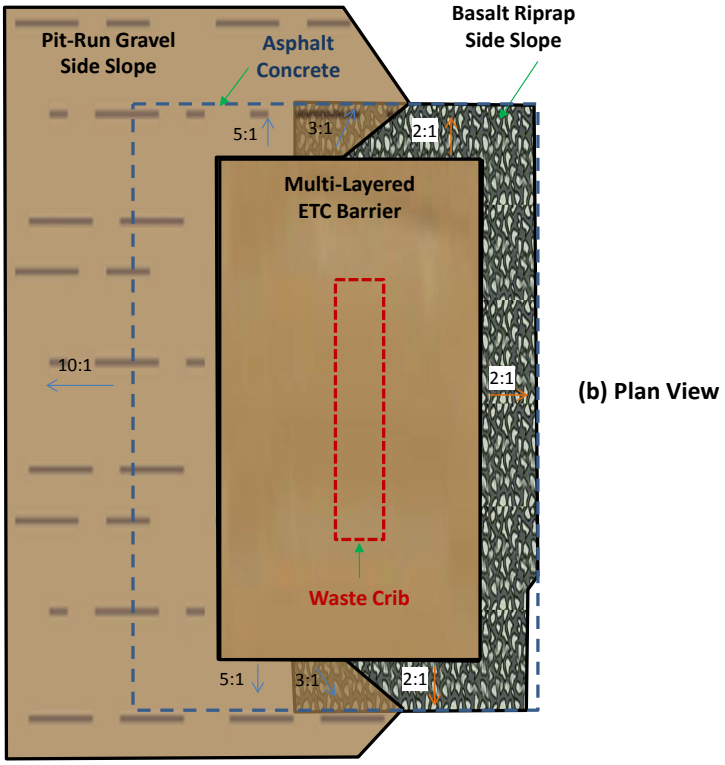

Figure 2.4. Schematic of the PHB: (a) cross-section view (west-east) and (b) plan view (approximate scale).

The ETC barrier is composed of multiple layers (Figure 2.5) of natural materials and uses a capillary break (sand filter and gravel) to increase the storage capacity of the top silt loam ET layer. The silt loam layers were constructed with a 2% slope from the crown (north-to-south centerline) to promote runoff of excess precipitation. The dry bulk density of the ETC barrier admix after construction was 1380±0.121 kg m^{-3} (Gee et al. 1995). Each layer of the ETC barrier serves a distinct purpose, as given in Table 2.5.

The west side slope is a 10:1 (horizontal:vertical) pit-run gravel side slope. It contains a small amount of fine (e.g., sand and silt) particles. The east side slope is made of basalt riprap with a size of about 0.2 to 0.3 m.

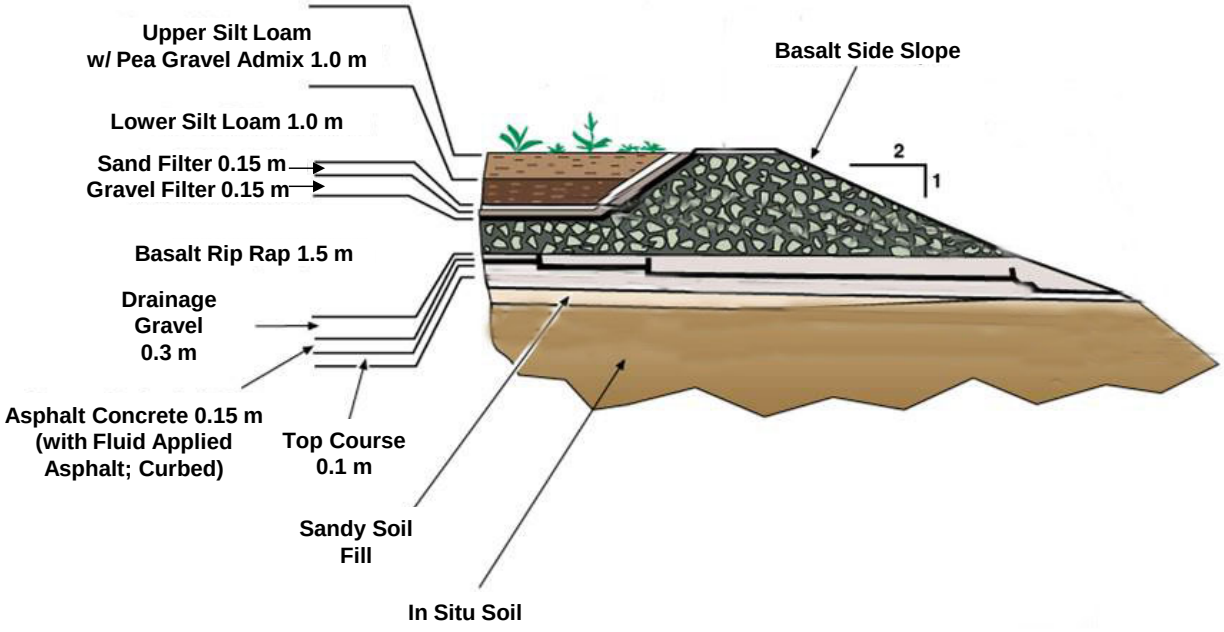

Figure 2.5. Prototype Hanford Barrier cross-section – basalt riprap side slope.

Table 2.5. The layers of the ETC barrier and their functions.

Layer No.	Materials	Thickness (m)	Function	Notes
0	Vegetation	NA	Release stored water into the atmosphere by evapotranspiration; protect barrier surface from wind and water erosion	Revegetated native plant species
1	Upper silt loam w/ pea gravel admix	1.0	Provide a medium for plant growth and water storage; the 15% pea gravel is to minimize soil loss by erosion	2% slope from the crown (north-south center line)
2	Lower silt loam	1.0	Provide a medium for plant growth and water storage	2% slope from the crown
3	Geotextile	NA	Prevent the fine silt loam from entering the underlying coarser sand layer during construction	Non-woven, needle-punched polypropylene geotextile
4	Sand filter	0.15	Prevent silt loam from falling into the gravel filter; form a capillary break with the overlying silt loam	2% slope from the crown
5	Gravel filter	0.3	Prevent gravel from falling into the basalt riprap; is a portion of the coarse layer that forms the capillary break	Top course material; 2% slope from the crown
6	Basalt riprap	1.5	Provide a physical control against digging by humans and burrowing animals; limit root penetration	A layer of shoulder ballast was used at the top of basalt riprap; 2% slope from the crown
7	Drainage gravel	0.3	Protect the underlying layer; provide a medium for lateral water movement	2% slope from the crown
8	Asphalt concrete	0.15	Divert infiltration water away from the waste zone; provide a barrier against noxious gases from the waste zone	AC with 5-mm-thick FAA coating; the layer is curbed and drainage water is guided out to a designated area; 2% slope from the crown
9	Top course	0.1	Provide a base for the asphalt concrete	Compacted to 95% of the maximum density; 2% slope from the crown
10	Compacted sandy soil fill	Variable	Provide a foundation for the top layers	Level north-south; 2% in the west-east direction from crown; compacted to 95% of the maximum density

The PHB is intended to perform for at least 1000 years without maintenance, making the function of the ETC barrier and structural stability critical to its success. Issues that could affect barrier functionality, structural stability, and longevity were addressed in the design and are briefly summarized below.

Issues related to barrier functionality:

- Vegetation sustainability. Perennial shrubs were established by collecting seeds from local populations growing on the silt loam soil, growing seedlings, and planting them on the surface of the barrier. Perennial grasses were established by hydroseeding. The silt loam used to construct the ETC barrier provides a medium for the growth of vegetation for transpiration. The bulk density of the silt loam layer was designed for optimal plant growth.

- Precipitation storage and release. The 2-m-thick silt loam layer acts as the storage layer from which ET processes recycle stored water back to the atmosphere. Coarser materials (sand overlying gravel) placed directly below the silt loam layer create a capillary break that inhibits the downward drainage of water from the silt loam into the coarser materials.
- Limited runoff (storm-water diversion). To reduce water erosion, the silt loam used to construct the barrier has sufficiently high permeability so that runoff rarely occurs, except during extreme precipitation events, when the 2% slope of barrier surface promotes runoff to limit the amount of water infiltrating into the barrier.
- Drainage diversion. The FAA-coated AC has very low permeability. The drainage gravel above the AC helps to promote lateral flow of any water that passes through the ETC barrier.
- Protection of noxious gases. The FAA-coated AC also functions as a barrier to noxious gases.

Issues related to barrier structural stability and longevity:

- Material degradation. Degradation of materials used to construct the barrier may compromise barrier functionality. Synthetic materials used for some conventional barriers are not expected to last for the life of the barrier. The PHB design is based on use of natural construction materials (e.g., fine soil, sand, gravel, cobble, basalt, asphalt). The only synthetic material used was the geotextile at the bottom of the silt loam layer to prevent the fine particles of silt loam from entering the underlying sand during construction.
- Wind and water erosion. To reduce wind and water erosion, the PHB uses both a pea-gravel admix and vegetation. The gravel admix was blended with the soil during construction and vegetation was planted after construction. The surface layer (top 1 m of soil) was amended by adding about 15 wt% (dry weight) pea gravel. The decision to use 15 wt% pea gravel was based in part on the results of wind tunnel tests (Ligotke 1993; Ligotke and Klopfer 1990), and was also a compromise between water storage in the surface layer for plant growth and erosion mitigation.
- Intrusion. The side slopes guard the barrier against plant, animal, and human intrusion from the sides, and the 1.5-m-thick basalt riprap layer below the barrier's storage layer is designed to inhibit intrusion from the barrier surface.
- Settlement. A compacted soil subgrade was constructed to prevent the barrier foundation from settling, which could lead to cracking or other types of damage. The 2% slope of the AC barrier prevents formation of standing water. Both the compacted soil and the elimination of standing water allow the barrier and the side slopes to maintain their shear strength and structural stability.
- Slope stability. The angularity of the riprap provides interlocking surfaces between adjacent rocks, allowing a relatively steep yet stable side slope. On the 10:1 pit-run gravel side-slope, the gentle angle of the slope itself provides stability.

2.3 Specific Barrier Tests Conducted during the Demonstration Period

Two specific tests were carried out at the PHB during the demonstration period: (1) an enhanced precipitation test from WY95 to WY97 and (2) a controlled fire test in 2008. In most of the years when no

tests were conducted, the performance of the PHB was monitored with relatively few breaks (except in FY99, FY00, FY05, and FY06) due to a shift in funding priorities and funding shortfalls.

2.3.1 Enhanced Precipitation Test

An enhanced precipitation test was used to test the barrier under both ambient (natural precipitation) and extreme climate (enhanced precipitation) conditions for a period of 3 water years (WY95 to WY97, within a time frame of 4 calendar years). The enhanced precipitation test was part of the overall treatability test documented in DOE-RL 1999. In late March of each year from 1995 to 1997, a 1000-year-return, 24-hour rainstorm event was simulated on the north section of the barrier. Although the simulated rainstorm was targeted to deliver 68 mm over a 24-hour period based on the analysis of precipitation from 1947 to 1969 (Stone et al. 1983), in practice, 69.4, 69.5, and 69.7 mm of water were applied over 8-hour periods on March 25 of 1995, March 26 of 1996, and March 27 of 1997, respectively.

For testing purposes, the barrier surface was divided into two treatments, or sections (Figure 2.6). The north section was designated to receive an elevated amount of precipitation (natural precipitation plus supplemental irrigation) to simulate extremely wet climatic conditions, while the south section received only natural precipitation.

Irrigation water was applied with a Lockwood® linear-move sprinkler irrigation system by Petty Irrigation (Toppenish, WA) (Gee et al. 1994). The system delivered water on the north section of the barrier at a mean rate of about 10 mm hr^{-1} with a coefficient of spatial variation of 6.7% (Appendix F). It took 15 to 17 minutes for the sprinkler system to complete a full pass, and the water applied was equivalent to about 2 to 3 mm of precipitation, depending on the inlet line pressure of the irrigation system. This created an intermittent application of water to the barrier surface and allowed infiltration of greater amounts of water stored on the surface in localized ponds than would normally occur during a natural rainstorm.

Water was usually applied at biweekly intervals, except in winter and depending on the weather. The amount of water applied in each irrigation event was usually calculated based on the amount of precipitation since the last irrigation cycle, with a 10.0 mm margin to allow for natural precipitation events. From May 11 to May 14, 1998, 209.6 mm was applied to the north section for instrument calibration. The barrier was exposed to the natural precipitation conditions in WY99 and thereafter.

The total meteoric precipitation and irrigation received by the north side was 493.3, 493.1, 499.7, and 363.0 mm (SPI = 4.83, 4.83, 4.90, and 3.27) for WY95 through WY98, respectively. The SPI values for WY95, WY96, and WY97 correspond to precipitation probabilities of 0.67, 0.67, and 0.47 times of precipitation in 1 million years, respectively.

The estimate of the 1000-year-return, 24-hour rainstorm using the same method as in Stone et al. (1983) was 57.8 mm with the addition of records from 1970 to 1991 (Gilmore and Walters 1993) and was 53.8 mm by including the records from 1992 to 2004 (Hoitink et al. 2005). Hence, tests based on the 68 mm in Stone et al. (1983) placed a higher stress on the surface cover.

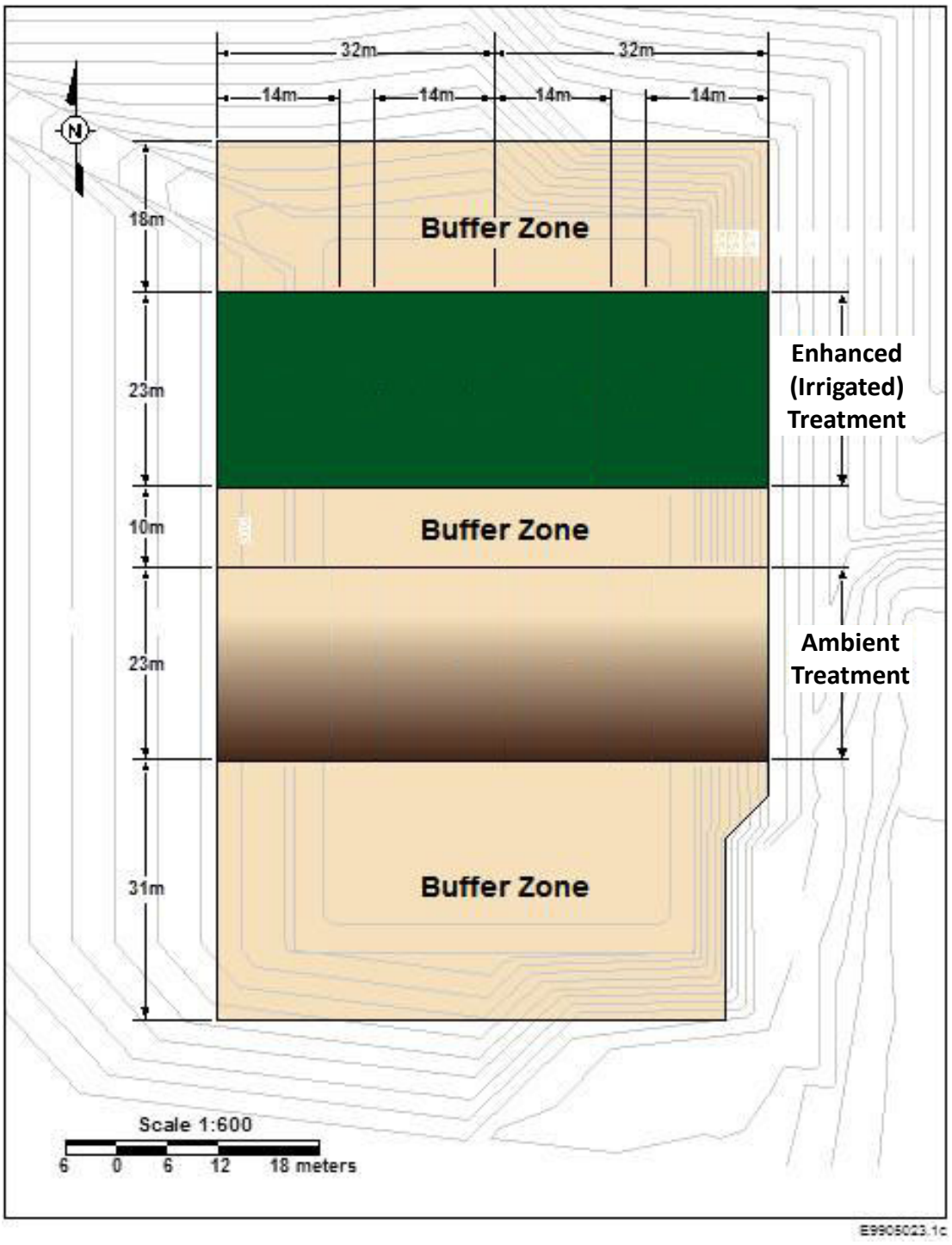

Figure 2.6. Plan view of the Prototype Hanford Barrier showing layout of the two precipitation treatments and three buffer zones.

2.3.2 Controlled Fire

A controlled burn was conducted on the formerly irrigated north section of the PHB in 2008 to understand the response of the ecosystems to wildfire and to quantify the effects of wildfire on the function of the ETC barrier. The test area encompassed the silt loam ETC barrier and the gravel side slope (Figure 2.7).

To ensure a complete burn, two loads (approximately 10.5 and 12.8 tonnes ha^{-1}, respectively) of tumbleweeds were imported to the burn area (Figure 2.7). Before starting the fire, a 3-m-wide line of fire retardant foam was applied to the buffer strip between the north and south sections of the barrier to protect the south section of the barrier during the fire. The fire was ignited with drip torches at 3:15 p.m. on September 26, 2008. The fire lasted approximately 7 minutes, by which time all of the imported tumbleweeds and most of the natural biomass had been consumed. Areas with incomplete combustion were burned off using a drip torch. More information about the controlled fire can be found in Ward et al. (2009) and Ward et al. (2010).

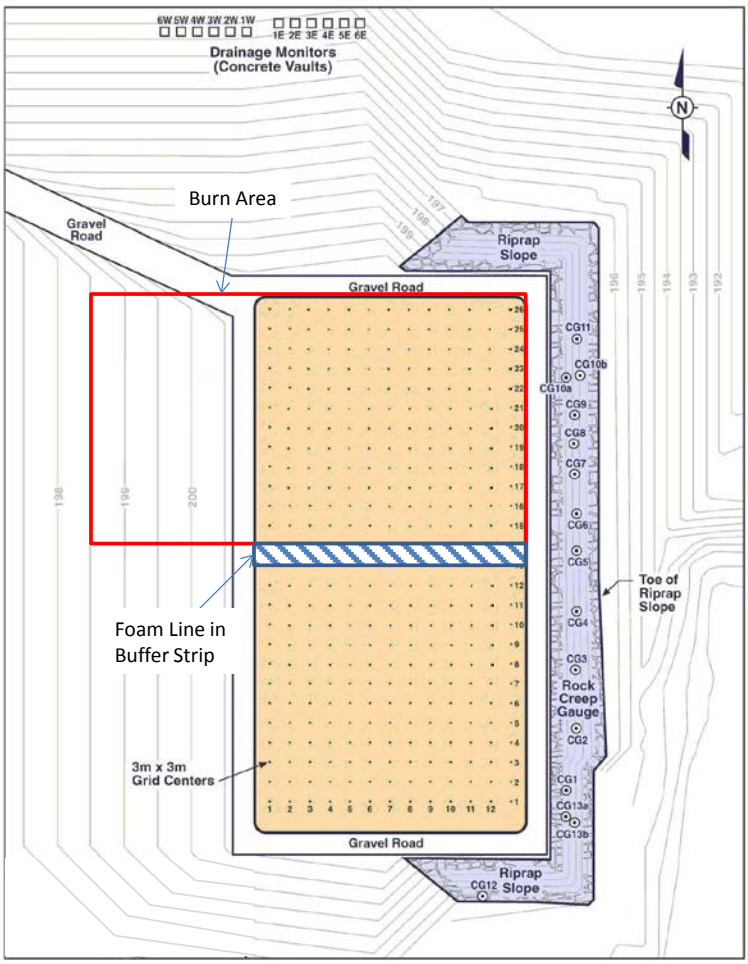

Figure 2.7. Schematic plan view of the barrier surface showing the burn area on the gravel side slope and the silt loam surface and the 3-m-wide line of fire retardant foam.

2.4 Barrier Monitoring

A comprehensive system was used to monitor the hydrology, structural stability, and ecology at the PHB. Details of the monitoring system are given in Appendix C and are briefly summarized below.

2.4.1 Hydrology

The primary hydrologic performance of the PHB was monitored using components of water balance, including precipitation and irrigation, surface runoff, water content (θ) and water storage within the ETC barrier, drainage through the ETC barrier and side slopes, and deep percolation through the AC. Secondary confirmative components monitored included water content at the bottom of the silt loam and beneath the AC, soil water pressure head (h) within the ETC barrier, and h below the AC.

Water balance measurements were focused on the silt loam layer. Twelve water balance monitoring stations, denoted as S1 through S12, were established on four silt loam plots (Figure 2.8). Two monitoring stations (S13 and S14) were located on the gravel side slope. Each monitoring station was equipped with a load cell (Revere Transducers, Cerrittos, CA) to record precipitation, a vertical aluminum access tube for a neutron probe (NP) (503 DR Hydroprobe, CPN Corporation, Martinez, CA), a time domain reflectometry (TDR) probe (MP-917 DM Meter, Environmental Sensors, Victoria, BC Canada), and a vertical access tube for a capacitance probe (Sentry 200-AP, Troxler Electronic Lab, Inc., Research Triangle Park, NC) to measure water content. The systems for monitoring hydrological variables also included heat dissipation units (HDUs) (229L, Campbell Scientific, Inc., Logan, UT) and fiberglass blocks (FGBs) (MC-314, ELE International, Inc., Lake Bluff, IL) for measuring soil water pressure, a pan lysimeter for percolation through the AC, and rain gauges for irrigation.

The soil water content and pressure of the silt loam barrier were monitored at the 12 water balance stations. Six of the stations were located in the north section and spaced 5 m apart. The other six stations were in the south section and were also spaced 5 m apart. Barrier water content was monitored at a vertical interval of 0.15 m using an NP deployed in a vertical (4.8-cm inner diameter) aluminum access tube extending 1.9 m below the barrier surface. The TDR probes generally were logged hourly. The capacitance probe was used only in FY1995.

Runoff and water erosion were monitored by measuring water volume and sediment yield from a 6-m-wide by 15-m-long flume installed on the soil surface (Figure 2.8). The flume was constructed of timber with an opening at the downslope end. A galvanized metal collector system received the water-sediment runoff for measurement by the automated ISCO monitoring system (ISCO, Inc., Lincoln, NE).

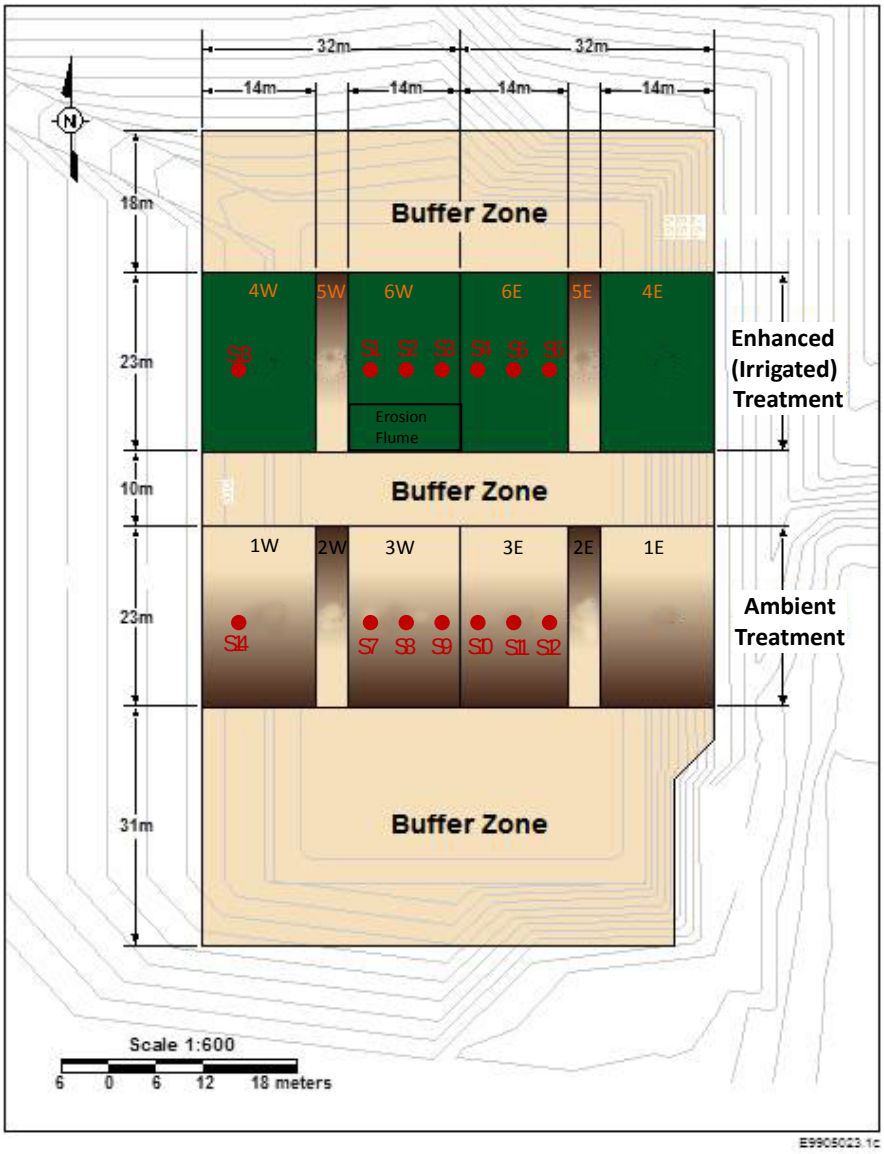

Figure 2.8. Plan view of the Prototype Hanford Barrier showing layout of the 2 precipitation treatments, 12 drainage plots (lW to 6W and lE to 6E), and 14 water balance stations (S1 to S14). The 12 plots represent three main types of barrier structure: ETC barrier (i.e., 3W, 3E, 6W, and 6E), side slopes (i.e., 1W and 4W for the west gravel side slope and 1E and 4E for the east riprap side slope), and transition zones (i.e., 2W, 2E, 5W, and 5E).

To measure the drainage rate through different parts of the PHB, the barrier surface was divided into 12 zones or plots (Figure 2.8), denoted as 1W through 6W for those located in the west half and 1E through 6E in the east half. These 12 plots represent three main types of barrier structure: ETC barrier (i.e., 3W, 3E, 6W, and 6E), side slopes (i.e., 1W and 4W for the west gravel side slope and 1E and 4E for the east riprap side slope), and transition zones (i.e., 2W, 2E, 5W, and 5E). A series of curbs divided a portion of the AC surface into 12 water collection zones corresponding to the 12 plots shown in Figure 2.8. Each curbed zone collected water beneath the plot, which was discharged to a concrete vault. Each collection zone with a vault is equivalent to a drainage lysimeter. The vaults were installed to the north and downgradient from the AC to allow the movement of water by gravity. Each vault contained an

Orenco® dosing siphon system (Orenco Systems, Inc., Sutherlin, OR) to discharge the collected water once the maximum water level was reached. The average dosing volume was 0.591 m^3, which is equivalent to 1.8 mm of drainage through the main plots (i.e., the silt loam and side slope plots) and 6.3 mm of drainage through the smaller transition plots. The drainage rate from each plot was also measured with a tipping bucket and a pressure transducer. Drainage water flowed into each vault via a tipping bucket, which allowed monitoring of low flows, e.g., through the ETC barrier or the transition plots. A submersed Druck® pressure transducer (Instrumart, South Burlington, VT) monitored the intermediate-to-high flow rates by recording hydrostatic pressure at intervals ranging from 10 minutes to 1 hour. Each vault was equipped with a lid to prevent precipitation from entering it and was covered with a thick tarp to prevent the water in the vault from freezing in the winter or evaporating in the summer.

The systems for monitoring hydrological variables also included HDUs and FGBs for measuring soil water pressure (which is a driving force for unsaturated flow), a pan lysimeter for measuring percolation through the AC, rain gauges for irrigation, and load cells for precipitation. Except for the NP and rain gauges, data collection from the instruments was controlled by data loggers connected to the required peripherals (e.g., batteries, solar panels, and multiplexers).

A robust system for long-term monitoring is expected to have a long duration of service and produce representative data that are valid, stable, and complete. Overall, the highest tier of monitoring systems included the NPs, tipping buckets, and rain gauges. The second tier of less reliable, but still functioning, systems included the MP-917 TDR with long probes, the HDUs, and the pan lysimeter. The third tier consisted of systems that did not perform to specification, including the MP-917 TDR with short probes, the FGBs, and load cells.

Future barrier monitoring should use the first two tiers of systems, with emphasis on the highest-performing systems. Data from the second-tier monitoring systems should be used with caution and after proper data screening or as confirmative information. The third tier monitoring systems should not be used for barrier performance evaluation. Based on this evaluation, the NP-measured soil water content was used to describe barrier water balance and water movement processes. The tipping-bucket-measured drainage was used for the silt loam and transition plots, and the pressure transducer measured drainage was used for the side slopes.

2.4.2 Structural Stability

Structural stability of the PHB was evaluated by measuring the water and wind erosion from the barrier surface, settlement of the subgrade below the AC, elevation change of the barrier surface, and displacement in the riprap side slope.

Two wind monitors were installed on top of the barrier and a third was installed on the gravel side slope (Figure 2.9). Wind speed sensors were installed at elevations of 0.25, 0.50, 1.0, and 2.0 m above the ground surface. Monitoring was carried out from 1994 through 1997. To quantify the shear stress exerted on the barrier surface, the time-averaged (monthly) wind velocity distribution was described by the semi-empirical relationship of a log wind profile (Oke 1987):

$$u_z = \frac{u_*}{k} \ln\left(\frac{z}{z_0}\right) \qquad [2.2]$$

where u_z is wind velocity (m s^{-1}) at height z, u_* is friction or shear velocity (m s^{-1}), $k \approx 0.41$ is the von Karman constant, and z_0 is the surface roughness (m). The surface roughness accounts for how objects on the ground surface affect wind. Typically, the roughness length is between 1/10 and 1/30 of the height of the objects (e.g., vegetation) on the ground.

Three sand saltation stations were installed at the southeast quadrat of the barrier surface (Figure 2.9). The measurement was terminated a year later because of a lack of saltation source as a result of the rapid vegetation growth and high soil moisture content at the barrier surface.

Subsidence or settling of the AC barrier was quantified by measuring the change in the elevation of settlement markers, DSG1 and DSG2, attached to the AC. These two settlement markers, 14 m apart, were installed at the north end of the barrier during barrier construction (Figure 2.9).

Elevation changes of a barrier surface indicate the inflation or deflation of the barrier as well as subsidence. Elevation surveys were taken at 338 (13 × 26) locations marked by wood stakes, 3 m apart (Figure 2.9).

Because of its steepness (2:1), the riprap slope was considered to have potential for movement. A total of 15 creep gauges (CGs) were installed at 13 locations (Figure 2.9) in the riprap slope during or after barrier construction to monitor slope displacement.

From the start of monitoring in 1994 through 2003, elevation and horizontal locations were measured by an electronic distance measurement (EDM) system. From 2004 to 2013, a real-time-kinematic global positioning system (Trimble Navigation Ltd., Sunnyvale, CA) was used because of a malfunction in the EDM system. The data for 1998 are questionable because they deviate considerably from other years, and hence these data were not included in the analysis. In total, 18 surveys were conducted for the surface elevation, 19 for the elevation of the settlement markers, and 19 for the locations of the CGs.

Soil inflation and deflation are likely to occur after a fire with the loss of plant cover. The patterns of inflation and deflation before and after the controlled fire were mapped using 66 erosion pins on the burned section of the barrier. The height above the soil surface at the 66 steel stakes was measured with a meter stick. The 66 measurement erosion pins were not distributed uniformly, but rather were placed around the edges and throughout the central region of the burned section.

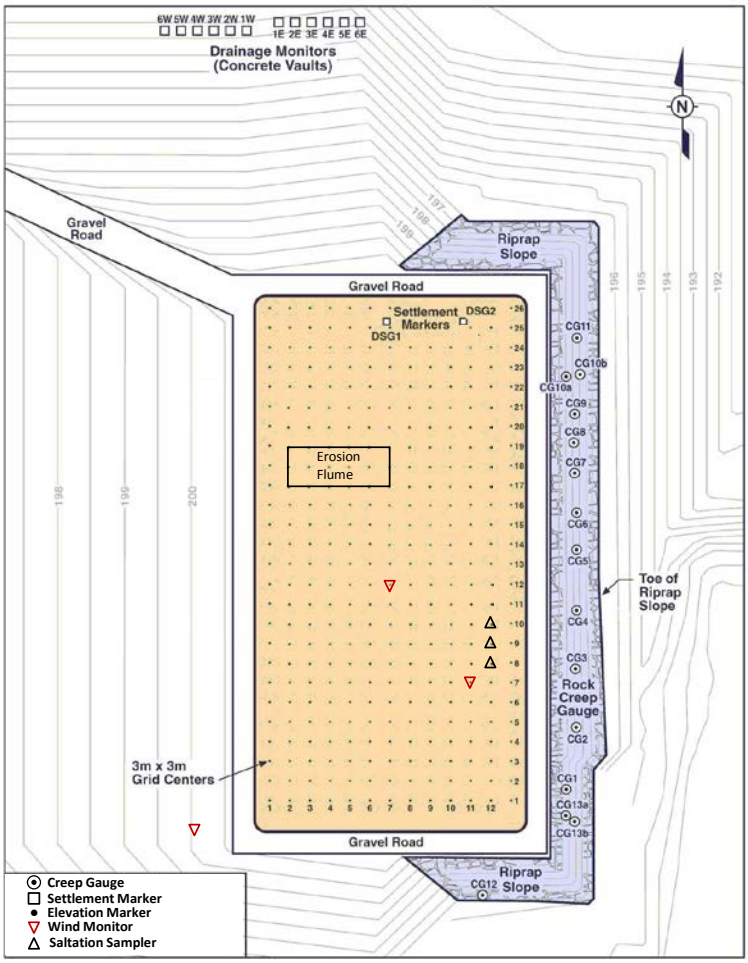

Figure 2.9. Plan view schematic showing the 338 elevation markers, 2 settlement markers, 3 wind monitors, 3 saltation samplers, 15 creep gauges, and the erosion flume. The elevation markers also marked the corners of 300 quadrats of 3 × 3 m^2.

2.4.3 Ecology

Ecology monitoring included the characteristics of vegetation and animal activities. The primary variables monitored included canopy characteristics (e.g., canopy dimension, species composition, reproduction, survivorship, and leaf area), root density and distribution, and physiological activities (transpiration, photosynthesis, and xylem pressure). Most of the vegetation characteristics were measured on 300 quadrats of 3 × 3 m^2 (Figure 2.9). For some items, only a limited number of samples were measured. Not all the variables were monitored at all ecological survey locations.

Animal activities were monitored in the 300 quadrats by examining animal evidence on the barrier surface and intrusion (burrowing) by insects and mammals. Evidence of animal use included direct observation (traps) as well as the presence of droppings, tracks, nests, burrows, resting spots, and gall formation. Animal hole dimensions were manually determined during ecological surveys.

2.4.4 Fire

A simulated fire was conducted on the north section of the barrier in 2008. For monitoring purposes, the burn area on the barrier surface was divided into nine 12 × 12 m^2 plots (Figure 2.10). In the center of each plot, a flame-height pole equipped with thermocouples was installed for visual observation of flame height and to quantify fire intensity. Soil properties were measured before the fire and at 1 week, 6 months, and 1 year after the fire. The field-saturated hydraulic conductivity was measured using a Guelph Permeameter (Reynolds and Elrick 1985) and the unsaturated hydraulic conductivity was measured using a Guelph Tension Infiltrometer (Reynolds 1993) at each of the nine plots. Soil water repellency was measured in situ on pre-burn and post-burn soil samples using the water-drop penetration time test (Dekker and Ritsema 1994). Soil macro-nutrients (i.e., N, P, and K) and selected micro-nutrients (i.e., Ca, Mg, and Na) were measured before the fire and again 1 week and 1 year after the fire by Northwest Agricultural Consultants (Kennewick, WA) using standard methods (Gavlak et al. 2003). Soil pH, electric conductivity, organic matter, cation exchange capacity, and specific surface area were also measured. Soil mineralogy was analyzed using the X-ray diffraction method for selected samples.

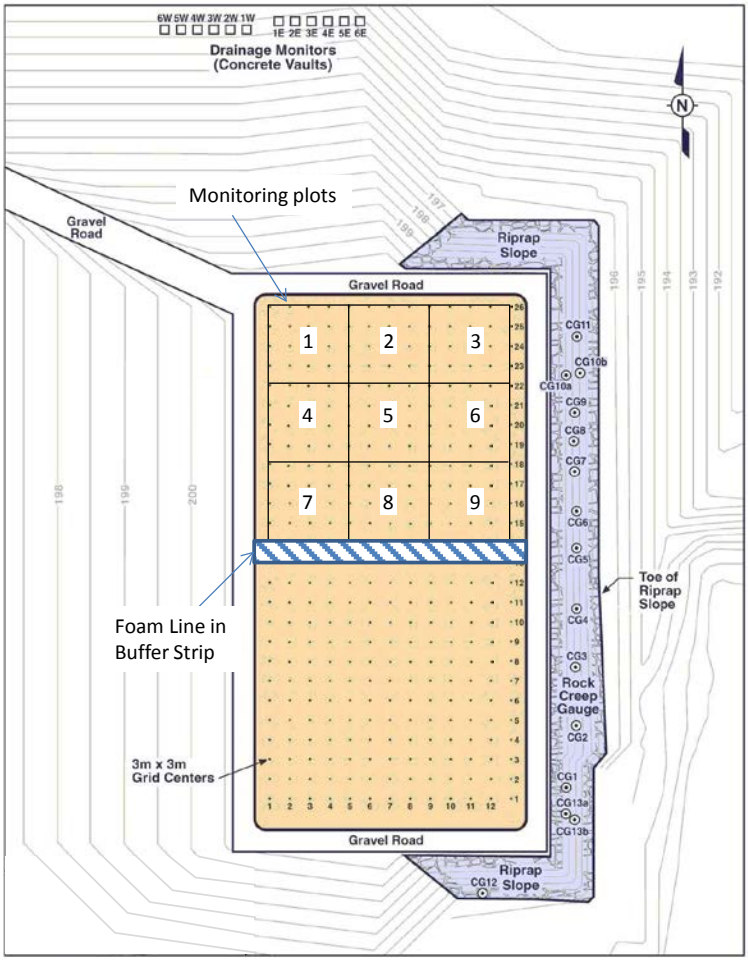

Figure 2.10. Schematic plan view of the barrier surface showing the nine 12 × 12 m plots for monitoring the fire.

2.5 Data Processing

Calculation of soil water content was based on the NP measurements at the 14 water balance stations. Barrier water content was monitored at a vertical interval of 0.15 m using an NP deployed in a vertical (4.8-cm inner diameter) aluminum access tube extending 1.9 m below the barrier surface. The NP was calibrated on April 5, 1995, in the vertical access tube:

$$\theta = a_0 + a_1 N + a_2 N^2 \qquad [2.3]$$

where N is the 16-sec. neutron count, a_0 = -0.01649, $a_1 = 1.449 \times 10^{-5}$, and $a_2 = 3.234 \times 10^{-10}$. On April 20, 2003, the NP received a new neutron counter. Cross-calibration with another NP before and after installation of the new counter showed that the new counter recorded only 96% of the values recorded using the old counter. Hence, the count values using the new counter were scaled by a factor of 1.041 for vertical logging so that Eq. [2.3] could be used to calculate water content. Radioactive decay was corrected for all the measurements before data analysis.

Arrays of HDUs were installed in September 1994 to monitor soil water pressure at depths of 0.075, 0.225, 0.45, 0.80, 1.25, and 1.75 m below ground surface. Before each measurement, the HDU was heated for a fixed period with a needle-type heater inside the HDU. The rate of heat dissipation was controlled by the water content of the HDU's porous matrix because water conducts heat much faster than air. The temperature increase caused a voltage change in the HDU's thermocouple, and the voltage was measured. The heat dissipation was determined as the difference between two voltages (ΔV), one measured after 1 sec. of heating and the other measured after a 30-sec. heating time. The relationships between the HDU-measured temperature and output voltage indicated that the variation among the HDUs was very small. Selected HDUs were calibrated in Tempe cells in a laboratory and the general calibration curve was used to convert the voltage change to soil-water pressure:

$$h = \begin{cases} a\exp(b\Delta V) & if \quad \Delta V \geq 1000 \\ c(1000-\Delta V)^2 + d(1000-\Delta V) - 1 & if \quad \Delta V < 1000 \end{cases} \qquad [2.4]$$

where $a = -1.514 \times 10^{-3}$, $b = 6.556 \times 10^{-3}$, $c = -1.338 \times 10^{-5}$, $d = 7.331 \times 10^{-3}$, h is negative under unsaturated conditions, and ΔV is the voltage change in millivolts. It is noted that the upper limit of water pressure measured by an HDU generally is considered to be approximately -1 m (CSI 2009; Flint et al. 2002; Reece 1996). However, the HDUs used at the PHB were first generation sensors and seemed to lack clear, distinct air entry pressures because of the existence of large pores.

To quantify the total amount of water in the barrier, water storage within the 2-m-thick silt loam layer was calculated based on neutron logging of soil water content at 12 depths between 0.15 and 1.80 m. The measurements at the 0.15-m depth were extrapolated to ground surface and those at 1.80-m depth were extrapolated to the 2-m depth.

Assuming water flow in the barrier is vertical only, ET can be estimated based on the mass balance equation:

$$ET = P - R - D - \Delta W \quad [2.5]$$

Using Eq. [2.5], ET was estimated for the north and south sections and for the winter (ET_w) and summer (ET_s) seasons for the years with sufficient data. Monthly ET (ET_m) was calculated for the summer months from WY95 to WY97. There were not sufficient observations to calculate the monthly ET for years from WY98 to WY13. The measured precipitation from the Hanford Meteorological Station, which is about 3.1 miles west of the PHB, was used to calculate ET.

To calculate the storage change (ΔW) for the winter season (ΔW_w) and the summer season (ΔW_s), water storage on November 1 and April 1 of each year was estimated by interpolating the measured water content of the two nearest neutron loggings. Interpolation of ΔW was conducted for the first day of the month when monthly ET was calculated.

Additionally, the monthly ET for the summer months from WY95 to WY97 was decomposed into the contributions from precipitation (ET_m^p) and soil (ET_m^s). When calculating ET_m^p and ET_m^s, it was assumed all the monthly precipitation (P_m) was released to the atmosphere via ET in the same month, and ET_m^s is the difference between the ET_m and P_m, i.e., $ET_m^p = P_m$, $ET_m^s = ET_m - P_m$. Sometimes negative ET_m^s was produced, suggesting that only part of the P_m contributed ET_m and the rest entered the barrier.

3.0 Results and Discussion

This section summarizes the results of barrier performance over the monitoring period. Results are presented for the different components of the PHB, including the ETC barrier, transition zone, side slopes, and the AC. Vegetation controlled ET for the ETC barrier, and therefore it is discussed in the ETC barrier performance section below. Structural stability results are presented, including results of animal activity. For more details, refer to Appendix E for performance of the silt loam storage layer, Appendix G and Appendix H for the hydrological characteristics of the PHB, Appendix I for the structural stability, Appendix J and Appendix K for vegetation characteristics and physiology, Appendix L for animal activities, and Appendix M and Appendix N for effects of the controlled fire.

3.1 ETC Barrier Performance

In this section, ETC barrier performance is summarized in terms of vegetation and hydrologic performance. After a description of vegetation characteristics, the water content results are analyzed for the winter season, summer season, sloped barrier surface, and controlled burn test. Water balance components for the north and south sections for each water year are tabulated in Tables G.3 through G.8 in Appendix G.

3.1.1 Vegetation Characteristics

After planting, roots grew to the bottom of a viewing tube (about 1.75 m) in the first year for the irrigated section and by the second year in the ambient precipitation section. These roots were primarily those of *Artemisia tridentata* (big sagebrush). This indicates that deep-rooted *A. tridentata* shrubs rapidly accessed nearly the entire soil profile for the barrier after construction. Forty-nine species were observed between 1995 and 2011, with the highest numbers observed 2 years after construction (35 species) and 2 years after the controlled fire (34 species). The minimum number of species observed was 11 in 2008, before the fire. *A. tridentata* density on the unburned section of the surface was 0.77 plants per m^{-2}, which was significantly greater than that on an unburned portion of the McGee Ranch (0.437 plants per m^{-2}), which is about 10 miles west to the PHB and is the source of the silt loam used for the PHB. *A. tridentata* was the dominant plant on the PHB until after the fire.

After the controlled fire in 2008, the mean leaf area index on the unburned section of the barrier (1.13±0.087) was significantly greater than that on the burned section (0.254±0.02) in 2009. *Machaeranthera canescens* (hoary tansyaster) became dominant on the burned section. In 2010, the ground surface coverage by *M. canescens* was 1.4% in the unburned section and 27.9% in the burned section; ground surface coverage by *A. tridentata* was 25.7% in the unburned section and 1.5% in the burned section. However, the plant communities on burned and unburned sections of the barrier surface were more similar to one another than to their counterparts at the McGee Ranch analog site (Link et al. 1994), indicating the vegetation community can develop naturally after a fire.

3.1.2 Hydrology in Winter Seasons

Recharge Process

The total winter season precipitation (meteoric precipitation plus irrigation), P_w, was 252.2, 339.9, 344.2, and 106.9 mm (with estimated probabilities of 1.04, 0.009, 0.007, and 3.9 times per 1000 years) for WY95, WY96, WY97, and WY98, respectively. (Note that in WY98, there was no irrigation in the winter season, but there was 209.6 mm of irrigation in the summer season). The P_w for WY95 was lower than planned because the start of the sprinkling system was delayed. The barrier had a net gain of water during the winter season of each WY, as shown in Figure 3.1, because ET was low and P was high in the winter season. During each winter season, the infiltration water gradually migrated from shallow to deep soil as more precipitation entered the soil. During the winter periods in WY95 through WY97, water contents increased to 0.20 m^3m^{-3} at depths of 1.55 m or deeper in the irrigated north section (Figure 3.1a) and from about 0.8 to 1.2 m in the south section (Figure 3.1b).

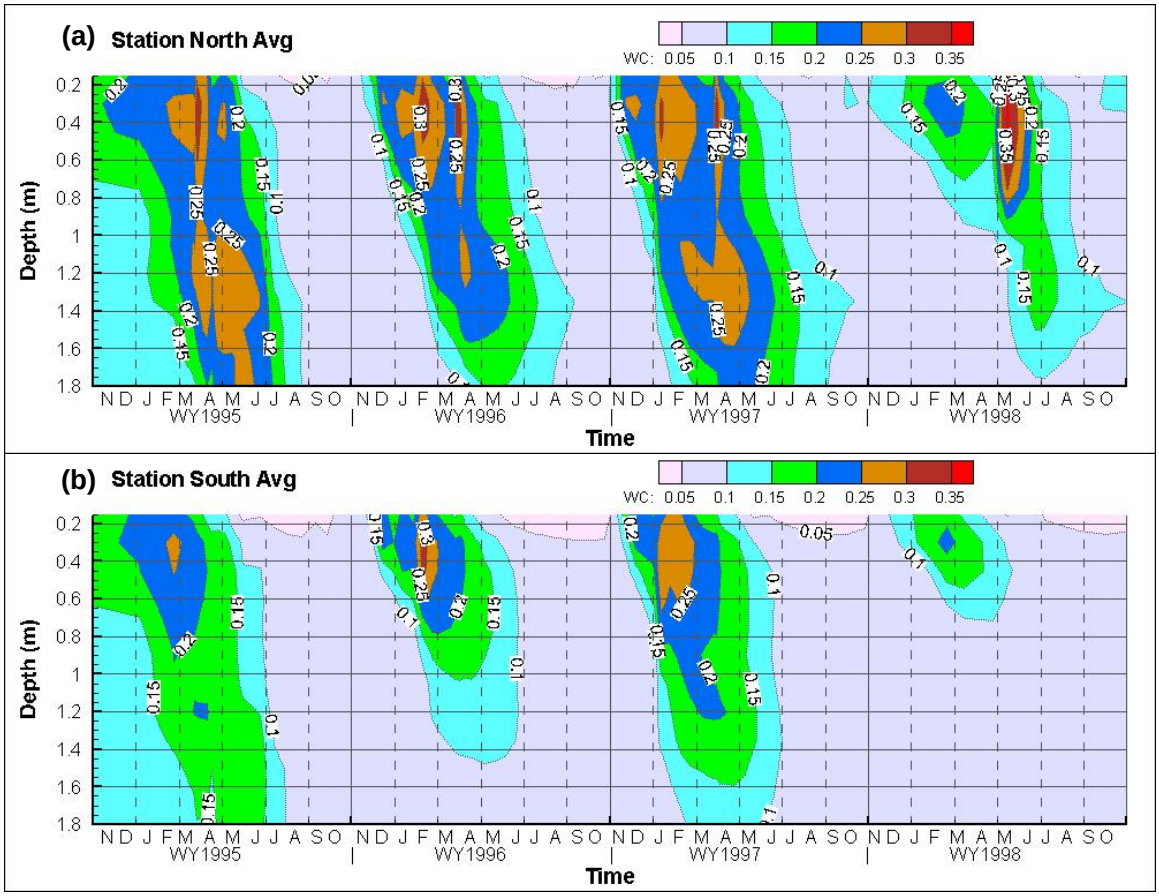

Figure 3.1. Average soil water content of six monitoring stations during the period from WY95 to WY98 for (a) the north section with enhanced precipitation and (b) the south section under ambient precipitation.

From WY99 to WY13, the entire barrier was exposed to only natural precipitation. The vegetation in the north section was burned by the controlled fire in September 2008 and was used to evaluate the impact of vegetation loss on soil water characteristics and natural plant community re-establishment. During this period, the winter season precipitation ranged from 49.3 to 144.5 mm, with an average of 96.2 mm. Of the

15 years, the P_w was moderate wet for 2 years, near normal for 12 years, and severe dry for 1 year. The water content contour plots in the *t*-*z* plane for the north section are shown in Figure 3.2a and Figure 3.2b. The results for the south section are similar to those for the north and hence are not shown. These results suggest that in near-normal precipitation years, the infiltration water is stored primarily in the top 0.8 m of the barrier profile, indicating very little chance to produce drainage.

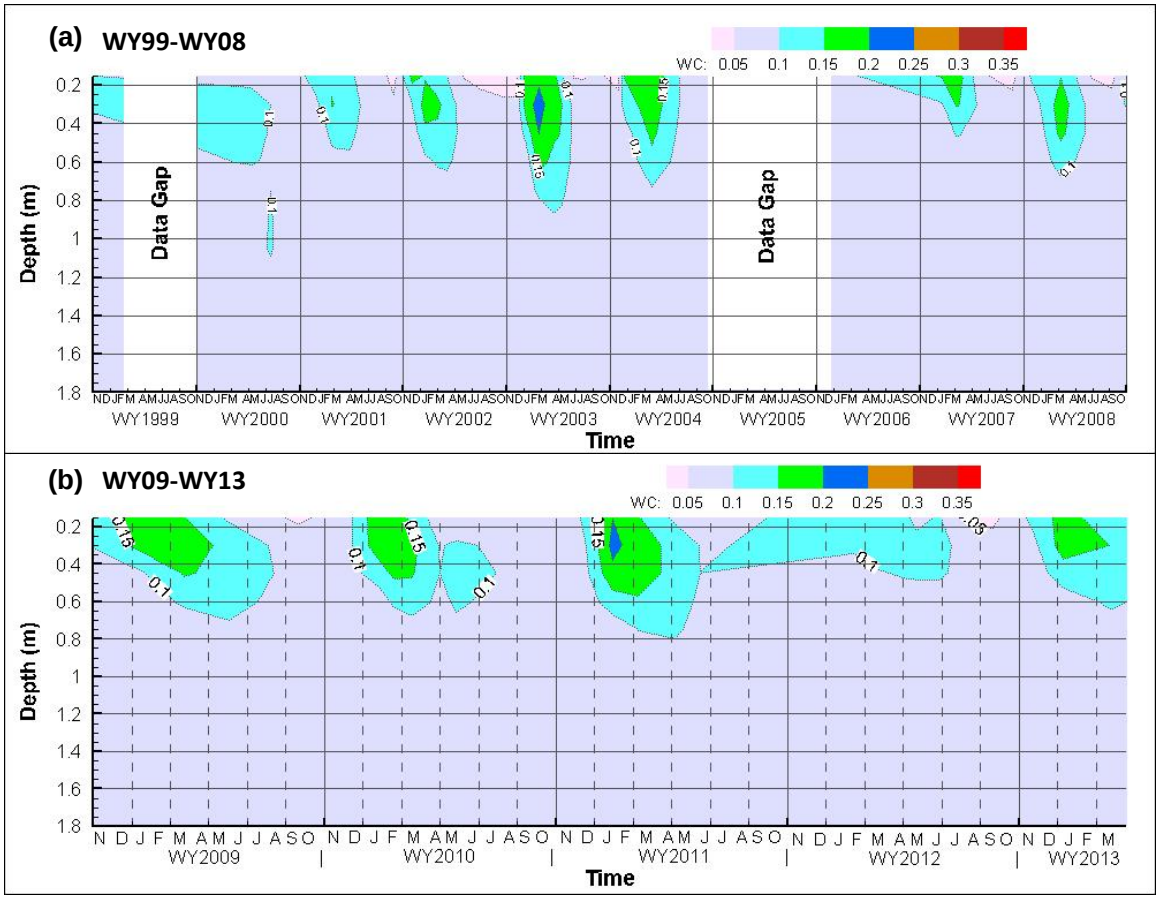

Figure 3.2. Average soil water content of six monitoring stations in the north section during the periods (a) WY99 to WY08 and (b) WY09 to WY13.

Drainage - A key quantitative performance measure of the enhanced precipitation test from WY95 to WY97 was to determine how much drainage through the ETC barrier would occur. Direct drainage measurements using tipping buckets showed that the maximum drainage rate of 0.18 mm yr^{-1} occurred in WY97 in the monitoring station at the northeast part of the barrier (Figure 3.3, 6E). The average drainage rate through the ETC barrier over the entire period was 0.005 mm yr^{-1}. The drainage rate after the enhanced precipitation test was no more than 8.5×10^{-4} mm yr^{-1}. These drainage rates are much less than the design drainage criterion of 0.5 mm yr^{-1}.

Drainage measurements for barriers have been conducted at a number of sites. Studies at the FLTF demonstrated that a vegetated, 150-cm-thick silt loam overlying sand and gravel layers prevented drainage from an annual precipitation of greater than 480 mm (Fayer and Gee 2006). Albright et al. (2004) reported the water balance of the ET or ETC barriers at 11 sites, 8 of which had an arid, semiarid, or sub-humid climate, for a test period up to 5 years. They found that the drainage rates from the ETC

barriers (with storage layer thicknesses between 0.6 and 2.5 m) in the arid, semiarid, and sub-humid sites were less than 1.5 mm yr^{-1} (0.4% of precipitation). Apiwantragoon et al. (2015) evaluated the water balance of ET and ETC barriers at 22 sites across the U.S. They found that, at semiarid and arid sites having low annual precipitation (<250 mm yr^{-1}), the drainage rates from ETC barriers of variable depths typically are less than 5 mm yr^{-1} and are frequently less than 1 mm yr^{-1}. Hence, the drainage rates measured at the PHB are in agreement with but better than those observed by others under similar conditions.

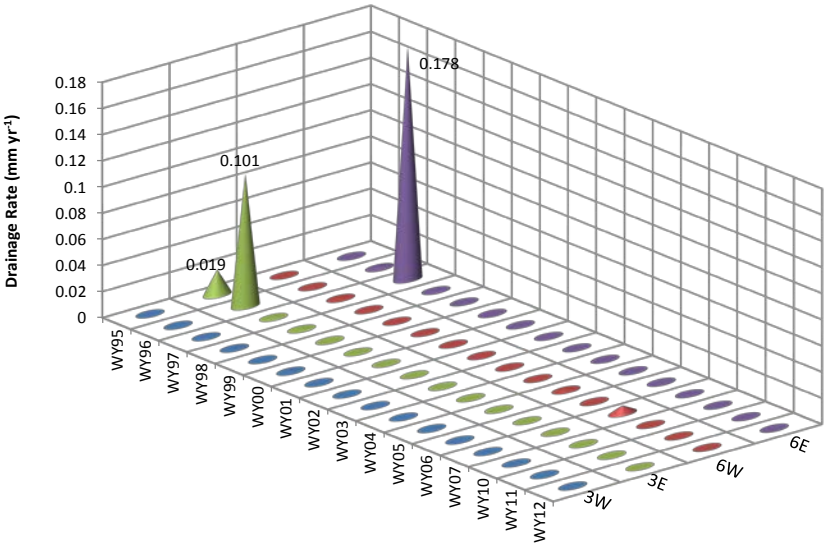

Figure 3.3. Drainage rate through the silt loam barrier plots.

Runoff - Runoff occurs when rainfall intensity exceeds the soil's infiltration capacity. In this report, runoff refers to the water moved out of the side boundary of the ETC barrier in the form of surface flow. Water movement at barrier surface within the barrier side boundary is not considered. Runoff may occur during a high-intensity rainstorm or when the soil's hydraulic conductivity is considerably reduced by processes such as freezing conditions or the soil has become hydrophobic following a wildfire. In March 1995, after the simulated 1000-year-return, 24-hour rainstorm to the newly vegetated surface, 1.79±0.11 mm of runoff was measured (Gee et al. 1995). Runoff of 36.3 mm was observed in the winter of 1997 and was attributed to the record precipitation of 93.7 mm in December 1996 and snowmelt on frozen ground (Ward et al. 1997). In January 2009, 4 months after the controlled fire, 0.016 mm runoff was observed. No runoff was observed during the rest of the monitoring period, including during the simulated 1000-year-return rainstorms in 1996 and 1997. Hence, the total runoff observed over the 19-year monitoring period was 38.1 mm.

Snowmelt events on frozen ground such as the one in January 1997 pose a higher risk for generating runoff, and hence soil erosion, than the 1000-year-return 24-hour rainstorms. This is because the ice in frozen soil blocks a fraction of the soil pores and the hydraulic conductivity of frozen soil is decreased. The magnitude of the decrease depends on the water and resulting ice content. Another large snowmelt event at the Hanford Site occurred in March 1985 and caused ponding of water at ground surface (Gee 1987).

Functionality of the Capillary Break - During the 3-year enhanced precipitation test, maximum storage was observed in WY97, with an average of 517.5 mm over the six monitoring stations in the north section with enhanced precipitation. A lysimeter test of a 1.5-m-thick Warden silt loam barrier showed that drainage did not occur as mass flow under 3X long-term precipitation (i.e., 480 mm yr^{-1}) in the lysimeters with vegetation (Fayer and Gee 2006; Gee et al. 1993). The test at the FLTF showed that the 1.5-m-thick barrier can store at least about 500 mm of water. The observed 518 mm is consistent with the findings at the FLTF. It is 98% higher than the field capacity (262 mm) and is 39% larger than the estimated value of 373 mm (assuming a water entry pressure of -0.15 m, or water content of 0.32 m^3m^{-3}) for the ETC barrier, based on the equilibrium of water pressure (e.g., Khire et al. 2000).

Vertical neutron logging at six stations in March, when the barrier was wettest during WY95, WY96, and WY97 (Figure 3.4), indicated that the water content at 1.8 m below ground surface was generally below 0.25 m^3m^{-3} (which is equivalent to a water pressure of about -0.4 m), except at the west end in 1997. Horizontal neutron logging at 1.9 m below ground surface (see Appendix H) also showed that water content was no more than 0.25 m^3m^{-3}. The high water content at the west end in 1997 (Figure 3.4c) was not observed by the horizontal neutron logging, suggesting this high water content might happen locally. The measured h at the 1.75 m depth (z) generally was less than -0.5 m, except h = -0.23 m at station S1 in March 1997. All of these results indicate that, although soil water increased near the bottom of the storage layer, the soil wetness near the bottom was still much lower than the near-saturation value needed to initiate water movement through the capillary break. Consequently, very little drainage occurred in spite of the enhanced precipitation. Based on the water content measurements (Figure 3.1a) and drainage rates (Figure 3.3), it appears that only minimal water flow (<0.18 mm yr^{-1}) across the capillary break occurred for the 3 years with enhanced precipitation. It is pointed out that the total winter precipitation (including irrigation) for WY96 and WY97 was very high, such that this magnitude of precipitation has a very low probability of occurring (0.001 times) during the 1000-year design life.

Water Storage - Water storage was generally the highest near the end of the winter season during each year. During the 19-year monitoring period, the maximum water storage occurred in late March of 1997 on the irrigated north section, and the mean with $\pm 1\sigma$ was 517.5±85.8 mm, which is less than the estimated 600 mm storage. From WY99 to WY12, the average storage with $\pm 1\sigma$ was 194.2±20.2 mm for the north section and 189.4±23.5 mm for the south section, meaning that only a very small fraction of the storage capacity was used, even at the wettest time. According to Zhang (2015), the Warden silt loam has an average plant unavailable water content of 0.058 m^3m^{-3}, which translates to 116 mm of storage for a 2-m-thick storage layer. These results indicate that, with near-normal precipitation, a barrier much thinner than 2 m would sufficiently store all winter precipitation.

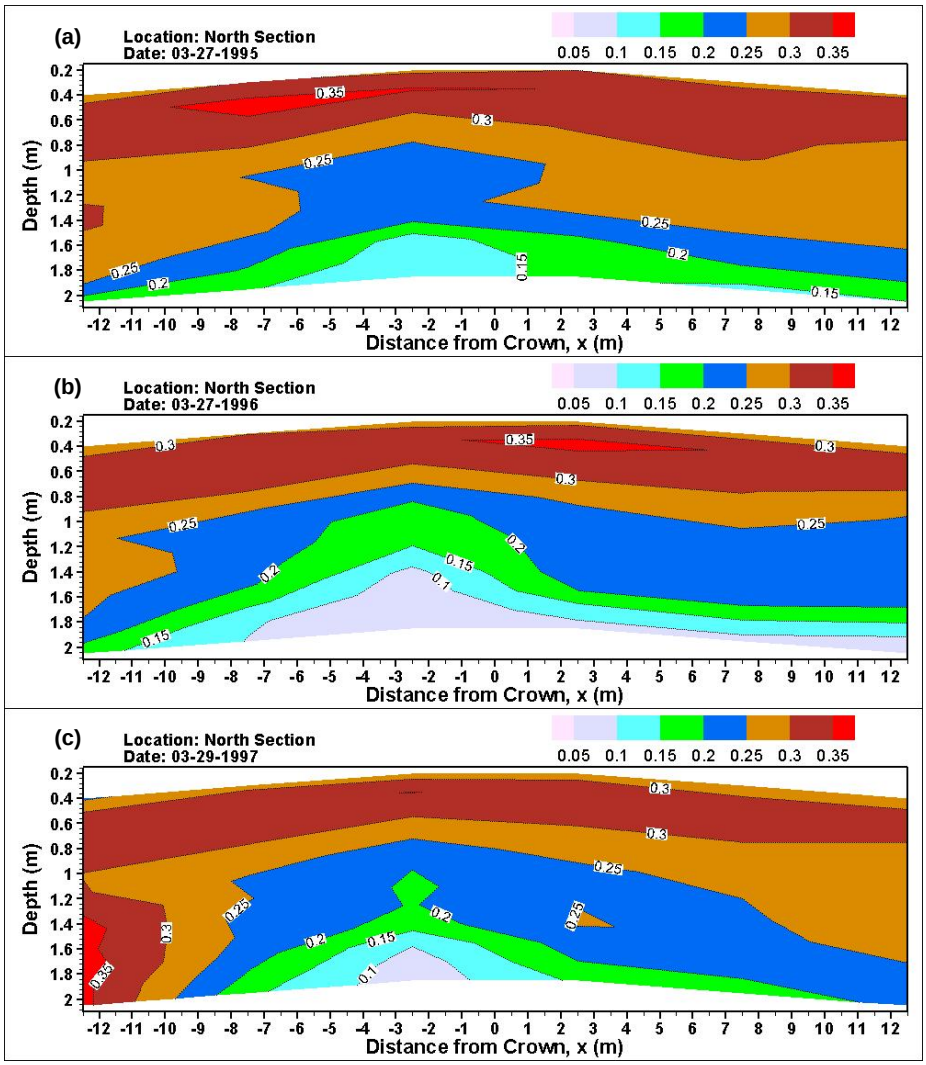

Figure 3.4. Average soil water content of six monitoring stations, based on NP measurements, of a west-east cross-section at the irrigated north section in late March, when the barrier was the wettest in WY95, WY96, and WY97.

The water storage findings have an important implication for determining the appropriate thickness (L) of the storage layer. Before construction of the surface barrier, the required storage capacity of the ETC barrier was estimated based on annual precipitation. Field data demonstrate that the precipitation in the summer season does not contribute to the storage at the PHB. During the winter season, all but about 47 mm of the precipitation infiltrates the barrier. Hence, it is more proper to determine the required storage capacity based on winter precipitation instead of annual values. Based on the analysis of winter precipitation, the estimated maximum P_w with a probability of 0.1% (approximately once in 1000 years) is 253 mm. Assuming that winter evaporation is at least 20 mm and the storage capacity is uniform over the whole thickness of the storage layer, the test at the PHB suggests that a 1-m-thick barrier has 201 mm of available storage. The 1000-year-return P_w of 253 mm would need a 1.2-m-thick barrier. The 100-year return P_w of 205 mm would need a 0.9-m-thick barrier. The estimated median P_w of 96 mm can be stored in a 0.4-m-thick barrier. Hence, for an ETC barrier that can store the 1000-year-return P_w, the lower portion of the barrier will have low water content for most of the years.

Evapotranspiration - The estimated ET during winter (ET_w) averaged 47.0 mm, with a σ of 23.1 mm, and showed no obvious trend (Figure 3.5a) from WY95 to WY13. The lack of correlation between ET_w and P_w suggests that ET_w was nearly independent of P_w. Because of the low temperature and near-dormant vegetation in the winter season, transpiration is nearly zero. Nevertheless, some water can be lost to the atmosphere through evaporation and occasional sublimation. Wallace (1977) estimated a 38.7-mm potential evapotranspiration (PET) for the winter season at Hanford using the Thornthwaite-Mather method (Thornthwaite and Mather 1955). The winter PET is about 38% of the average winter precipitation at Hanford, suggesting ET_w is primarily controlled by the winter PET, and an average of 62% of P_w is stored in the barrier. Because temperature, radiation, and wind, the main factors that determine PET, vary less than precipitation across years, ET_w had a relatively small variation across years and was nearly constant.

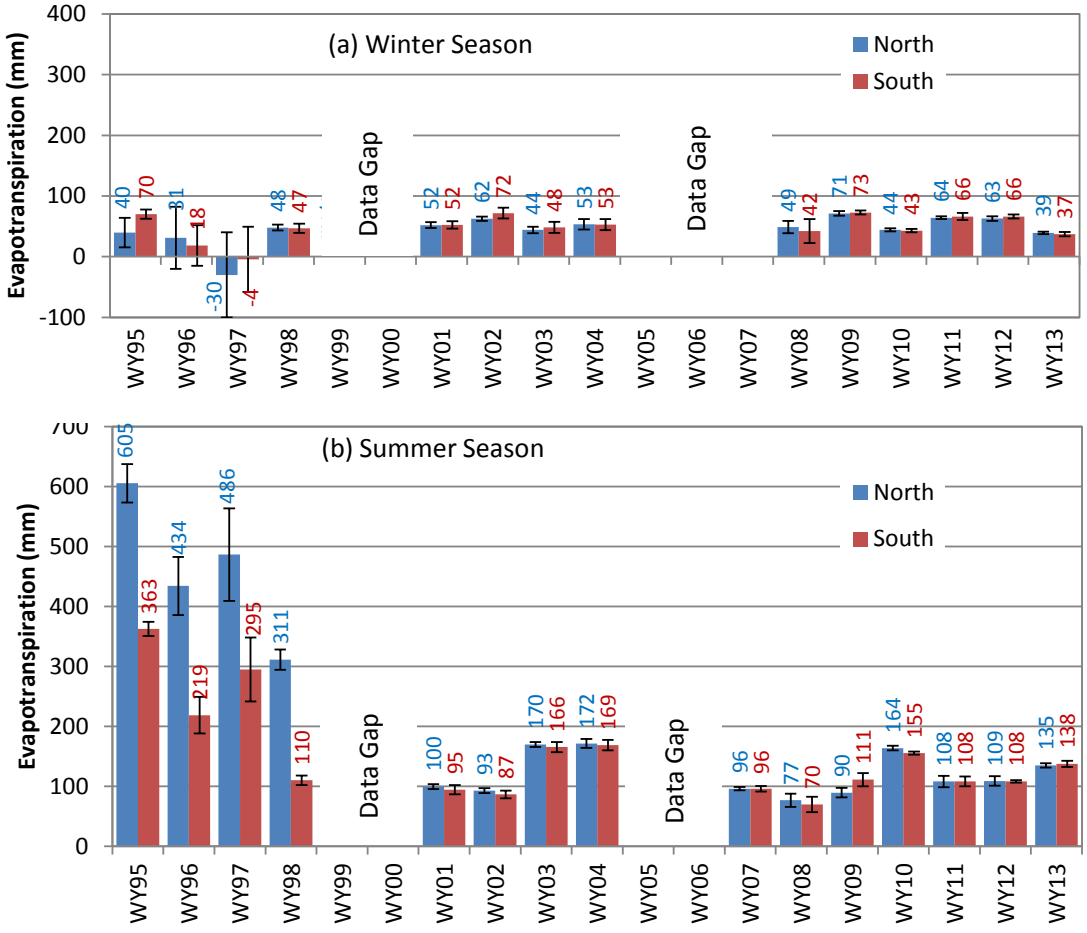

Figure 3.5. Average evapotranspiration of six monitoring stations in (a) the winter season and (b) the summer season. The numbers indicate the actual ET at the corresponding WY. The standard deviation was calculated among the six monitoring stations of each section and is shown as a capped vertical line at each bar. The data gaps were due to a shift in funding priorities and funding shortfalls.

3.1.3 Hydrology in the Summer Seasons

In the summer seasons, with a high air temperature, low precipitation, and high PET, the barrier had a net loss of soil water via ET as shown in Figure 3.1. The stored water was released into the atmosphere when ET exceeded precipitation. The soil water in shallow soil (roughly from 0 to 0.4 m deep) was released the quickest because both evaporation and transpiration took effect. When there was plant-available water stored at larger depth (e.g., from WY95 to WY98, Figure 3.1), the soil water at the intermediate depth (roughly from 0.4 to 1.2 m) was removed almost uniformly; the soil water at large depth (roughly below 1.2 m) was lost the slowest, possibly because there were relatively fewer roots in the deep soil.

In contrast to ET_w, the summer ET (ET_s) shows a clear trend with time, with much higher values from WY95 to WY97 for both the north and south sections than in other years (Figure 3.5b). The primary reason is that meteoric precipitation in these years was much higher than usual and was categorized as extremely to moderately wet. This also was the period of the enhanced precipitation test in the north section.

Figure 3.6 shows the monthly contribution of the soil water to *ET* (ET_m^s) from WY95 to WY97. There were not enough observations to calculate the monthly ET for years from WY98 to WY13. In WY95, ET_m^s first increased with time, reached the maximum in July, and then decreased in both the north and south sections. However, in WY96 and WY97, ET_m^s was nearly unchanged from April to June and then decreased with time. The different response in WY95 was probably because the vegetation, which was planted in November 1994, was small and hence the seedlings probably had limited need for soil water. As the plants grew, the low ET_m^s in April and May led to a high amount of available soil water and hence a very high ET_m^s in July 1995. The decrease of ET_m^s started in June or July, when the ET process was constrained by the supply of soil water. For all cases, ET_m^s approached nearly zero in September every year, meaning there was not much soil water available for the vegetation. In October, some negative ET_m^s values meant that the barrier soil had a net gain of water from precipitation in some years.

These results indicate that ET released most of the available water from roughly April to June at a rate controlled by the weather and plant conditions. ET released most of the remaining available water from July to September, but at a lower rate, possibly controlled by soil conditions. The results indicate that ET processes were strong enough to release to the atmosphere nearly all the stored water in the 2-m-thick storage layer even before the end of the summer season.

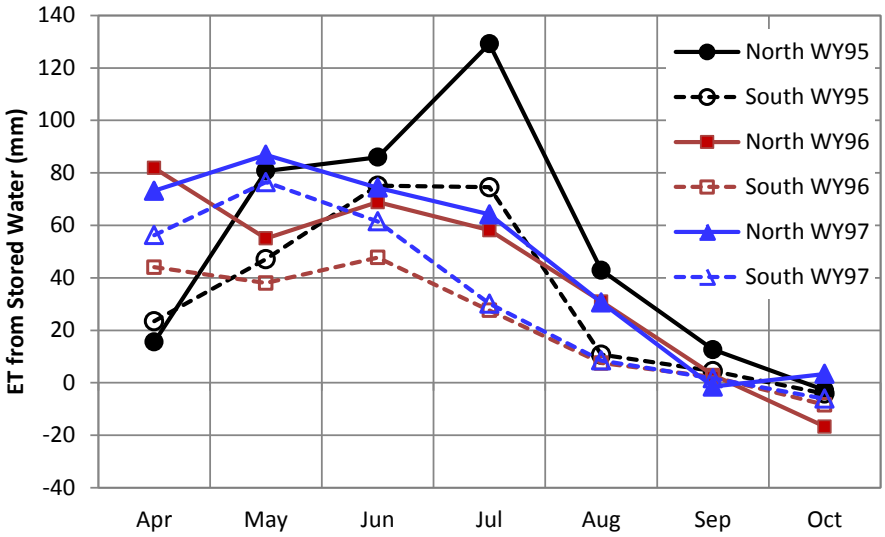

Figure 3.6. Monthly contribution of soil water (averaged over six monitoring stations) to ET during the summer seasons from WY95 to WY97.

3.1.4 Water Diversion by the Sloped Barrier Surface

Lateral water movement away from the crown but within the side boundaries of the ETC barrier is considered water diversion. The lateral water flow may occur above or below the 2% sloped barrier surface. The water content distribution in the west-east cross-section of the irrigated north section from WY95 to WY97 (Figure 3.4) shows that in late March of each of the 3 years, when the irrigated section was the wettest, there was a relatively low water content zone in the lower portion of the barrier profile near the crown. In contrast, water contents near the edges were higher, likely due to water diversion. To confirm that the observed water diversion was not caused by measurement bias, the HDU-measured *h* at the 1.75-m depth on March 29 of the 3 years was analyzed. The soil near the crown showed more negative *h* values, indicating a relatively drier condition. The horizontal NP logging at the 1.9-m depth also confirmed the existence of the drier zone below the crown. In the ambient south section, this diversion process was less obvious. These results indicate that the water-diversion process due to the 2% slope enhanced the barrier's capability to protect the area near the crown against heavy rainstorms.

3.1.5 Impacts of Controlled Fire on Hydrology

The impact of the controlled fire in September 2008 on soil water processes was delineated by comparing the water content distribution between the north (Figure 3.2b) and south (Figure 3.7) sections. The results indicate that the ET rate before the stored water was used up was slightly less in the burned section than it was in the unburned section. However, the lower ET in the burned section appeared high enough to release the stored water to the atmosphere, albeit over a slightly longer period. Neither section had detectable drainage, suggesting that the barrier performed well after the fire eliminated the vegetation. In a separate test of a 1.5-m-thick silt loam barrier without vegetation at the FLTF, the average drainage rate was no more than 0.2 mm yr^{-1} from 1987 to 2004 under ambient precipitation, and was no more than 16.4 mm yr^{-1} from 1987 to 2002 under the enhanced (2X before 1990 and 3X thereafter) precipitation (Fayer and Gee 2006). These results indicate that a wildfire would not compromise barrier performance under near-normal precipitation conditions.

Annual precipitation during the monitoring period after the fire (WY09 to WY13) was near normal. If extremely wet years had followed the fire, barrier performance might have been different. A comparable scenario was the simulated 1000-year-return, 24-hour rainstorm in March 1995, when the vegetation planted in November 1994 was still very small and the barrier surface was nearly bare. During this simulated rainstorm, 1.79 mm of runoff containing approximately 72 kg ha^{-1} of soil was observed.

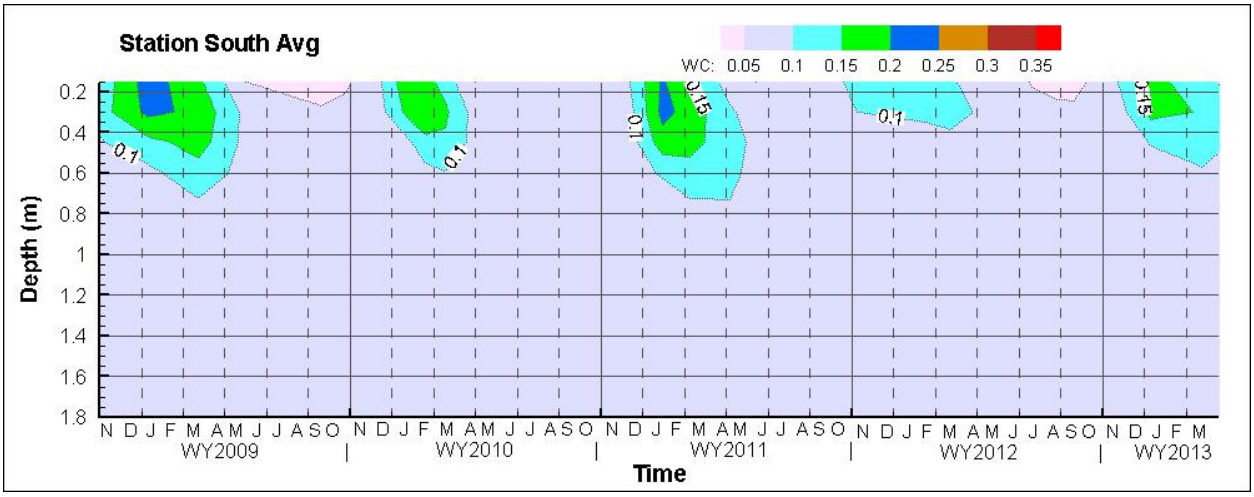

Figure 3.7. Average soil water content of six monitoring stations for the south section from WY09 to WY13.

3.1.6 Relationship between Water Storage, Transpiration, and Precipitation

Analysis of monitoring results revealed that the storage decrease in the summer season ($-\Delta W_s$) was nearly the same as the storage increase in the prior winter season (ΔW_w) of the water year (Figure 3.8):

$$\Delta W_w = -\Delta W_s \quad [3.1]$$

This result is not surprising because drainage was always less than 0.018 mm yr^{-1}, the runoff was generally negligible except in FY95, and the ET process in the summer season tended to use nearly all the water stored in the winter season, leaving only the tightly bound water on soil particles. These conditions are the essence of an ET barrier. If only a fraction of the stored water had been released, the rest would have been carried into the next winter season. If continued year after year, gradual accumulation of stored water could lead to drainage. However, none of the results from the PHB suggest that this will occur.

According to the law of mass conservation, ΔW_w cannot be more than P_w, assuming there is no run-on water. Field data suggested a near-constant winter ET (Figure 3.5a). Along this line, higher precipitation probably does not contribute much to ET_w, but infiltrates into the soil. Thus, the relationship between ΔW_w and P_w (Figure 3.9) was described by

$$\Delta W_w = P_w - ET_{w0} \quad [3.2]$$

where ET_{w0} = 47.0 mm is the average ET during the winter season. Note that runoff was assumed to be negligible in Eq. [3.2]. Should runoff be considerable for an ET barrier of different design or for different site conditions, the contribution of runoff needs to be re-evaluated.

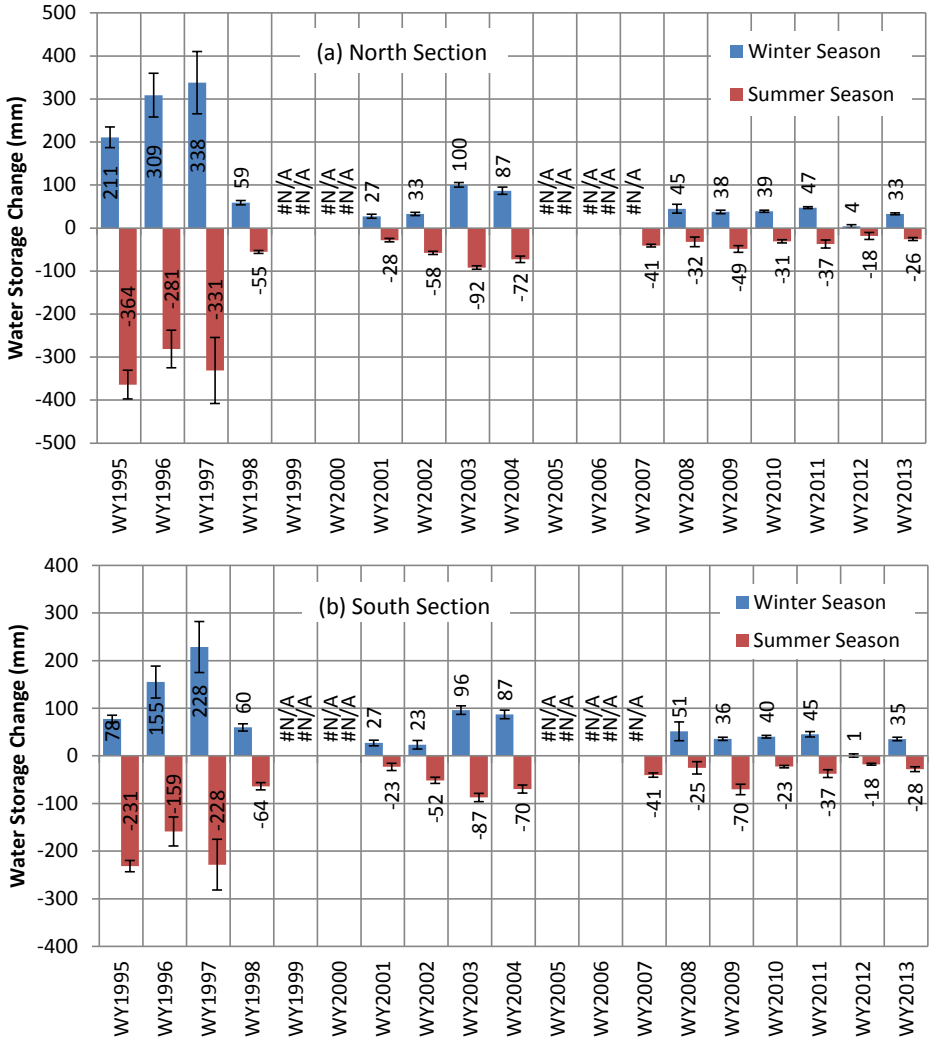

Figure 3.8. Soil water storage change (averaged over six monitoring stations) during the winter season (November to March) and the summer season (April to October) for (a) the north section of the barrier and (b) the south section of the barrier. The standard deviation was calculated among the six monitoring stations of each section and is shown as a capped vertical line at each bar. #N/A means there is no data or insufficient data to calculate storage change.

Based on Eqs. [3.1] and [3.2], the relationship between ET_s and P_a ($P_a = P_w + P_s$) is therefore

$$ET_s = P_a - ET_{w0} \quad [3.3]$$

According to Eq. [3.3], in an average water year, about 47 mm of precipitation is released into the atmosphere in the winter season and the rest is released in the summer season. To demonstrate the use of Eq. [3.3], the predicted ET_s for both the north and south sections is shown in Figure 3.10 as a function of WY precipitation. Generally, Eq. [3.3] yielded good predictions of ET_s, with slight underestimation when P_a is high (e.g., P_a > 250 mm).

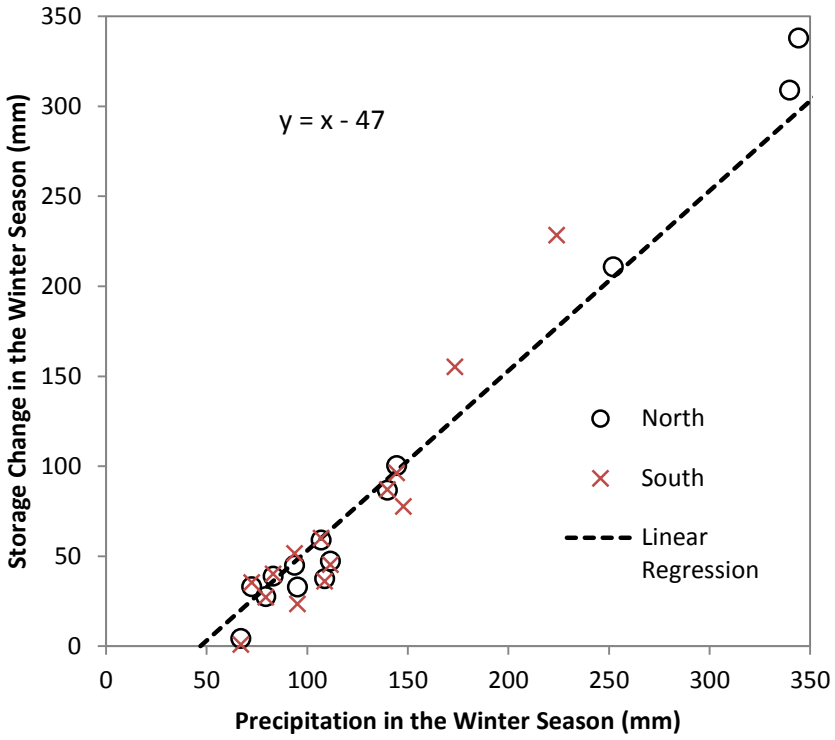

Figure 3.9. Water storage as a function of precipitation received in the winter season.

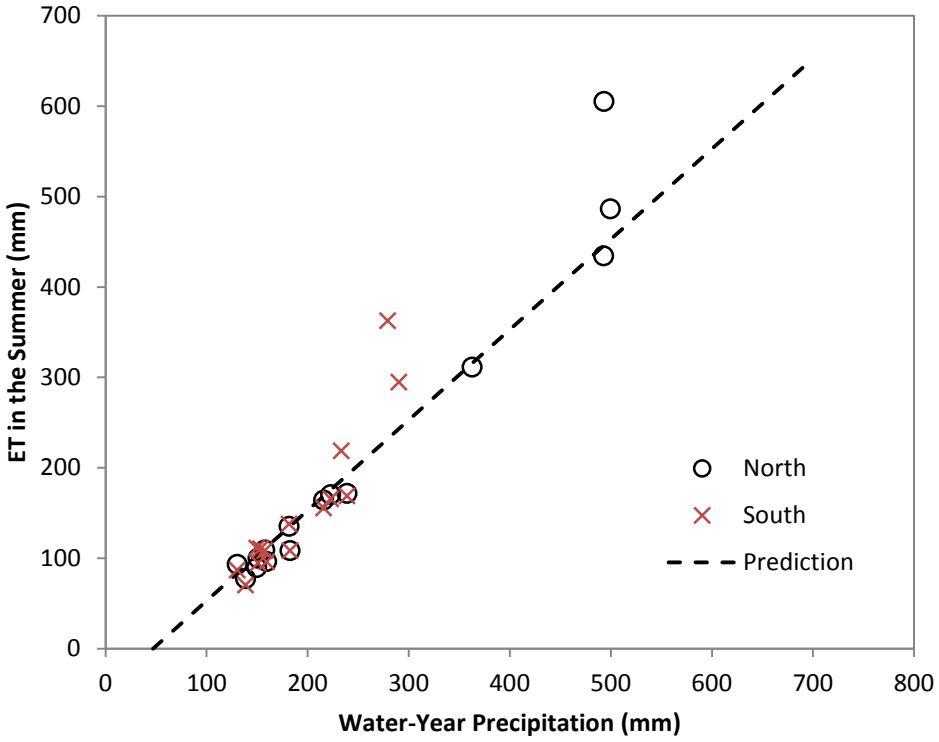

Figure 3.10. Observed and predicted summer ET in the north and south sections of the barrier.

3.2 Hydrology at the Transition Zones, Side Slopes, and AC Barrier

This section discusses the temporal variation of soil water in the gravel side slope, along with the impacts of side slopes and the AC barrier.

3.2.1 Seasonal Variation of Soil Water in the Gravel Side Slope

Water storage in the top two meters of the gravel side slope from 1995 to 2013 varied between about 118 and 239 mm (Figure 3.11). Although the north section was irrigated to an average precipitation of 495.4 mm (approximately 3X the average precipitation) from WY95 to WY97, there was little difference in water storage between the irrigated and the non-irrigated sections during winter seasons, meaning the maximum storage capability of the gravel side slope was reached. Water storage in the irrigated north section in the summers of 1996 and 1997 was slightly higher than it was in the non-irrigated south section.

Compared to the gravel side slope, the field-averaged 2-m water storage in the ETC barrier varied between 111 and 518 mm. Although the high values for the gravel side slope were much lower than those for the ETC barrier, the low values were nearly identical. This indicates that soil type has a strong influence on storage capacity and drainage, and hence the construction material for the side slope should be selected with great care.

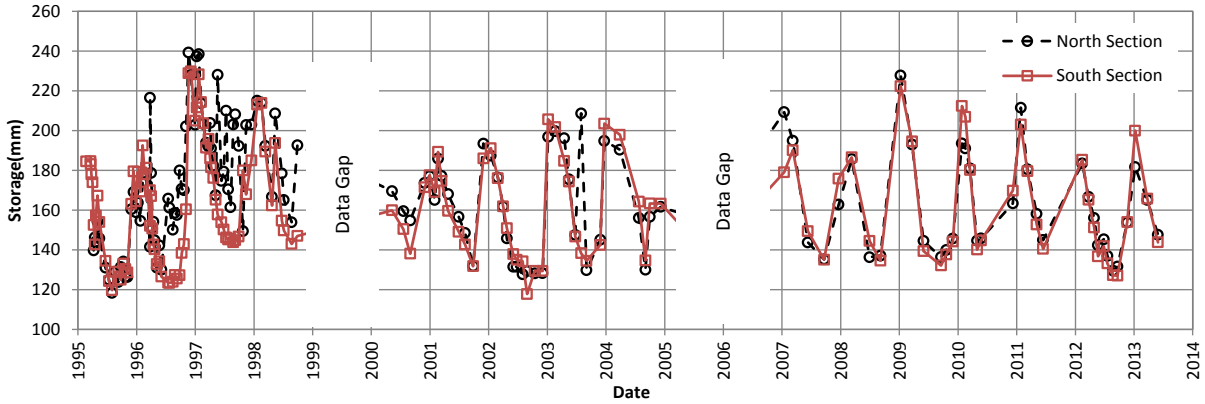

Figure 3.**11**. Water storage in the top 2 m of the gravel side slope.

3.2.2 Drainage through the Side Slopes

Figure 3.12 compares the rates of WY drainage through the side slopes. Because the drainage measuring system was not ready until March 1995, the drainage for WY95 is a cumulative value from March to October. The maximum drainage under enhanced precipitation was 283.0 mm yr^{-1} for the riprap side slope and 231.1 mm yr^{-1} for the gravel side slope. The maximum drainage under natural precipitation was 143.1 mm yr^{-1} for the riprap side slope and 171.4 mm yr^{-1} for the gravel side slope. All maxima occurred in WY97, which had the highest precipitation (290 mm, 1.7X the average) during the monitoring period. During the 3-year enhanced precipitation condition, the average P_a over the north section was 495.3 mm yr^{-1}; the average drainage rates were 130.7 mm yr^{-1} (i.e., 26% of P_a) at the gravel side slope and 139.9 mm yr^{-1} (i.e., 28% of P_a) at the riprap side slope. During the same period, under ambient

condition, the average P_a was 367.6 mm yr^{-1}; average drainage rates were 83.5 mm yr^{-1} (i.e., 23% of P_a) at the gravel side slope and 61.7 mm yr^{-1} (i.e., 17% of P_a) at the riprap side slope.

From WY98 to WY12, natural precipitation (from 0.81X to 1.32X average precipitation) was near normal, and hence the drainage rate was relatively low, with an average of 12.4 mm yr^{-1} (i.e., 0.067P_a) for the gravel side slope and 13.1 mm yr^{-1} (i.e., 0.072P_a) for the riprap slope. These results indicate that precipitation played a critical role in the drainage rate through the side slopes.

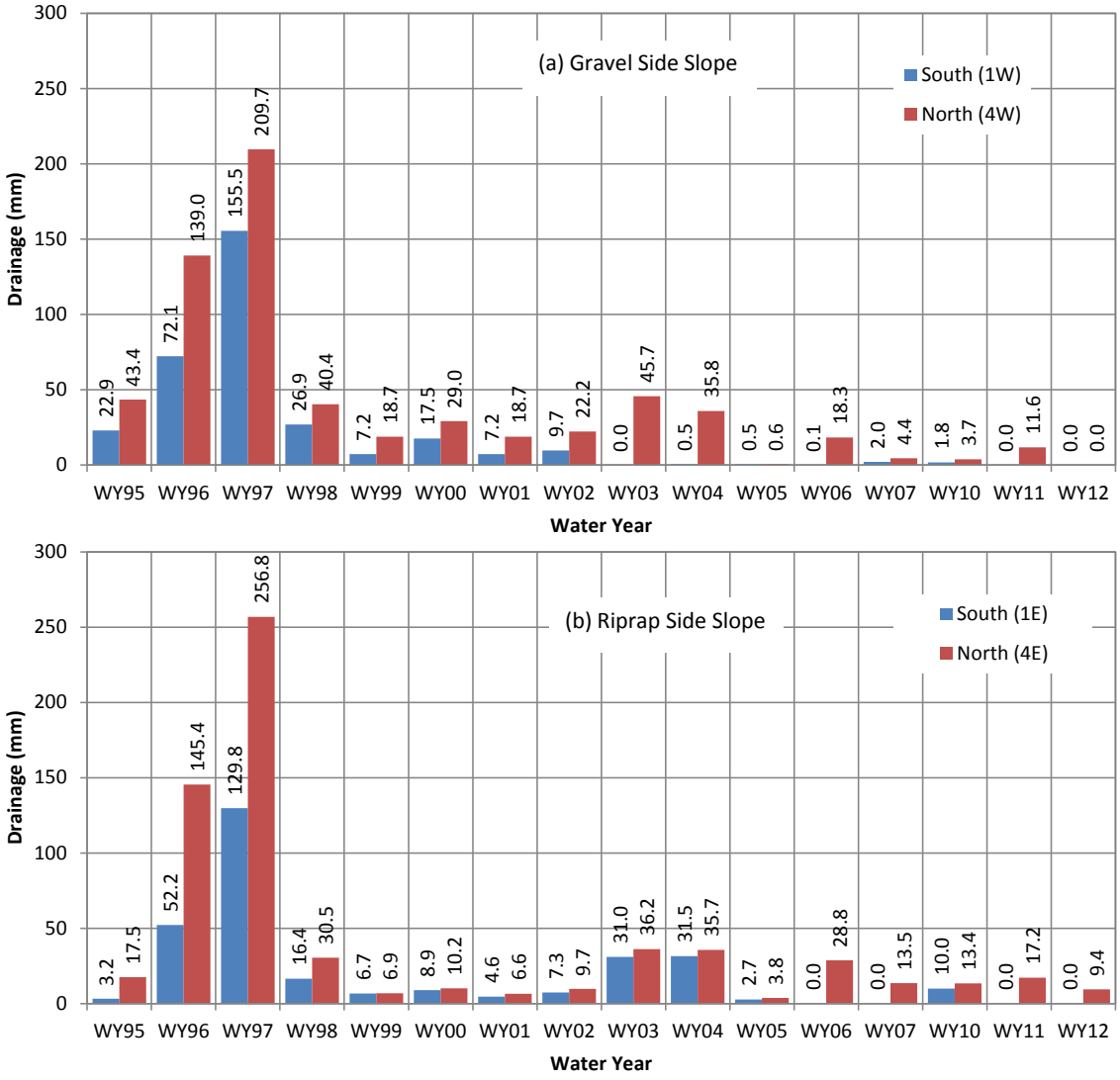

Figure 3.12. Annual drainage through (a) the gravel side slope and (b) the riprap side slope. The north section was irrigated from WY95 to WY98. The drainage for WY95 is from March to October.

Figure 3.13 shows the relationship between WY drainage rate and annual precipitation. For both types of side slopes, when P_a was less than about 140 mm yr^{-1}, the drainage approached zero, indicating nearly all precipitation was first stored in the side slope soil and then released into the atmosphere via ET for the gravel side slope and via evaporation for the riprap side slope. When P_a was greater than about 140 mm yr^{-1}, roughly 46% (43% for the gravel side slope and 49% for the riprap side slope) of the

additional annual precipitation became drainage. In other words, when $P_a \leq 140$ mm yr^{-1}, all the precipitation becomes ET; when $P_a > 140$ mm yr^{-1}, about 54% of the additional precipitation becomes ET, i.e., ET $\approx 140+0.54(P_a - 140)$. For example, for an average year with 172 mm yr^{-1} precipitation, the estimated drainage through the side slopes is 14.7 mm yr^{-1} (8.6% of P_a) and ET is 157.3 mm yr^{-1} (91.4% of P_a). These results indicate that ET released most of the precipitation back to the atmosphere despite the low storage capacity of the side slopes.

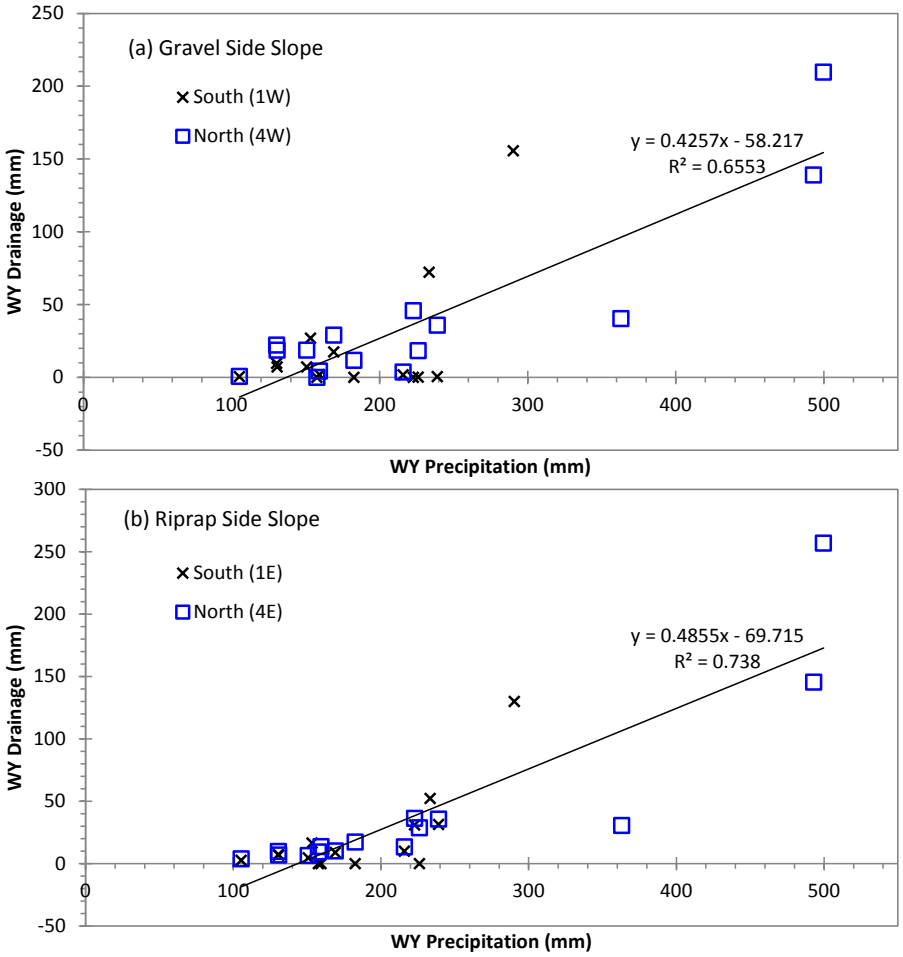

Figure 3.13. The relation between drainage and precipitation for (a) the gravel side slope and (b) the riprap side slope. The lines indicate linear regressions. The observations from WY95 are excluded because the measuring system was not completely ready.

3.2.3 Flow at the Transition Zones

Based on the barrier design, the silt loam-sand interface at the side boundaries of the ETC barrier (see Figure 2.4b) forms a capillary break, preventing the capillary water in the silt loam from entering the coarser materials unless the silt loam is nearly saturated. Because the storage layer has a shape similar to an inverted isosceles trapezoid, the silt loam is thinner near the boundaries than it is inside the layer. As a result, the silt loam above the slanted capillary break has less storage capacity.

Different from inside the ETC barrier, where flow tends to be one-dimensional vertically, flow in the silt loam near the boundary is expected to be multi-dimensional and likely migrates both vertically and laterally because of the slanted interface between silt loam and sand. Theoretically, after the infiltrating water reaches the slanted side capillary break, the water is expected to move downward along the slanted boundary. After arriving at the bottom of the silt loam layer, the infiltration water tends to move laterally into the silt loam because of the capillary break at the bottom. When there is enough water at the bottom to overcome the capillary break, some water will enter the underlying coarser layers and become drainage.

Figure 3.14 shows water content measurements at the bottom of the silt loam layer in time-space planes along two lateral monitoring lines, one for the north section and the other for the south section. From WY95 to WY97, there was a seasonal variation of water content at the bottom of the silt loam in the irrigated north section (Figure 3.14a), indicating the infiltration water reached the bottom of the silt loam layer in the winter seasons. The increase in water content during the winter seasons was much more pronounced near the boundaries (marked by dashed lines in Figure 3.14) than in the middle of the silt loam layer. For instance, along the west-to-east line for north section (Figure 3.14a) on March 29, 1997, the maximum was 0.238 m^3m^{-3} near the west boundary, 0.201 m^3m^{-3} near the east boundary, and 0.069 m^3m^{-3} in the middle, meaning infiltration water accumulated near the slanted side boundaries of the barrier. The higher water content near the side boundaries (Figure 3.14a) also suggests that the infiltration water moved laterally toward the inside of the storage layer by as much as about 10 m in the irrigated north section in WY95 and WY97. However, the water content was still much less than the estimated breakthrough water content of 0.320 m^3m^{-3}, indicating no drainage occurred across the capillary break at the bottom of the silt loam layer. In the non-irrigated south section, the infiltration water reached the bottom of the storage layer near the side boundaries only in the spring of 1997, when the winter precipitation was 2.2X the average. From 1998 to 2013, the WY precipitation was moderate wet for only 1 year and near normal or less in other years. Thus, the water content at the bottom of the silt loam layer stayed at low θ (< 0.075 m^3m^{-3}) almost all the time (Figure 3.14a, b), suggesting the infiltration water never reached the bottom of the silt loam layer, even at the side boundaries, for these years. The above results show that the moisture accumulation along the silt loam boundaries was evident only under the enhanced (3X average) precipitation condition. No moisture accumulation was observed under natural precipitation conditions.

During the monitoring period, WY drainage rates from the transitional plots exceeded the 0.5 mm yr^{-1} design criterion only in five instances. Four instances (7.5 mm yr^{-1} or less) occurred in the irrigated section and the fifth (i.e., 0.9 mm yr^{-1}) occurred in the ambient east boundary in WY97 with a 2.2X winter precipitation. The maximum drainage rate was 7.5 mm yr^{-1} and occurred in the irrigated northeast boundary (5E in Figure 2.8) in WY97, indicating lateral flow. The maximum drainage rate through the side boundaries was much greater than the maximum drainage rate through the silt loam (0.18 mm yr^{-1}), but much less than the maximum rate through the side slopes (283.0 mm yr^{-1}) reported above. From WY98 to WY13, the drainage rate through the side boundaries was no more than 0.002 mm yr^{-1} when the winter precipitation was no more than 1.4X the long-term average.

The above results indicate there is an edge effect on the flow in the ETC barrier, and that the strength of this effect depends on the water storage near the barrier edge. Hence, the horizontal extent of an ETC barrier needs to be larger than that of the underlying waste zone. For the worst-case scenario during the 3X enhanced irrigation test, the distance of lateral flow was about 10 m. Fayer (1987) conducted a series of numerical simulations and found that a 10-m overhang was sufficient to mitigate the edge effect of a

barrier over a loam sand. They also pointed that a finer soil beneath the barrier would have stronger edge effect.

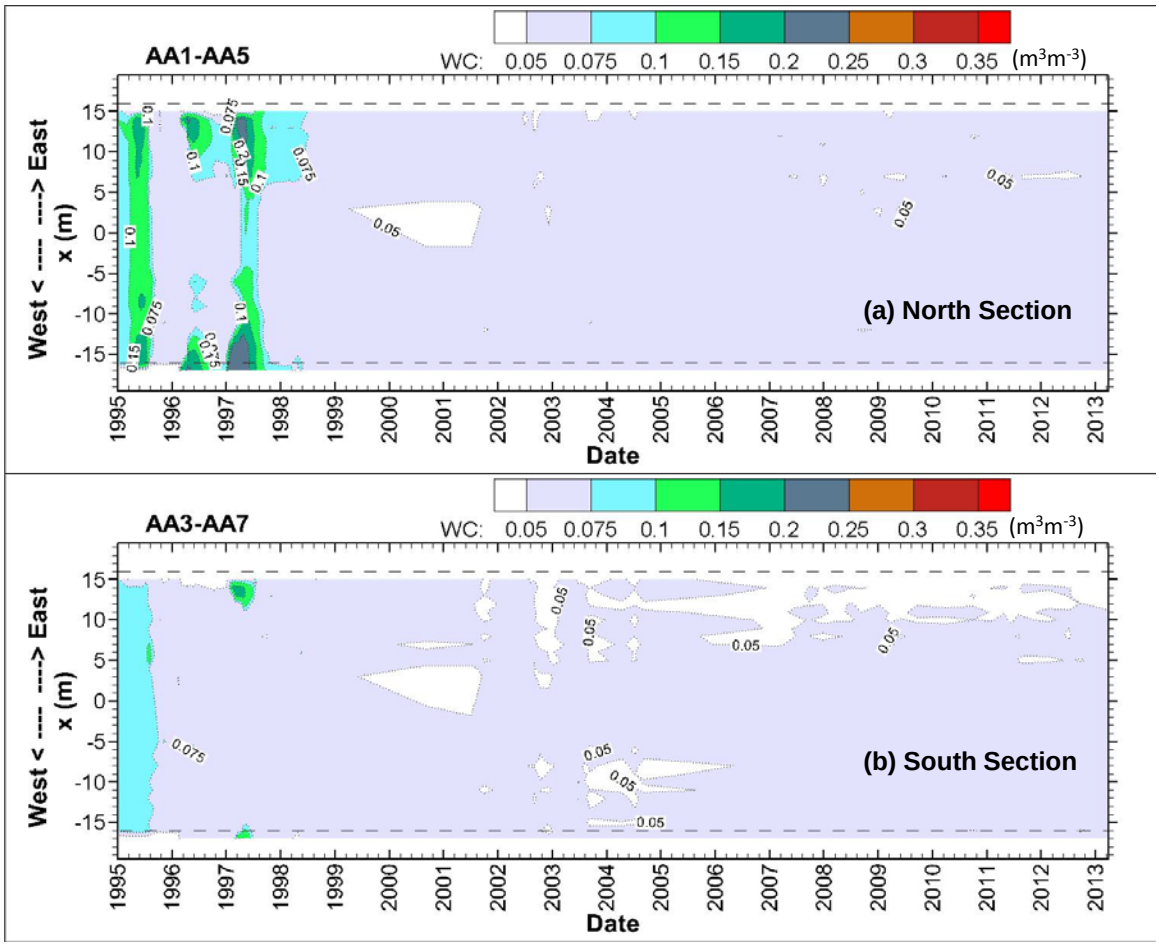

Figure 3.14. Soil water content near the bottom of the silt loam in the time-space plane along the horizontal lines (a) in the north section and (b) in the south section. The edges of the silt loam layer at the ground surface were at x = -19.3 m and x = 19.3 m and those at the bottom of the silt loam layer at x = -16 m and x = 16 m (marked by horizontal dashed lines).

3.2.4 Effects of Asphalt Concrete

The average water content from 26 observations below the AC barrier (excluding the outer 6 m, i.e., x = 0 to 26 m) is illustrated in Figure 3.15. From 1995 to about 2000 there was a trend of decreasing water content, but the changes were generally very small (< 0.005 m^3m^{-3}) because initial water content at the time of construction was relatively low (about 0.10 m^3m^{-3}). The trend of decreasing water content suggests the soil was losing water, likely because of downward movement of antecedent soil water due to gravity. If there was any water input from above during this period, it was less than the water loss from this zone. From 2000 to 2013, the water content stayed relatively stable, meaning the soil water was nearly immobile. Note that the neutron counter and probe sleeve for the NP used were replaced by new parts in April 2003, and this might have caused a slight (< 0.005 m^3m^{-3}) increase in observations starting in early 2003.

The soil water pressure below the AC barrier, measured at the northeast section with six FGBs, was almost always less than -300 m. Despite the large uncertainty of FGB-measured *h* (about a factor of 3; see Appendix F), the measured *h* was comparable to the commonly recognized permanent wilting point of -150 m (Or and Wraith 2001; Romano and Santini 2002). The cumulative percolation through the AC barrier, measured with the pan lysimeter, was only 0.14 mm (average 0.012 mm yr^{-1}) over a period of about 12 years. The percolation through the AC barrier is very low compared with the design criterion of 0.5 mm yr^{-1}.

In summary, stable or decreasing water content, stable soil water pressure, and very low percolation rate all demonstrate negligible water percolation through the AC barrier over the 19-year monitoring period. However, pan lysimeter data suggest that the FAA-coated AC barrier should be permeable.

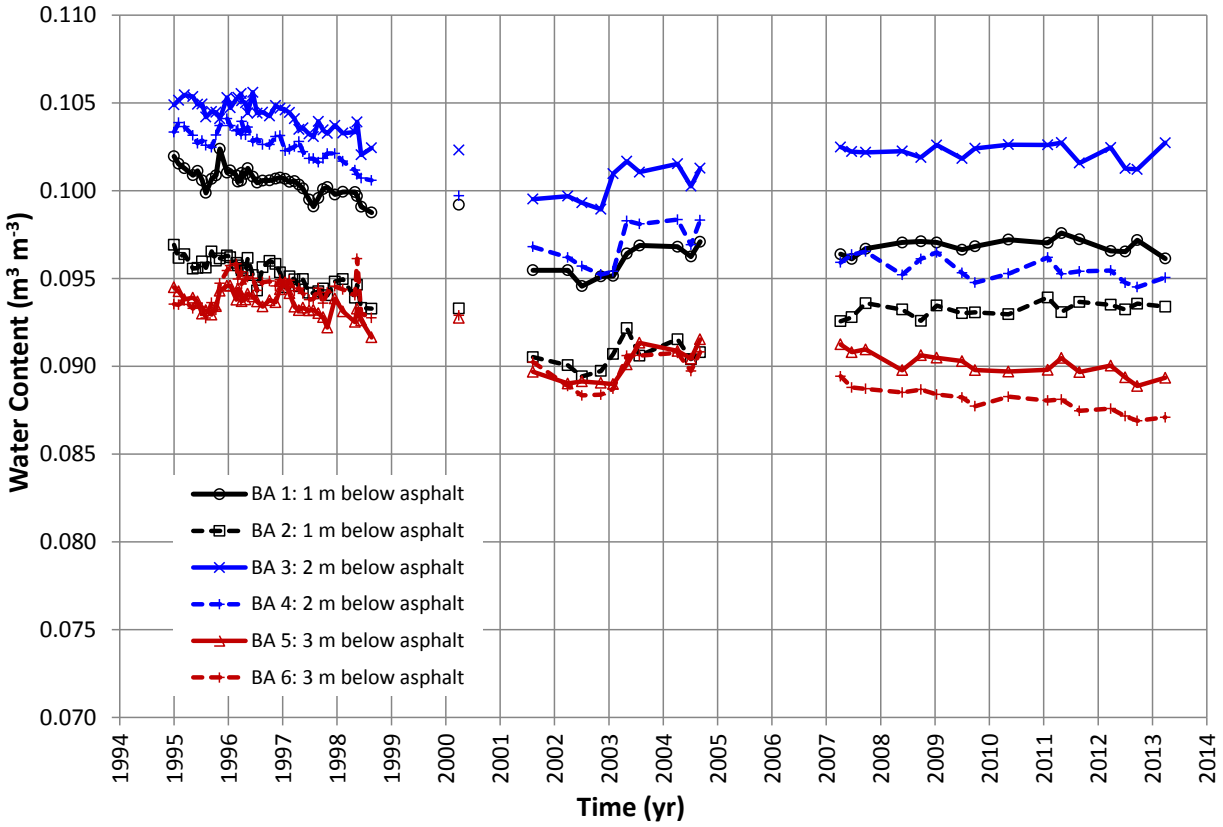

Figure 3.15. Average water content from x = 0 to 26 m. (x is the distance from the centerline of the barrier. The edge of the AC barrier is at x = 32 m.)

3.3 Structural Stability

This section presents the observed results of erosion, elevation changes of the AC barrier and barrier surface, displacement of the riprap side slope, and animal activities.

3.3.1 Wind and Water Erosion

Vegetation obstructs air flow above the ground surface. Vegetation's effectiveness at protecting the ground surface against wind erosion is a function of surface roughness, which is the height at which wind velocity is reduced to zero. Higher surface roughness means better protection against wind erosion. Surface roughness generally increases with the height and/or coverage of vegetation. Based on the monthly average wind speed profile and Eq. [2.2], estimates of barrier surface roughness were made for each month and are shown as points in Figure 3.16.

From the planting of vegetation on the barrier in November 1994 until about April 1995, the surface roughness was near zero. After May 1995, when the vegetation was established, the surface roughness varied seasonally in each year, with higher values generally in the summer season. This is most likely due to increased leaves and/or flowers of sagebrush during the growing season and higher coverage of annuals and limited bi-annuals. Hence, the vegetation had a greater ability to reduce wind in the summer. This implies that, for a given year, the barrier was more resistant to wind erosion in the summer season than in the winter season. Across different years, the low values of z_0 at stations 1 and 2 (Figure 3.16) on the barrier surface (roughly in early spring) increased from near zero in 1995 to about 0.05 m in 1997. This increase suggests that the barrier was likely well protected from wind erosion year round in 1997. Additionally, the stronger wind in late spring and summer coincided with higher surface roughness. As a result, the strong wind in the spring/summer was offset by higher roughness of the barrier surface. The results indicate that the vegetation increased the height of zero wind velocity above the barrier surface and suggest reduced possibility of wind erosion.

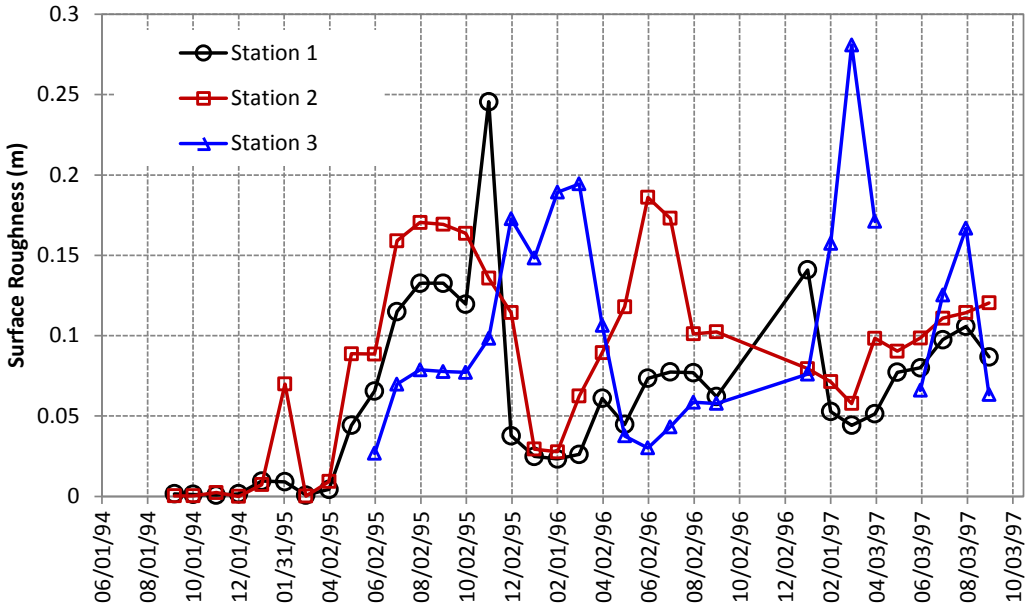

Figure 3.16. Barrier surface roughness based on monthly average wind profiles.

During the simulated 1000-year-return, 24-hour rainstorm (69.4 mm of water over an 8-hour period) on the newly vegetated surface in March 1995, erosion occurred on the surface of the barrier (Gee et al. 1995). Initial sediment concentrations collected during the test were approximately 7 g L^{-1}. This amount fell to approximately 1 g L^{-1} at the end of the water application. The results showed a decreasing pattern of erosion, indicating less soil was eroded, possibly because more pea gravel was exposed. The estimated soil erosion was 72 kg ha^{-1} in total. No soil erosion was observed during the rest of the monitoring period, including during the simulated 1000-year-return rainstorms in 1996 and 1997, during the snowmelt event in the January 1997, and after the controlled fire in 2008. The primary reasons for the lack of runoff and erosion were the sufficiently high soil hydraulic conductivity and the increased coverage of vegetation on the ground surface. The 15 wt% pea gravel in the top 1 m of the barrier protects the barrier surface from erosion because of its weight, and hence protects against the formation of runoff channels such as rills or gullies (Gilmore and Walters 1993). As an analog, a similar mixture of gravel appears to the primary reason for longevity of natural bergmounds formed from ice-rafted glacial debris about 13,000 years ago (Bjornstad 2014; Chamness 1993; Fecht and Tallman 1978).

3.3.2 Barrier Settlement and Compression

From 1994 to 2012, the average elevations with ±1σ of the two settlement markers were 201.956±0.007 m and 201.685±0.012 m, respectively, without clear trends over time (Figure 3.17). For both markers, the elevation variations were between -0.03 and 0.02 m, indicating near-zero settlement. Considering that the small variations were probably measurement noise, the results suggest a very stable AC barrier, subgrade, and waste zone.

The contour plots of the barrier surface for the 18 surveys from 1994 to 2012 are given in Appendix I. Plots for the first survey in 1994 and last survey in 2012 are shown in Figure 3.18. The plots reflect the 2% slope from the crown.

The spatially averaged elevation change over time is shown in Figure 3.19. During the 18-year monitoring period, the shape of the barrier surface stayed relatively constant. From 1994 to 2012, the average elevation change with 1σ was 0.003±0.018 m, which is negligible. There is no noticeable difference between the north and the south sections. The north section was irrigated to 3X the long-term average precipitation from WY95 to WY97 and the vegetation on it was burned by the controlled fire in 2008, while the south section was exposed to natural conditions for the duration of the study. The results indicate that neither settlement nor compression occurred during the 18-year monitoring period.

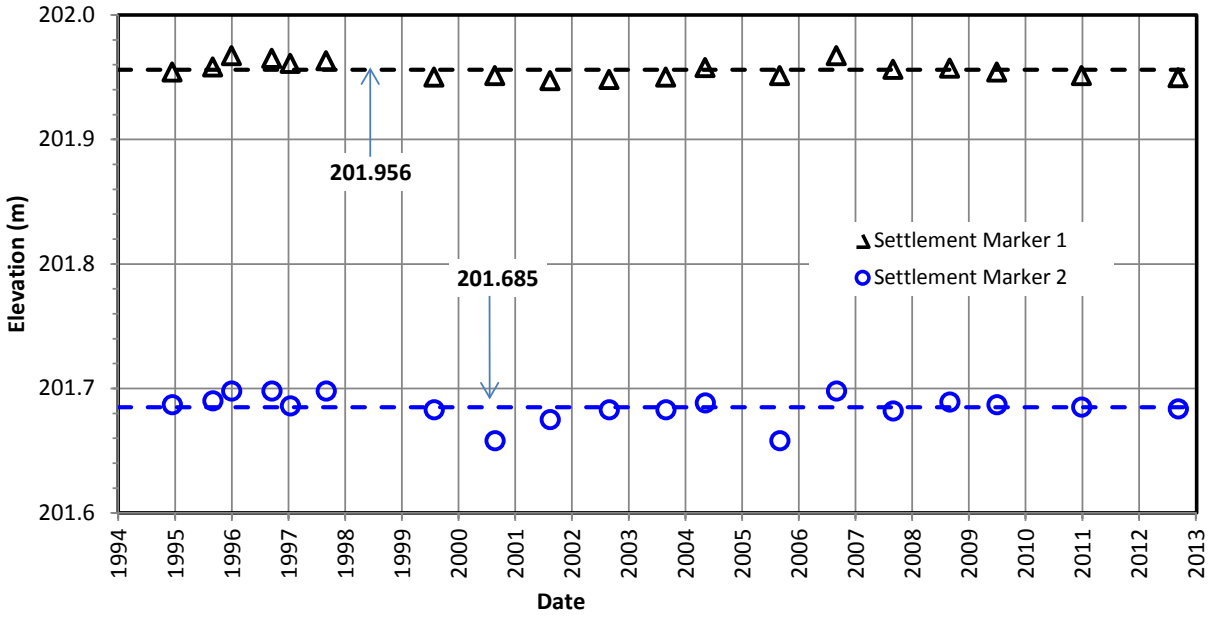

Figure 3.17. Elevation of settlement markers. Dashed lines indicate the average values.

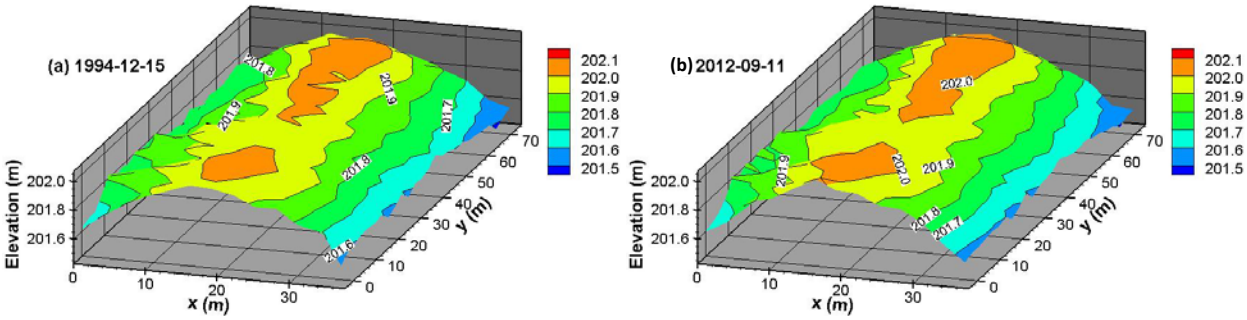

Figure 3.18. Surface elevation contours of the Prototype Hanford Barrier in (a) 1994 and (b) 2012.

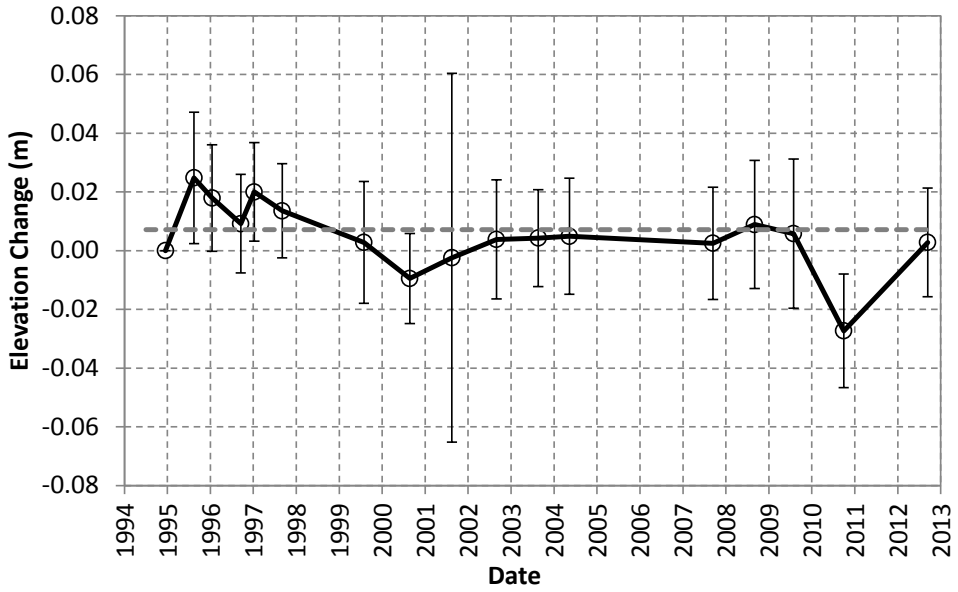

Figure 3.19. Average surface elevation change over 338 observations of the Prototype Hanford Barrier. Vertical lines indicate one standard deviation.

3.3.3 Riprap Side Slope Displacement

Negligible movement of the riprap side slope was observed during the 18-year monitoring period. Time plots of the CGs are reported in Appendix I; this section only compares the first and last surveys. Figure 3.20 shows the positions of the CGs in the final survey in 2012 (2011 for CG12 and 2010 for CG10a) relative to their corresponding initial positions in 1994. Of the 15 CGs, 12 had positive changes up to 0.083 m to the outward east, 13 had positive changes up to 0.033 m to the north, and 13 had negative changes down to -0.018 m (shown as the empty circles) in the vertical direction. On average, over the 15 CGs, the changes with 1 σ are dx = 0.023±0.032 m, dy = 0.020±0.012 m, and dz = -0.007±0.006 m. The average changes are comparable to the standard deviation, indicating that any changes are beyond detection and the riprap side slope was very stable during the monitoring period.

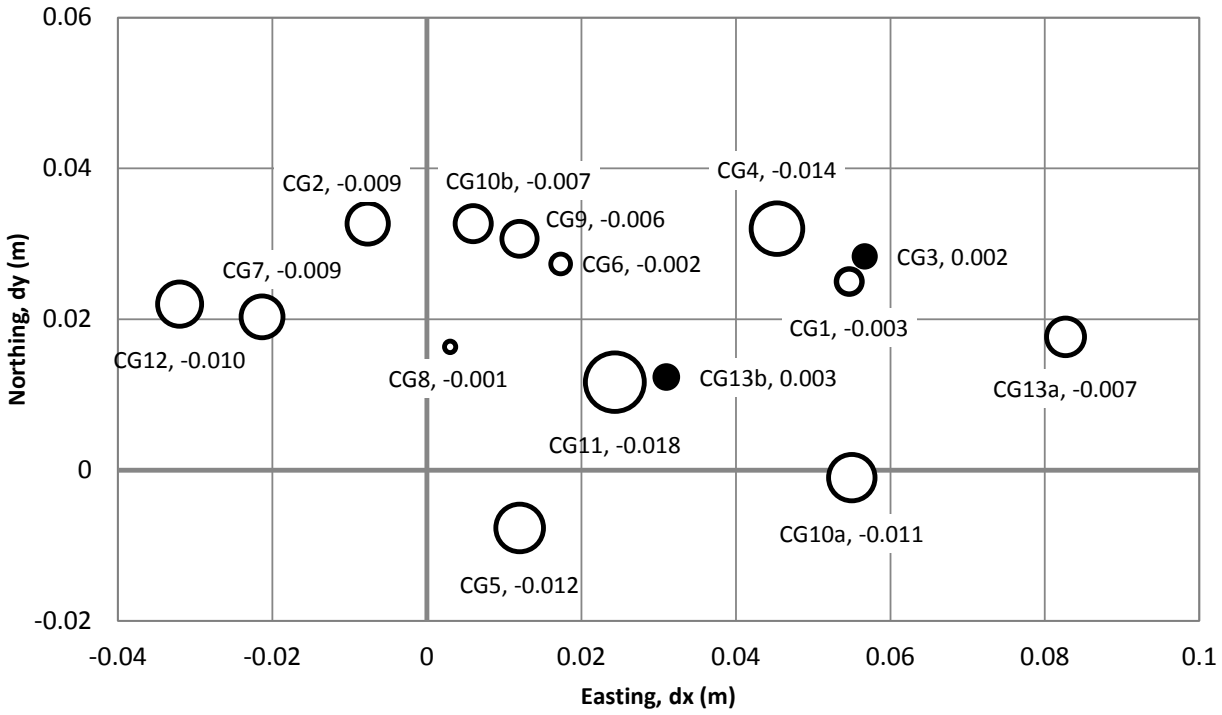

Figure 3.20. Positions of creep gauges in 2012 (2011 for CG12 and 2010 for CG10a) relative to their corresponding initial positions. A positive *dx* value indicates lateral movement of the side slope outward. A filled bubble indicates an increase in CG elevation, while an empty bubble indicates a decrease. The area of the bubble indicates the change in elevation as shown by the number nearby.

3.3.4 Surrounding Area of the PHB

The surface conditions of the PHB and surrounding area were recorded by aerial images taken approximately annually. Quality images for 2013 and 2015 were also obtained from Google Earth. The images provide an opportunity for qualitative visual comparison of the surface conditions of the PHB and surrounding area. Figure 3.21a and b show the aerial images taken in 1994, when the PHB construction was completed, and 21 years later, in 2015. Other than the vegetation that developed on the PHB and the surrounding area, there is no visual difference between the main components of the PHB, i.e., the ETC barrier and side slopes. However, the images show obvious changes in the terrain of subgrade at the east side to the PHB and the terrain of the north portion of the gravel side slope. The rectilinear slope of the exposed subgrade (Figure 3.21a) is less steep in 2015 and the sharp edge is rounded. The subgrade consists of the local sandy soil, which is highly erodible.

In May 2004, after severe thunderstorms, runoff water from the elevated BY-BX Tank Farm surface (southeast of the PHB) flowed down-gradient to the region between the Tank Farm and the PHB, eroding a channel about 1.1 m deep at the base of the east side of barrier side slope (Figure 3.22). The channel extended into the sandy subgrade below the riprap side slope.

The occurrence of the flood and the soil erosion by the PHB indicates that the topology around the barrier, the resultant run-on/runoff, and the surrounding surface hydrology can play an important role in

barrier integrity. Therefore, barrier design needs to consider protection of the toes of side slopes, particularly riprap side slope.

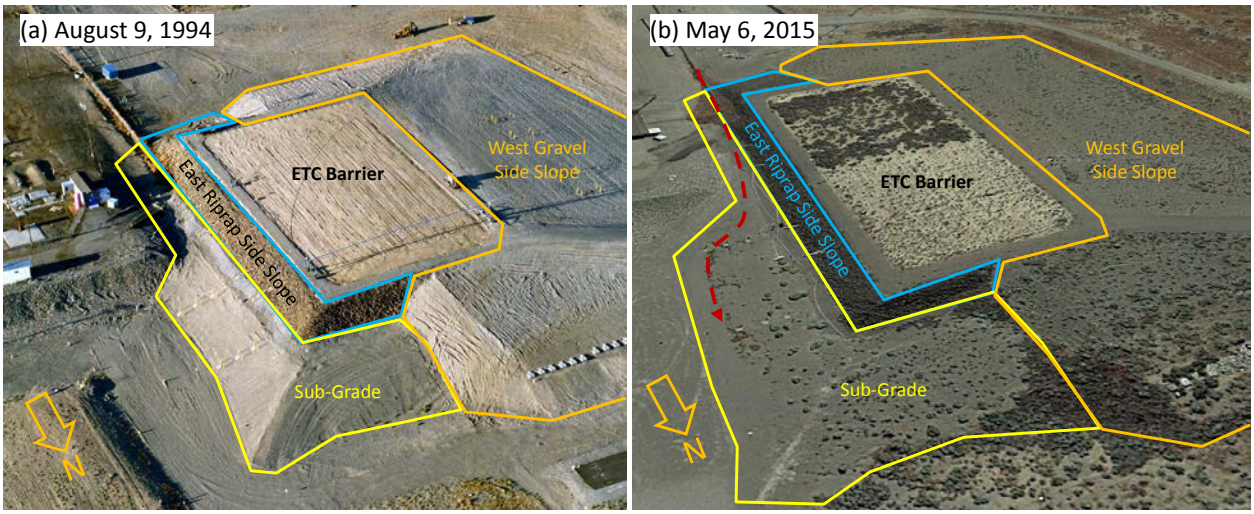

Figure 3.21. Aerial view of the Prototype Hanford Barrier (a) in 1994 after the completion of construction and (b) in 2015. The solid lines show the approximate boundaries of some barrier components. The dashed line indicates the approximate path and direction of the runoff water in May 2004 after severe thunderstorms. The image in (b) is from Google Earth.

Figure 3.22. North-facing photograph taken on June 16, 2004. The orange lines indicate the path and direction of the runoff water in May 2004 after severe thunderstorms.

3.3.5 Animal Activities

Potential risks to barrier function from animal activities include the formation of large holes, mounding, and damage to plants.

During regular surveys of activities at the PHB, the largest hole from animal activity was 0.09 m in diameter and 0.3 m deep. There was one mound observed that was 0.09 m tall. Rabbits were noted on the surface by the presence of feces, which positively correlated with percent cover of *Elymus wawawaiensis* (Snake River wheatgrass). A hole about 0.6 m deep and 0.3 m diameter, dug by an identified large animal, was observed and filled in during a visit to the site.[1] This hole was not recorded in the planned surveys of animal activities. Holes like these, if left unfilled, may become preferential flow channels if runoff flows into the holes. Insect galls were found on *A. tridentata* (sagebrush), making the plants appear to be under stress. Insect gall on *A. tridentata* may eventually weaken the shrubs with heavy infestation and can lead to their death.

The pre-PHB studies conducted at the Hanford Site (Cadwell et al. 1989; Landeen 1990, 1991, 1994) indicate that most animal burrows do not extend below 1 m since most favorable environmental conditions (e.g., food, water, shelter, and temperature) are found within the top 1 m below ground surface, with the exception of the Western harvester ant (Gano and States 1982). An Animal Intrusion Lysimeter Facility was constructed in FY88 near the Hanford Meteorological Station to evaluate the impacts of burrowing animals on engineered surface barrier performance. The results of these studies (Cadwell et al. 1989; Landeen 1990, 1991, 1994) are briefly summarized below.

- Soil brought to the surface by burrowing animals can be more susceptible to erosion. However, the erosion can be mitigated by adding gravel admix to the upper portion of the soil or installing a bio-barrier.
- Although deep percolation can occur, most water in the animal holes was later removed by a variety of processes (e.g., drying via ventilation effects from open burrows and transpiration from plants). Abandoned badger burrows were often quickly backfilled with soil and organic debris.
- The presence of small mammal burrows did not have a considerable impact on deep percolation.

Based on the pre-PHB studies of animal activities, animals at the PHB do not appear to significantly affect barrier function.

3.3.6 Barrier Maintenance

After the completion of the PHB construction and the revegetation in 1994, there was very little maintenance at the PHB, other than instrumentation, except the filling of an animal hole that was about 0.6 m deep with a 0.3 m diameter. The runoff channel after the severe thunderstorms in May 2004 at the base of the east side of barrier side slope was repaired in FY05.

[1] Personal communication with Chris Strickland and Ray Clayton of PNNL.

3.4 Impacts of Controlled Fire on Barrier Properties

The impacts of controlled fire on barrier properties are summarized in Appendix M and Appendix N. During the controlled fire, the maximum flame heights exceeded 9 m and the maximum temperatures ranged from 250°C at 1.5 cm below ground surface to over 700°C at 1 m above ground surface. Based on the measurements with 66 erosion pins before and nearly a year after the fire, the average change in measurement with one standard deviation was 1.3±7.1 cm. The large uncertainty in the measurements suggests that the measurements with the erosion pins are inconclusive with respect to barrier surface inflation and deflation following the fire.

One week after the fire, barrier soils significantly decreased in wettability, hydraulic conductivity, air-entry pressure, organic matter, and porosity relative to pre-fire conditions, whereas dry bulk density increased. Decreases in hydraulic conductivity and wettability led to a 0.016 mm surface runoff event in January 2009. There was a significant increase in soil macro-nutrients, pH, and electrical conductivity.

One year after the fire, wettability returned to pre-burn levels, with only 16% of the samples still showing a decrease. Hydraulic conductivity and air-entry pressure returned to pre-burn levels at one third of the locations but remained similar to values recorded immediately after the fire at the other two thirds. Soil nutrients, pH, and electrical conductivity remained elevated. Species composition on the burned surface changed considerably from prior years relative to the unburned surface and two analog sites.
The proportion of annuals and biennials increased, as is characteristic of burned surfaces that have become dominated by ruderal species.

3.5 Expected Future Barrier Performance

Future barrier performance depends on barrier stability and hydrology. Therefore, predicting barrier performance requires estimates of barrier stability and hydrology throughout its 1000-year design life.

3.5.1 Stability

The stability of a surface barrier refers to its ability to resist change when exposed to stresses such as soil erosion (Rumer and Mitchell 1995), differential settlement of the barrier or barrier foundation (Benson et al. 1999; Jessberger and Stone 1991; Lagatta 1992; Levitt et al. 2005), or sliding of the side slope (Blight 2008; Koerner and Soong 2000; Merry et al. 2005). Factors that may affect PHB stability in the future include soil erosion, barrier settlement, aging of asphalt, intrusion, and natural disasters. Each is described below.

Erosion of the ETC Barrier - The 19-year PHB record showed practically no evidence of wind or water erosion of the ETC barrier, despite 3 years of triple the mean annual precipitation; three simulated 1000-year-return, 24-hour precipitation events; and an intense, controlled fire that burned off all vegetation across half the barrier surface. The only evidence of water erosion occurred during the first simulated 1000-year-return rainstorm in March 1995, about half a year after PHB construction, when the vegetation was only in the seedling stage.

To understand how the barrier might behave over longer periods, Chatters and Gard (1991) reviewed and analyzed archaeological literature on 44 ancient human-made mounds or mound groups with ages ranging

from decades to millennia. They found that the most durable mound is conical and is built in successive layers on a prepared surface (much like the PHB).

Bjornstad and Teel (1993) and Chamness (1993) studied bergmounds, which have a gravel admix on the surface, as an analogue for the design of an erosion-resistant surface cover, and used those findings to guide the design of the PHB. In addition to the gravel admix, plants growing on the surface reduce the erosive force of rain and wind, and help to strengthen and protect the surface soil through root proliferation and mulching. Even in the absence of vegetation (e.g., following a fire), the pea gravel added to the silt loam protected the barrier surface from wind and water erosion. As the PHB testing showed, plants return to the barrier surface naturally within the year following a burn and re-establish their protection. Overall, the monitoring results have confirmed that the PHB design is resistant to water and wind erosion and that resistance is expected throughout the barrier's 1000-year design life.

Erosion of the Exposed Subgrade - An intense rainstorm in May 2004 generated runoff from surrounding areas located upslope of the PHB. As it flowed past by the PHB, the runoff water eroded some of the subgrade sandy soil just beyond the toe of the east riprap side slope. The amount eroded was noticeable but did not affect the side slope's stability. The PHB design process had not anticipated such events and thus had not provided for erosion protection of the subgrade. In retrospect, it is clear that the hydrology of the area surrounding and upslope of the barrier can play an important role in barrier integrity, and hence the design needs to consider protection of the riprap side slope toe. With such protection, the PHB can be expected to withstand such events in the future.

Settlement - During the nearly two decades of PHB monitoring, the two settlement markers indicated that the subgrade remained stable (i.e., did not settle). This can be explained by the absence of significant voids, other than 30.5-cm-diameter corrugated steel pipe left in place within the waste zone, and by the careful placement and compaction of the subgrade fill. Because no viable mechanism exists to alter the stability of the material beneath the barrier, the chance of differential settlement in the future is expected to remain very low.

Asphalt Aging - As asphalt ages, its average molecular size increases because of oxidative reactions that combine smaller molecular weight materials into larger molecules. The increase in molecular size is one of the primary factors in age hardening of asphaltic materials. Freeman et al. (1994) studied buried archaeological asphalt artifacts, ranging in age from 500 to 4000 years, analogous with the asphalt component of the PHB. The percentage of large molecular size materials was quantified. The fraction of large molecular size materials increased from about 0.4% for fresh asphalt to about 2.4% for 4000-year-old asphalt artifacts. These results indicate that, under buried conditions (i.e., no ultraviolet light; reduced oxygen), the aging processing appears to be extremely slow. Based on these results, the buried asphalt is expected to remain intact and functional well beyond the barrier's 1000-year design life.

Intrusion - Intrusion by plant roots and burrowing animals as well as inadvertent intrusion by humans is expected to be deterred by the 1.5-m-thick riprap layer. DOE intends to maintain active control of the Hanford Site (e.g., using fences, patrols, alarms) for the foreseeable future. If active control should ever cease, passive measures (e.g., signs, markers) are expected to be used. However, intentional activities such as stealing of the barrier materials (e.g., soil or rock) could dramatically damage the barrier integrity.

Natural Disruptive Events - Large-scale disruptive events such as tornados, volcanos, and earthquakes have the potential to affect barrier stability. Myers and Duranceau (1994) evaluated the historical

evidence for such events near the Hanford Site. Wind data collected at the Hanford Site and surrounding locations were used to develop probabilistic straight-wind and tornado hazard assessments. Straight-wind velocities that equal or exceed tornado velocities have return periods of about 100,000 years. Hence, tornado winds are expected to be extremely rare on the Hanford Site.

The nearest volcano is the extinct Goat Rock volcano in the Cascade Range (46°29′19″N 121°24′21″W[1]), more than 70 miles west of the Hanford Site. Tephra from the Cascade volcanos has been found in the sediments in and around the Hanford Site. During the 1980 volcanic eruption of Mount St. Helens (46.20°N 122.18°W[2], 120 miles southwest of Hanford), about 1 cm (0.39 in.) of ash fell on the northern part of the Hanford Site (Myers and Duranceau 1994). The volcanic hazard depends on the Cascade eruptive activity and the meteorological conditions that control the direction and distance of air transport. A small amount of volcanic ash is not expected to affect PHB performance.

The Columbia River Plateau region is an area of low magnitude seismicity compared to the rest of the western U.S. The most significant earthquake relative to the Hanford Site is the 5.75 magnitude quake that occurred in 1936 near Milton-Freewater, Oregon, which is more than 90 km (56 miles) to the southeast. Hence, the probability of PHB damage by tornados, volcanos, and earthquakes appears to be very low.

Side Slope Stability - Natural stable landforms generally have a curvilinear shape that is often convex near the upper area and concave near the lower area (Chatters and Gard 1991; Schor and Gray 2007). In contrast, the side slopes of the PHB were constructed with constant gradients. Because the west gravel side slope is very gentle (10:1) and merges well with the surrounding environment, it is expected to last for the long term. The steep (2:1) riprap slope led to the exposure of sub-grade. The erosion that occurred in May 2004 at the toe of the riprap side slope suggests that the steep slope may not be stable over the long term and improvement is needed.

3.5.2 Hydrology

The hydrology of the PHB refers to how the barrier interacts with the water cycle to (1) minimize runoff and (2) store and release precipitation such that drainage is nearly eliminated. Factors that will affect barrier hydrology in the future include climate change, soil development, plant community change, capillary break degradation, preferential flow, and geomorphic processes such as swale-dune formation. Each is described below.

Climate Change - Changes in climate (e.g., precipitation, temperature, wind) can affect the water balance and may alter the structure, root depth, and distribution of plants. These changes will affect water movement in the surface barrier.

An extensive body of research has indicated that the global average temperature and precipitation are expected to have an increasing trend (e.g., Christensen et al. 2007). In the next century, the projected average precipitation could increase by as much as 30%. The future climate for the next millennium is largely unknown, but it may be inferred from the past. Petersen (1994) extracted the pollen record from the lake bottom sediments of Carp Lake, located near Goldendale, Washington, about 100 miles

[1] https://en.wikipedia.org/wiki/Goat_Rocks.
[2] https://en.wikipedia.org/wiki/Mount_St._Helens.

southwest of the Hanford Site. This pollen record, dating back 75,000 years or more, indicates the types of vegetation that once grew near the lake and thus indicates the climate conditions necessary to support the growth of those types of vegetation. Based on the Carp Lake pollen record, Petersen (1994) stated that the mean annual precipitation 75,000 years ago ranged from 25% to 50% below to 28% above modern levels.

As discussed in Section 2.1, the estimated annual precipitation at the 99.9th percentile (0.1% probability) is 350 mm. Assuming that the mean annual precipitation will increase by 30% in the future and the temporal variation will remain nearly the same as current, then the P_a at the 99.9th percentile would be 455 mm. During the 3-year enhanced precipitation test, the average P_a was 496 mm, larger than the projected P_a at the 99.9th percentile. Hence, the PHB with the current design will likely perform well hydrologically in the next millennium, even with climate change.

There is a growing concern that the greenhouse effect will lead to global warming. According to Petersen (1994), the mean temperature 75,000 years ago ranged from 7°C to 10°C below to 2°C above modern levels. Warmer climate is expected to cause higher PET, which will reduce soil water storage and thus reduce the likelihood for drainage. Warmer climate may also change the composition of the plants that inhabit the surface of the barrier. As discussed below, barrier performance does not depend on a specific plant community composition.

In summary, nothing in the climate record from the past or the climate predictions for the future suggests conditions will be outside the range of those tested at the PHB, and thus barrier performance should continue to meet the design criteria.

Soil Change - Soil change refers to the changes to soil properties that may affect the hydrologic performance of a barrier. For an engineered system, soil changes can occur in response to the soil formation processes of illuviation, eluviation, and pedoturbation (Schaetzl and Anderson 2005), erosion-deposition, and fire. Illuviation and eluviation processes differentiate a uniform soil mass into distinctive layers (horizons) through transformation and translocation of soil components (e.g., clay, Fe, Al, humus, carbonate, and silica). Pedoturbation processes tend to inhibit soil horizonation by mixing layers formed previously. When acting simultaneously, layer formation still occurs, but it is in response to both processes.

Because of soil formation processes, natural soils generally contain several horizons (or layers) that are used to classify soils. For example, the Warden silt loam soil series at Hanford (Hajek 1966) typically has a surface layer that is underlain by a calcareous zone. When a barrier is built, no layering exists; however, given enough time, soil formation processes will slowly transform the material into something resembling a natural soil. This implies that the silt loam used for the barrier surface material will slowly evolve to be similar to a Warden silt loam soil, possibly over centuries or millennia. Based on data from Rockhold et al. (1988), the particle size distribution and hydraulic properties of Warden silt loam at the 20-cm depth are similar to those at the 60-cm depth, suggesting that the developed soil layers do not have considerably different hydraulic properties. Thus, soil formation within the silt loam layer is not expected to affect the hydrologic performance of the barrier in the next 1000 years.

The pedoturbation processes that mix soil components, usually at relatively shallow depths, can be caused by burrowing animals, soil fauna (e.g., worms), plant root growth, and paired processes such as freezing-thawing, wetting-drying, and swelling-shrinking. The pedoturbation processes keep the soil in a dynamic

condition so that channels for potential preferential flow, such as old animal burrows, root channels, and soil structures, are destroyed gradually after they are formed. Benson et al. (2007) observed that the hydraulic properties of cover soils converge to common values over time. Sometimes pedoturbation creates large conduits that could be avenues for preferential flow; this issue is treated separately below.

Soil can also change in response to erosion-deposition and fire. Erosion removes surface soil, which reduces the thickness of the water-storage layer. Deposition (e.g., wind-transported dust and sand, volcanic ash) increases the thickness of the water-storage layer, and its impact on barrier performance will depend on the properties and depth of the deposited material. The 19-year PHB record shows no evidence of erosion or deposition. The review of volcanic activity revealed very little ash deposition in the last 10,000 years.

When fire burns off the vegetation, it leaves behind residue that affects barrier soil properties, e.g., a reduction in wettability, hydraulic conductivity, air-entry pressure, organic matter, and porosity. The results of the controlled fire in 2008 showed such impacts to soil properties following a very hot fire, but the main impacts diminished within several years. More importantly, there were no discernible impacts to barrier performance.

Plant Community Change - Because ET surface barriers rely on soil evaporation and plant transpiration to release stored soil water into the atmosphere, the loss of vegetation may reduce surface barrier efficiency because of the reduced transpiration. The variety and growth habits of the species that comprise the plant community may change (thus changing transpiration) in response to climate or disturbances such as fire or biological intrusion by non-native species. Short-term PHB performance does not depend on plant transpiration, and long-term performance does not depend on a specific mix of plant species. For example, after the controlled fire in 2008, new vegetation developed naturally on the barrier, but the new plant species were dominated by shallow-rooted grass species. The test results show that, under near-normal precipitation conditions, the ET (predominantly evaporation) after a fire is sufficient to release the stored water. Lysimeter tests conducted at Hanford from 1987 to 2004 showed that a 1.5-m-thick silt loam barrier without vegetation could release nearly all (99.9%) of the stored water via only evaporation (Fayer and Gee 2006). Given these results, the barrier is expected to remove stored water effectively for the next 1000 years regardless of any plant community changes.

Capillary Break Change - The long-term performance of the barrier depends in part on maintaining the capillary break (texture discontinuity) at the bottom of the silt loam. Over time, soil fines could settle or migrate downward, partially or completely filling the matrices of the underlying gravel layer. The process could make the capillary break less effective at limiting downward unsaturated flow, thus reducing the storage capacity of the fine-grained storage layer. Waugh et al. (1994) conducted an analog study at the Hanford Site and found that many locations showed texture discontinuity. In some cases, the gravels were matrix free, comparable to the coarse layer in the PHB design, while in other cases, gravels were filled with poorly sorted sand and silt. The latter cases were likely the result of rapid deposition during the cataclysmic flooding that emplaced the sediments more than 10,000 years ago. Because the amount of water moving through the capillary break is expected to be extremely small, the translocation of fine soil particles (e.g., colloids, clay, dissolved salts and organic compounds) through the capillary break is expected to be very small, suggesting that the capillary break will retain its form and functionality throughout the design life.

Preferential Flow - Animal burrows and dead plant roots can act as channels for preferential flow when water exists at positive pressure, such as during runoff events caused by rainstorms or snowmelt. During the 19-year monitoring period at the PHB, runoff was observed only three times, in very small amounts, indicating that the barrier surface absorbed nearly all of the precipitation. When water in the silt loam is at negative pressure (i.e., the soil is unsaturated), water is retained and moves within the soil matrix because of the capillary effect; under these conditions, the burrows and channels are empty (except for air) and can actually enhance evaporation (Cadwell et al. 1989; Landeen 1990, 1991, 1994). Channels for preferential flow decrease with depth in direct proportion to the decrease in animal and plant activity. With sufficient silt loam depth, which the PHB has, the barrier can tolerate these channels and still store and release water and prevent drainage of water through the barrier. The channels are local and ephemeral; they occur in the vicinity of individual animals and plants and last until pedoturbation processes destroy them and create new channels.

Swale-Dune Topography Formation - The silt loam used to construct the PHB came from the nearby McGee Ranch. The dune-swale topography at the McGee Ranch appears to be associated with the distribution of vegetation clumps, which were called “coppice dunes” by Melton (1949). The dunes are generally the accumulated eolian dust or sand around the base of shrubs. At McGee Ranch, coppice dunes are circular to oblong with diameters of 1 to 3 m and heights between 0.2 and 0.7 m (Link et al. 1994; Waugh et al. 1994). The time needed to form coppice dunes is uncertain. The formation of dune-swale topography could influence water flow processes and soil water balance of the ETC barrier. The coppice dunes may enhance local runoff during rainstorms or snowmelt events, causing more infiltration in the swales between the dunes. Because the vegetation can grow on and between the dunes, the basic store-and-release mechanism will still function. Observations at the PHB over the past two decades show no evidence of the formation of the coppice dunes or the deposition of sand around the shrubs on the barrier surface.

3.5.3 Summary of Expected Future Barrier Performance

Future barrier performance depends on the stability and hydrology of the barrier. Given the 19-year record of successful performance and consideration of all the processes and mechanisms that could degrade the stability and hydrology in the future, the results suggest the PHB is very likely to perform for at least the remainder of its 1000-year design life. This conclusion is based on two assumptions: (1) the exposed subgrade receives protection against erosion and (2) institutional controls prevent inadvertent human activity at the barrier.

4.0 Summary of Findings

Findings from the 19-year PHB record are grouped below into the categories of vegetation, hydrology of the ETC barrier, hydrology of the transition zone and side slopes, structural stability, and fire impact to soil properties.

Vegetation

- *The plant community on the PHB was robust*. Forty-nine species were observed between 1995 and 2011, with the highest number of species (35) observed 2 years after construction and the fewest (11) observed in 2008, just prior to the controlled fire. In 2009, 1 year after the fire, there were 12 plant species on the unburned side, but many more species (24) on the burned side. *Artemisia tridentata* (big sagebrush) was the dominant plant when there was no fire. The results indicate a normal vegetation community for the Hanford climate.
- *The vegetation community recovered after the fire*. Burned and unburned plant communities were more similar to each other than to their counterparts at the McGee Ranch analog site, meaning that the vegetation community gradually recovered after the fire.

Hydrology of the ETC Barrier

- *The ETC barrier was able to store all winter precipitation, including that received during the precipitation stress tests*. As expected, water storage peaked in the winter months, when ET is low. Peak total water storage during the enhanced precipitation treatment was 517.5±85.8 mm in the 2-m-thick silt loam, which is 98% higher than the field capacity because of the underlying capillary break. The average is less than the 600-mm design storage, suggesting that the ETC barrier could have stored even more water. From WY99 to WY13, total water storage was 194.2±20.2 mm for the north section and 189.4±23.5 mm for the south section, meaning that no more than one third of the pores were filled, even during the wettest time of the year.
- *The ETC barrier was able to recycle to the atmosphere, via ET, nearly all precipitation stored during the winter and received during the summer*. Water stored near the soil surface was released the quickest whereas water stored at the largest depths was released the slowest. The rate of water removal by ET was constant from April to June and decreased thereafter. The results indicate that ET was sufficiently strong to reduce soil water storage to minimum values even before the end of the summer season.
- *The maximum drainage below the barrier components was well below the intended design*. The average drainage rate was 0.005 mm yr^{-1}, which is a factor of 100 less than the design criterion of 0.5 mm yr^{-1}. The maximum annual drainage observed during the monitoring period was 0.18 mm, and occurred during the enhanced precipitation test.
- *Snowmelt events on frozen ground such as the one in January 1997 pose a higher risk for generating runoff than rainstorms*. During the monitoring period, three events contributed a total runoff of 38.1 mm, of which 36.3 mm (95%) was due to a snowmelt event.
- *The 2% slope successfully diverted water during the enhanced precipitation test*. After the enhanced precipitation test and during the ambient precipitation test, there was no detectable water diversion, suggesting that ET kept water content small enough to preclude noticeable lateral movement.

- *The barrier demonstrated resilience to fire*. After the controlled fire in September 2008, the burned section revegetated naturally, predominantly by shallow-rooted grasses with some annuals, bi-annuals, and shrubs. From WY09 to WY13, precipitation was near normal and the plant community on the burned section was able to remove all the stored water, albeit at a slower rate than the mature plant community (with shrubs) in the unburned section. Despite the significant change in plant community in the burned section, there was no discernible increase in drainage rates.

Hydrology of the Transition Zones, Side Slopes, and Asphaltic Concrete

- *Water in the silt loam of the transition zones migrated both vertically and laterally*. The accumulation of soil moisture along the silt loam boundaries was noticeable only under the enhanced precipitation conditions and was minimal under natural precipitation conditions. The measured maximum drainage rate through the transition zones was much higher than the rate through the silt loam layer, but much lower than the rate through the side slopes.
- *Drainage through the side slopes was high*. Drainage through the two side slopes was highest in winter and lowest in summer. The annual drainage rate from both side slopes was very high (135.3 mm yr^{-1} on average) during the enhanced precipitation treatment. After the enhanced precipitation test, the rate decreased to an average of 12.8 mm yr^{-1}. Although these rates are much lower than they were during the enhanced precipitation test, they are still far in excess of the barrier design rate of 0.5 mm yr^{-1}, suggesting that side slopes, if included in the design, need to be evaluated for their impact on overall performance. No obvious difference in seasonal pattern of drainage or rate of drainage was observed between the two types of side slopes.
- *The AC barrier minimized water percolation to rates below detection*. The level of soil water pressure below the AC was comparable to the permanent wilting point, meaning the soil water was tightly bound to soil particles and thus fairly immobile. The stable or decreasing water content, stable soil water pressure, and very low percolation rate all indicate that the amount of water that percolated through the AC was negligible.

Structural Stability

- *The PHB surface resisted erosion by wind*. The vegetation increased the height of zero wind velocity above the barrier surface and suggested reduced possibility of wind erosion. A small amount (72 kg ha^{-1}) of water erosion was observed during the first simulated 1000-year return rainstorm in March 1995, about 6 months after construction when the vegetation was at the seedling stage. No soil erosion was observed during the rest of the monitoring period, which included the simulated 1000-year rainstorms in 1996 and 1997, the snowmelt event in the January 1997, and the controlled fire in 2008.
- *The PHB did not subside or compact*. From 1994 to 2012, the spatially averaged elevation of the barrier surface decreased by only 0.003±0.018 m, meaning undetectable soil loss or gain because of wind or water erosion or barrier settlement. The elevation of the asphalt layer varied between -0.03 and 0.02 m, indicating near-zero settlement and a very stable asphalt surface and subgrade.
- *PHB side slopes were stable*. During the 18-year monitoring period, the CGs at the riprap slope moved an average of 0.023±0.032 m outward to the east, 0.020±0.012 m to the north, and 0.007±0.006 m lower in elevation. These small changes demonstrate that the riprap side slope was very stable during the monitoring period.

- *Animal activity did not affect barrier performance*. The number and sizes of animal holes or mounds on the barrier surface were generally small (no more than 0.09 m in diameter and 0.3 m deep). One large hole about 0.6 m deep with a 0.3-m diameter was observed and filled. These holes presented little risk to barrier function.
- *Exterior processes affected the periphery of the PHB*. The rainstorm event in May 2004 led to runoff from nearby facilities that eroded a small section of the toe of the steep riprap side slope. The barrier design did not consider an event of this nature. The erosion did not affect the stability of the side slope and was repaired.

Fire Impact to Soil Properties

The impact of the controlled fire on soil properties diminished gradually over several years. The controlled fire in 2008 caused decreases in wettability, hydraulic conductivity, air-entry pressure, organic matter, and porosity relative to pre-fire conditions, whereas dry bulk density increased. One year after the fire, hydrophobicity had returned to pre-burn levels, with only 16% of the samples still showing signs of decreased wettability. Hydraulic conductivity and air-entry pressure returned to pre-burn levels at one third of the locations but remained similar to values recorded immediately after the fire at the other two thirds. Soil nutrients, pH, and electrical conductivity remain elevated.

Comparison with Performance Objectives

Table 4.1 compares the key findings from the 19-year monitoring record for the PHB to the performance objectives established during the treatability test (DOE-RL 1999). Overall, the PHB performance objectives were met, with an exception for minimal maintenance.

Table 4.1. Performance objectives and findings.

Objectives	Findings at PHB
1. Function in a semi-arid to sub-humid climate	The PHB functioned in Hanford's semi-arid climate as designed according to the observations of the hydrology within the silt loam layer and surrounding area, the structural stability of barrier surface and side slopes, and the vegetation and animal activities.
2. Have a design life of 1000 years	The enhanced precipitation events in WY95 through WY97, which have a low probability over the design life (estimated to be less than once in a million years), did not compromise the PHB. The PHB is expected to function normally under current Hanford precipitation conditions as well as conditions expected under climate change and a 1000-year return rainstorm. The monitoring results indicate that the PHB is structurally stable and there was negligible soil loss or gain from soil or wind erosion or barrier compression.
3. Limit drainage through the silt to less than 0.5 mm yr^{-1}	The average drainage rate was 0.005 mm yr^{-1}, two orders of magnitude lower than the design criterion. The maximum drainage rate ever observed was 0.18 mm yr^{-1} during the first year of the enhanced precipitation stress test, less than the design criterion of 0.5 mm yr^{-1}.
4. Limit runoff	In total, 38.1 mm runoff was observed at the PHB in three events. The silt loam has sufficient high hydraulic conductivity and the hydraulic properties appear to be stable over time.
5. Be maintenance free	There was near-zero maintenance at the PHB except to fill one animal hole and to repair a channel at the toe of the riprap side slope that was caused by an unusual runoff event that originated from the surrounding area.
6. Minimize biotic intrusion	Animal burrows were generally shallow, indicating no deep intrusion. The potential intrusion of plant roots into the layers beneath the silt loam was not monitored.
7. Minimize erosion	The only soil erosion observed was during the first simulated 1000-year return, 24-hour rainstorm in 1995, when there were loose soil particles on the surface of added gravels. No other soil erosion was observed.
8. Meet or exceed RCRA performance criteria[a]	The thickness of the ETC barrier exceeded the construction criteria and the drainage rate was less than the performance criteria for the RCRA C or D barrier.
[a] There are no clearly defined RCRA performance criteria. Generally, the design life for a RCRA cover is 30 years and the thickness is 0.91 m.	

The PHB functioned as designed from the completion of construction in 1994 to 2013. Monitoring activities included hydrological stress tests that far exceeded stresses expected over the next 1000 years. Most importantly, PHB performance demonstrated that the barrier satisfied nearly all key objectives. The PHB functioned in Hanford's semi-arid climate, limited drainage to well below the 0.5 mm yr^{-1} performance criterion, limited runoff, minimized erosion, and far exceeded RCRA criteria. Although the test period represented only 2% of the design life, the observed surface and side slope stability suggests the PHB is robust enough to endure for at least 1000 years under similar stress conditions.

The toe of the east riprap side slope was impacted by an unexpected runoff event from the surrounding area. This showed that nearby operations and facilities could affect barrier performance, suggesting that barriers like the PHB may require a design modification to protect against such events, which can be easily accomplished. Although not listed as a key objective, maintenance of monitoring sensors and equipment needs to be considered for barriers that require extended monitoring.

5.0 Recommendations

The nearly two-decade record of successful PHB performance is encouraging with respect to establishing surface barriers as a viable remediation technology. The data provide insights that offer an opportunity to identify recommendations for improvement. Recommendations for the PHB and future barrier development are summarized below. Additional detail regarding the recommendations and lessons learned can be found in Appendix P.

Extend the period of PHB performance monitoring

One of the challenges facing deployment of surface barriers is convincing stakeholders that the technology will be effective and long-lasting. A longer period of performance monitoring will help to address this challenge. Other reasons for extending the period include the following:

- The two-decade monitoring period accounts for only 2% of the 1000-year design life. Extrapolation of past performance into the future is subject to significant uncertainty, including the possible effects of climate change. Extending the monitoring period improves the predictive ability of extrapolation.
- Extreme events happen very infrequently, perhaps on time scales of decades or longer. Extending the monitoring period increases the likelihood that extreme events will occur and barrier performance will be observed.
- The vegetation on the north section of the PHB was still dominated by the shallow-rooted grasses 4 years after the controlled burn. Precipitation levels during this period were normal and were never high enough to stress the barrier. Extending the monitoring period allows for more-complete observation of vegetation recovery and PHB performance.

The monitoring systems that performed well during the PHB demonstration are recommended for continued monitoring at the accepted frequency. Continued monitoring of hydrology is recommended, including neutron logging to monitor water content and storage (manual logging, quarterly), drainage from 12 plots (automated logging, hourly), and runoff (automated logging, hourly). Monitoring the elevation of the surface barrier, stability of the riprap side slope, and ecological conditions once every 5 years is recommended. These monitoring activities may also be carried out if a severe unexpected event (e.g., fire, flooding, severe erosion, slope slide, death of a large portion of vegetation, considerable change in elevation in part or the whole barrier) occurs at the PHB.

Improve monitoring systems.

With some attention, some but not all of the PHB monitoring systems are adequate for extended barrier monitoring. Given the importance of establishing a defensible record of barrier performance, the monitoring systems that are functioning should be overhauled to improve robustness and reproducibility and to focus on the types of processes that will need to be monitored in the future. More robust sensors and the remote sensing technology for long-term cost-effective monitoring should be evaluated.

Improve design tools

The PHB record suggests there are ways to modify the barrier design to reduce costs yet retain the necessary performance. To support design optimization activities, analytic and numerical design tools

should be developed that account for the impact to performance of changing features such as soil thickness, soil type, and protection from off-site events. The tools should be able to address new monitoring capabilities and sensors, the effective depth (below the barrier) of barrier influence, and the integration of surface barriers with other remediation technologies. Finally, the tools should be able to represent (for barrier design purposes) the influence of the topography and hydrology that surrounds a barrier. Given the need to project barrier performance beyond the monitoring period, the design tools should be compared with the monitoring data in a rigorous validation exercise. In addition, the latest generation of sensors and data analytics should be evaluated and deployed to evaluate performance.

6.0 Quality Assurance

The PNNL Quality Assurance (QA) Program is based on the requirements as defined in DOE Order 414.1D, *Quality Assurance*, and 10 CFR 830, *Energy/Nuclear Safety Management*, Subpart A -- Quality Assurance Requirements (a.k.a. the Quality Rule). PNNL has chosen to implement the following consensus standards in a graded approach:

- ASME NQA-1-2000, *Quality Assurance Requirements for Nuclear Facility Applications*, Part 1, Requirements for Quality Assurance Programs for Nuclear Facilities.
- ASME NQA-1-2000, Part II, Subpart 2.7, Quality Assurance Requirements for Computer Software for Nuclear Facility Applications, including problem reporting and corrective action.
- ASME NQA-1-2000, Part IV, Subpart 4.2, Guidance on Graded Application of Quality Assurance (QA) for Nuclear-Related Research and Development.

The procedures necessary to implement the requirements are documented through PNNL's "How Do I…? (HDI), a system for managing the delivery of laboratory-level policies, requirements, and procedures.

The *DVZ-AFRI Quality Assurance Plan* is the minimum applicable QA document for all Deep Vadose Zone – Applied Field Research Initiative (DVZ-AFRI) projects. This QA plan also conforms to the QA requirements of DOE Order 414.1D and 10 CFR 830, Subpart A. The DVZ-AFRI is subject to the *Price Anderson Amendments Act*. Implementation of the DVZ-AFRI QA program is graded in accordance with ASME NQA-1-2000, Part IV, Subpart 4.2.

Four technology levels are defined for this DVZ-AFRI QA program:

- **Basic Research** consists of research tasks that are conducted to acquire and disseminate new scientific knowledge. During basic research, maximum flexibility is desired in order to allow the researcher the necessary latitude to conduct the research.
- **Applied Research** consists of research tasks that acquire data and documentation necessary to assure satisfactory reproducibility of results. The emphasis during this stage of a research task is on achieving adequate documentation and controls necessary to be able to reproduce results.
- **Development Work** consists of research tasks moving toward technology commercialization. These tasks still require a degree of flexibility and there is still a degree of uncertainty that exists in many cases. The role of quality on development work is to make sure that adequate controls to support movement into commercialization exist.
- **Research and Development Support Activities**. Support activities are those that are conventional and secondary in nature to the advancement of knowledge or development of technology, but allow the primary purpose of the work to be accomplished in a credible manner. An example of a support activity is controlling and maintaining documents and records. The level of quality for these activities is the same as for developmental work.

Within each technology level, the application process for QA controls is graded such that the level of analysis, extent of documentation, and degree of rigor of process control are applied commensurate with their significance, importance to safety, life cycle state of a facility or work, or programmatic mission. The work for this report was performed under the technology level of Applied Research.

6.1 Quality Assurance of Data Collection

The PHB demonstration was operated under the PNNL QA plan OHE-002, Rev. 6. Procedures that are specific to the PHB project include the following:

- PNL-PSB-2.0, *Procedure for Operational Use of Prototype Barrier Linear Irrigation Equipment*
- PNL-PSB-4.0, *Procedure for Routine Maintenance and Calibration of Dosing Siphons at the Prototype Surface Barrier*
- PNL-PSB-5.0, *Procedure for Surface Composition Analysis of the Prototype Surface Barrier*
- PNL-PSB-9.0, *Procedure for Calibration of Precipitation Meter Load Cells at the Prototype Surface Barrier*
- PNL-PSB-10.0, *Procedure for Measuring Soil Moisture Using the Neutron Probe in the Neutron Access Tube Vertical and Horizontal Arrays*
- PNL-PSB-11.0, *Soil Sampling and Testing Procedure for Verification of Hydrologic Performance at the Hanford Prototype Surface Barrier*

6.2 Quality Assurance of the Raw Data

The raw or original monitoring data were organized into multiple data qualification packages. Each data qualification package generally pulls the raw monitoring data of the same type together in EXCEL files with proper headings and descriptions. The data files received an independent technical review.

6.3 Quality Assurance of Data Processing

The QA-controlled raw data were used as inputs for further processing and analysis. Data reduction was applied to the frequently (e.g., hourly or sub-hourly) collected data using data loggers at multiple levels, such as daily or multi-daily, monthly, and annually. The final results were presented as tables or plots. Processing of raw data was documented in multiple computer-assisted calculations packages. These calculation packages and the associated data files received an independent technical review to ensure that the scientific and technical documents and records are technically adequate, complete, and correct.

During the near two-decade field monitoring, it was not unusual to have questionable data for many reasons. The issues may cause the loss of data or the generation of invalid data. Invalid data are defined as those beyond the reasonable physical range. During data processing, the invalid data were treated in the same way as the missing data, as described below.

1. *Discard the problematic data*. This happens (a) in the calculation of average or statistical analysis (e.g., average of water content over multiple monitoring stations), and (b) in the reduction of data logger data (e.g., the average of pressure head over a period such as a day or a month).

2. *Find the best estimates*. A general way to fill in the missing data is by interpolation either in space or time.

- Interpolation in space. In processing data from the neutron loggings that were conducted from once a week to once every several months, to calculate the water storage over the profile, the missing data may be filled by spatial interpolation using data for the adjacent depths of the same profile.
- Interpolation in time. In processing the drainage data, the values for total drainage over a certain period (e.g., a day or a month) were to be calculated. Hence, the data must be filled in for the total values to meaningful. In this case, interpolation in time was conducted.

3. *Discard all the related data for a calculation.* In the calculation of integrated values (e.g., water storage in the 2-m thick silt loam), all the data for a profile may be left unconsidered when several data items were missing or an interpolation was inappropriate.

7.0 References

10 CFR 830. *Energy/Nuclear Safety Management*, Code of Federal Regulations.

Albright, WH, CH Benson, GW Gee, AC Roesler, T Abichou, P Apiwantragoon, BF Lyles, and SA Rock. 2004. "Field Water Balance of Landfill Final Covers," *Journal of Environmental Quality*, 33(6):2317-2332.

Albright, WH, CH Benson, and WJ Waugh. 2010. *Water Balance Covers for Waste Containment Principles and Practices*. ASCE Press, Reston, Virginia.

Apiwantragoon, P, CH Benson, and WH Albright. 2015. "Field Hydrology of Water Balance Covers for Waste Containment," *Journal of Geotechnical and Geoenvironmental Engineering*, 141(2):04014101. doi:10.1061/(asce)gt.1943-5606.0001195.

ASME NQA-1-2000. *Quality Assurance Requirements for Nuclear Facility Applications*, New York, New York.

Benson, CH, DE Daniel, and GP Boutwell. 1999. "Field Performance of Compacted Clay Liners," *Journal of Geotechnical and Geoenvironmental Engineering*, 125:390-403.

Benson, CH, A Sawangsuriya, B Trzebiatowski, and W Albright. 2007. "Post-Construction Changes in the Hydraulic Properties of Water Balance Cover Soils," *J. of Geotech. and Geoenv. Engr*, 133(4):349-359.

Bjornstad, BN. 2014. "Ice-Rafted Erratics and Bergmounds from Pleistocene Outburst Floods, Rattlesnake Mountain, Washington, USA," *Quaternary Science Journal*, 63(1):44-59. doi:10.3285/eg.63.1.03.

Bjornstad, BN and SS Teel. 1993. *Natural Analog Study of Engineered Protective Barriers at the Hanford Site*, PNL-8840, Pacific Northwest Laboratory, Richland, Washington.

Blight, G. 2008. "Slope Failures in Municipal Solid Waste Dumps and Landfills: A Review," *Waste Management & Research*, 26:448-463.

Cadwell, LL, LE Eberhardt, and MA Simmons. 1989. *Animal Intrusion Studies for Protective Barriers: Status Report for FY 1988*, PNL-6869, Pacific Northwest Laboratory, Richland, WA.

Chamness, MA. 1993. *An Investigation of Bergmounds as Analogs to Erosion Control Factors on Protective Barriers*, PNL-8841, Pacific Northwest Laboratory, Richland, Washington. Available at http://www.iaea.org/inis/collection/NCLCollectionStore/_Public/25/059/25059205.pdf.

Chatters, JC and HA Gard. 1991. *Archaeological Mounds as Analogs of Engineered Covers for Waste Disposal Sites Literature Review and Progress Report*, PNL-7718, Pacific Northwest Laboratory, Richland, WA.

Christensen, JH, B Hewitson, A Busuioc, A Chen, X Gao, I Held, R Jones, RK Kolli, W-T Kwon, R Laprise, V Magaña Rueda, L L. Mearns, CG Menéndez, J Räisänen, A Rinke, A Sarr, and P Whetton. 2007. " Regional Climate Projections." In *Climate Change 2007: The Physical Science Basis.*

Contribution of Working Group I to the Fourth Assessment Report of the Intergovernmental Panel on Climate Change eds. S Solomon, D Qin, M Manning, Z Chen, M Marquis, KB Averyt, M Tignor, and HL Miller. Cambridge University Press, Cambridge, United Kingdom and New York, NY, USA.

CSI. 2009. *229 Heat Dissipation Matric Water Potential Sensor*, Campbell Scientisic, Inc., Logan, Utah.

Dekker, LW and CJ Ritsema. 1994. "How Water Moves in a Water-Repellent Sandy Soil: I. Potential and Actual Water Repellency," *Water Resources Research*, 30:2507-2517.

DOE-RL. 1992a. *200 East Groundwater Aggregate Area Management Study Report*, DOE/RL-92-19, U.S. Department of Energy Richland Operations Office, Richland, Washington.

DOE-RL. 1992b. *200 North Aggregate Area Management Study Report*, DOE/RL-92-44, U.S. Department of Energy Richland Operations Office, Richland, Washington.

DOE-RL. 1992c. *200 West Groundwater Aggregate Area Management Study Report*, DOE/RL-92-16, U.S. Department of Energy Richland Operations Office, Richland, Washington.

DOE-RL. 1993. *Phase I Remedial Investigation Report for the 200-BP-1 Operable Unit*, DOE/RL-92-70, Rev. 0, U.S. Department of Energy Richland Operations Office, Richland, Washington.

DOE-RL. 1994. *Constructability Report for the 200-BP-1 Prototype Surface Barrier*, DOE/RL- 94-76, U.S. Department of Energy Richland Operations Office, Richland, Washington.

DOE-RL. 1999. *200-BP-1 Prototype Barrier Treatability Test Report*, DOE/RL-99-11 Rev. 0, U.S. Department of Energy Richland Operations Office, Richland, Washington.

DOE-RL. 2013. *Hanford Site Cleanup Completion Framework*, DOE/RL-2009-10, Rev. 1, U.S. Department of Energy Richland Operations Office, Richland, Washington. Available at http://www.hanford.gov/files.cfm/Comp_Framework_Jan_%201-23-13-lfm.pdf.

DOE Order 414.1D. *Quality Assurance*, Washington, D.C.

EPA. 2013. *National Priorities List*. Accessed on April 1, 2015 at http://www.epa.gov/superfund/sites/npl/.

Fayer, MJ. 1987. *Model Assessment of Protective Barrier Designs: Part II*, PNL-6297, Pacific Northwest Laboratory, Richland, WA.

Fayer, MJ and GW Gee. 2006. "Multiple-Year Water Balance of Soil Covers in a Semiarid Setting," *Journal of Environmental Quality*, 35(1):366-377.

Fayer, MJ and JM Keller. 2007. *Recharge Data Package for Hanford Single-Shell Tank Waste Management Areas*, PNNL-16688, Pacific Northwest National Labratory, Richland, Washington. Available at http://www.osti.gov/energycitations/servlets/purl/917585-FNQXEV/.

Fecht, KR and AM Tallman. 1978. *Bergmounds Along the Western Margin of the Channeled Scablands, South-Central Washington* RHO-BWI-SA-11, Rockwell International, Richland, Washington. Available at http://www.osti.gov/scitech/servlets/purl/6431635.

Flint, AL, GS Campbell, KM Ellett, and C Calissendorff. 2002. "Calibration and Temperature Correction of Heat Dissipation Matric Potential Sensors," *Soil Sci. Soc. Am. J.*, 66:1439-1445.

Freeman, HD, RA Romine, and AH Zacher. 1994. *Hanford Permanent Isolation Barrier Program: Asphalt Technology Data and Status Report- FY 1994*, PNL-10194, Pacific Northwest Laboratory, Richland, Washington.

Gano, KA and JB States. 1982. *Habitat Requirements and Burrowing Depths of Rodents in Relation to Shallow Waste Burial Sites*, PNL-4140, Pacific Northwest Laboratory, Richland, Washington.

Gavlak, R, D Horneck, RO Miller, and J Kotuby-Amacher. 2003. *Soil, Plant and Water Reference Methods for the Western Region*, WCC 103 publication WREP 125, 2nd edition, Oregon State University, Corvallis, OR.

Gee, GW. 1987. *Recharge at the Hanford Site: Status Report*, PNL-6403, Pacific Northwest laboratory, Richland, Washington.

Gee, GW, MJ Fayer, ML Rockhold, and MD Campbell. 1992. "Variations in Recharge at the Hanford Site," *Northwest Science*, 66(4):237-250.

Gee, GW, D Felmy, JC Ritter, RR Kirkham, SO Link, JL Downs, and MJ Fayer. 1993. *Field Lysimeter Test Facility: Status Report IV*, PNL-8911, Pacific Northwest Laboratory, Richland, WA.

Gee, GW, HD Freeman, WHJ Walters, MW Ligotke, MD Campbell, AL Ward, SO Link, SK Smith, BG Gilmore, and RA Romine. 1994. *Hanford Protoype Surface Barrier Status Report: FY 1994*, PNL-10275, Pacific Northwest Laboratory, Richland, Washington. Available at http://www.osti.gov/energycitations/servlets/purl/10113304-5D9ZgI/webviewable/.

Gee, GW, JM Keller, and AL Ward. 2005. "Measurement and Prediction of Deep Drainage from Bare Sediments at a Semiarid Site," *Vadose Zone Journal*, 4:32-40.

Gee, GW, AL Ward, and MJ Fayer. 1997. "Surface Barrier Research at the Hanford Site," *Land Contamination & Reclamation*, 5(3):233-238.

Gee, GW, AL Ward, BG Gilmore, MW Ligotke, and SO Link. 1995. *Hanford Prototype-Barrier Status Report: FY 1995*, PNL-10872, Pacific Northwest National Laboratory, Richland, Washington. Available at http://www.osti.gov/energycitations/servlets/purl/177965-nd9isN/webviewable/.

Gilmore, BG and WH Walters. 1993. *Water Erosion Field Tests for Hanford Protective Barriers: FY 1992 Status Report*, PNL-8949 UC-603, Pacific Northwest Laboratory, Richland, Washington.

Hajek, BF. 1966. *Soil Survey Hanford Project in Benton County Washisngton*, BNWL-243, Pacific Northwest Laboratory, Richland, Washington. Available at http://www.fsl.orst.edu/rna/Documents/publications/Soil%20survey%20Hanford%20project%20in%20Benton%20county%20Washington.pdf.

Hoitink, DJ, KW Burk, JV Ramsdell (Jr.), and WJ Shaw. 2005. *Hanford Site Climatological Summary 2004 with Historical Data*, PNNL-15160, Pacific Northwest National Laboratory, Richland, Washington.

Jessberger, HL and K Stone. 1991. "Subsidence Effects on Clay Barrier," *Geotech*, 41:185-194.

KEH. 1993. *Prototype Surface Barrier at 200-BP-1 Operable Unit,* W-263-C2 Rev. 0, Kaiser Engineers Hanford Company, Richland, Washington.

Khire, MV, CH Benson, and PJ Bosscher. 2000. "Capillary Barriers: Design Variables and Water Balance," *Journal of Geotechnical and Geoenvironmental Engineering,* 126(8):695-708. doi:10.1061/(asce)1090-0241.

Koerner, R and T Soong. 2000. "Stability Assessment of Ten Large Landfill Failures," *Advances in transportation and geoenvironmental systems using geosynthetics (GeoDenver 2000),* 1-38 pp. Geotechnical Special Publication (GPS 103), Denver, CO.

Lagatta, MD. 1992. "Hydraulic Conductivity Tests on Geosynthetic Clay Liners Subjected to Differential Settlement," MS Thesis, University of Texas, Austin, Texas.

Landeen, DS. 1990. *Animal Intrusion Status Report for Fiscal Year 1989,* WHC-EP-0299, Westinghouse Hanford Company, Richland, Washington.

Landeen, DS. 1991. *Animal Intrusion Status Report for Fiscal Year 1990,* WHC-EP-0398, Westinghouse Hanford Company, Richland, Washington.

Landeen, DS. 1994. *The Influence of Small Mammal Burrowing Activity on Water Storage at the Hanford Site,* WHC-EP-0730, Westinghouse Hanford Company, Richland, Washington.

Levitt, DG, MJ Hartmann, KC Kisiel, CW Criswell, PD Farley, and C Christensen. 2005. "Comparison of the Water Balance of an Asphalt Cover and an Evapotranspiration Cover at Technical Area 49 at the Los Alamos National Laboratory," *Vadose Zone Journal,* 4(3):789-797. doi:10.2136/vzj2004.0171.

Ligotke, MW. 1993. *Soil Erosion Rates Caused by Wind and Saltating Sand Stresses in a Wind Tunnel,* PNL-8478, Pacific Northwest Laboratory, Richland, Washington. Available at http://www.osti.gov/energycitations/servlets/purl/6377761/.

Ligotke, MW and DC Klopfer. 1990. *Soil Erosion Rates from Mixed Soil and Gravel Surfaces in a Wind Tunnel,* PNL-7435, Pacific Northwest Laboratory, Richland, Washington.

Link, SO, WJ Waugh, JL Downs, ME Thiede, JC Chatters, and GW Gee. 1994. "Effects of Coppice Dune Topography and Vegetation on Soil Water Dynamics in a Cold-Desert Ecosystem," *Journal of Arid Environments,* 27:265-278.

McKee, TB, NJ Doesken, and J Kleist. 1993. "The Relationship of Drought Frequency and Duration of Time Scales," *Eighth Conference on Applied Climatology, American Meteorological Society,* 179-186 pp. Jan. 17-23, 1993, Anaheim, California.

McKee, TB, NJ Doesken, and J Kleist. 1995. "Drought Monitoring with Multiple Time Scales," *9th Conference on Applied Climatology,* Am. Meteorol. Soc., Dallas, Texas.

Melton, FA. 1949. "A Tentative Classification of Sand Dunes, Its Application to Dune History in the Southern High Plains," *J. Geol.*, 48:504-508.

Merry, SM, E Kavazanjian, and WU Fritz. 2005. "Reconnaisance of the July 10 2000 Payatas Landfill Failure," *ASCE Journal of Performance of Constructed Facilities,* 19:100-107.

Myers, DR and DA Duranceau. 1994. *Prototype Hanford Surface Barrier: Design Basis Document,* BHI-00007 Rev.0, Bechtel Hanford, Inc., Richland, Washington.

Oke, TR. 1987. *Boundary Layer Climates*. Second ed., Methuen, London.

Or, D and JM Wraith. 2001. "Soil Water Content and Water Potential Relationships." In *Soil Physics Companion,* ed. AW Warrick, pp. 49-84. CRC Press, Boca Raton.

Petersen, KL. 1994. The Long-Term Climate Change Task of the Hanford Permanent Isolation Barrier Development Program. In GW Gee and NR Wing *Proceedings of Thirty-Third Hanford Symposium on Health and the Environment, November 7-11,1994,* Battelle Press, Columbus, Ohio.

Reece, CF. 1996. "Evaluation of Line Heat Dissipation Sensor for Measuring Soil Matic Potential," *Soil Sci. Soc. Am. J.,* 60:1022-1028.

Reynolds, WD. 1993. "Unsaturated Hydraulic Conductivity: Field Measurement." In *Soil Sampling and Methods of Analysis,* ed. MR Carter, Canadian Society of Soil Science, pp. 633-644. Lewis Publishers, Boca Raton, Florida.

Reynolds, WD and DE Elrick. 1985. "In Situ Measurement of Field-Saturated Hydraulic Conductivity, Sorptivity and the A-Parameter Using the Guelph Permeameter," *Soil Science,* 140(4):292-302.

Rickard, WH and BE Vaughan. 1988. "Plant Community Characteristics and Responses." In *Shrub-Steppe: Balance and Change in a Semi-Arid Terrestrial Ecosystem, Developments in Agricultural and Managed-Forest Ecology,* eds. WH Rickard, BE Vaughan, and LE Rogers, Vol 20, pp. 109-179. Elsevier, Amsterdam.

Rockhold, RL, MJ Fayer, and GW Gee. 1988. *Characterization of Unsaturated Hydraulic Conductivity at the Hanford Site,* PNL-6488, Pacific Northwest Laboratory, Richland, WA.

Romano, N and A Santini. 2002. "Field." In *Methods of Soil Analysis Part 4 Physical Methods,* eds. JH Dane and CT Topp, pp. 721-738. Soil Science Society of America, Inc., Madison, Wisconsin USA.

Rumer, RR and JK Mitchell, eds. 1995. *Assessment of Barrier Containment Technologies: A Comprehensive Treatment for Environmnetal Remediation Applicaitons*, Springfield, VA.

Schaetzl, R and S Anderson. 2005. *Soils Genesis and Geomorphology*. Cambridge University Press, New York.

Schor, HJ and DH Gray. 2007. *Landforming: An Environmental Approach to Hillside Development, Mine Reclamation and Watershed Restoration*. John Wiley and Sons, Inc., Hoboken, NJ.

Stone, WA, JM Thorp, OP Gifford, and DJ Hoitink. 1983. *Climatological Summary for the Hanford Area,* PNL-4622, Pacific Northwest Laboratory, Richland, Washington.

Thom, HCS. 1966. *Some Methods of Climatological Analysis,* WMO Technical note 81, Secretariat of the WMO, Geneva, Switzerland.

Thornthwaite, CW and JR Mather. 1955. "The Water Balance," *Publications in Climatology, Drexel Institute of Climatology, Centerton, NJ,* 8(1):1-104.

Wallace, RW. 1977. *A Comparision of Evapotranspiration Estimates Using ERDA Hanford Climatological Data*, PNL-2698, Battelle Pacific Northwest Laboratories, Richland, Washington.

Ward, AL and GW Gee. 1997. "Performance Evaluation of a Field-Scale Surface Barrier," *Journal of Environmental Quality*, 26(3):694-705.

Ward, AL, GW Gee, and SO Link. 1997. *Hanford Prototype-Barrier Status Report: FY 1997*, PNNL--11789, Pacific Northwest National Laboratory, Richland, Washington. Available at http://www.osti.gov/energycitations/servlets/purl/569021-3NLXw0/webviewable/.

Ward, AL, KD Leary, SO Link, GT Berlin, JW Cammann, ML Mandis, and LC Buelow. 2009. "Short and Long-Term Fire Impacts on Hanford Barrier Performance," *Waste Management Symposium 09*, Phoenix, Arizona.

Ward, AL, SO Link, KD Leary, and GT Berlin. 2010. "Fire Impacts on an Engineered Barrier's Performance: The Hanford Barrier One Year after a Controlled Burn," *WM 2010 conference*, March 7-11, 2010, Phoenix, Arizona.

Waugh, WJ, JC Chatters, GV Last, BN Bjornstad, SO Link, and CR Hunter. 1994. *Barrier Analogs: Long-Term Performance Issues, Preliminary Studies, and Recommendations*, PNL-9004, Pacific Northwest Laboratory, Richland, WA.

Wing, NR and GW Gee. 1994. "Quest for the Perfect Cap," *Civil Engineering*, 64(10):38-41.

Zhang, ZF. 2015. "Field Soil Water Retention of the Prototype Hanford Barrier and Its Variability with Space and Time," *Vadose Zone Journal*, 14(8):1-10. doi:10.2136/vzj2015.01.0011.

Appendix A

The Standardized Precipitation Index at Hanford

Appendix B

Prototype Hanford Barrier: Barrier Design, Enhanced Precipitation Test and Controlled Burn Test

Appendix C

Prototype Hanford Barrier Monitoring

Appendix D

Properties of Materials for Barrier Construction

Appendix E

Field Soil Water Retention of the Prototype Hanford Barrier and Its Variability with Space and Time

Appendix F

Evaluating of the Hydrological Monitoring Systems at the Prototype Hanford Barrier

Appendix G

Nineteen-Year Hydrological Characteristics of the Prototype Hanford Barrier: The Silt Loam Storage Layer

Appendix H

Nineteen-Year Hydrological Characteristics of the Prototype Hanford Barrier: The Side Slopes and Asphalt Concrete Barrier

Appendix I

Structural Stability of the Prototype Hanford Barrier

Appendix J

Plant Community after Revegetation, Irrigation, and Fire at the Prototype Hanford Barrier

Appendix K

Plant Structure and Function at the Prototype Hanford Barrier

Appendix L

Animal Activities at the Prototype Hanford Barrier

Appendix M

Controlled Fire at the Prototype Hanford Barrier

Appendix N

Fire Impacts on the Performance of the Prototype Hanford Barrier

Appendix O

Aerial Photographs of the Prototype Hanford Barrier

Appendix P

Prototype Hanford Barrier: Elements Worked, Lessons Learned and Recommendations

Appendix Q

Monitoring Data

Appendix R

Prototype Hanford Barrier Publications